File: A-023-IDA

5

Investigation of Natural Sealing Processes in Irrigation Canals and Reservoirs

Charles E. Brockway

A dissertation presented in partial fulfillment
of the requirements for the degree

of

Doctor of Philosophy

in

Engineering

Idaho Water Resources Research Institute
University of Idaho
Moscow, Idaho

April 1977

INVESTIGATION OF NATURAL SEALING PROCESSES IN IRRIGATION CANALS AND RESERVOIRS

by

Charles Edward Brockway

A Dissertation
Submitted in partial fulfillment
of the requirements for the degree

of

DOCTOR OF PHILOSOPHY

in

Engineering

This project was supported primarily with funds provided by the Office of Water Research and Technology as authorized under the Water Resources Research Act of 1964, as amended.

Idaho Water Resources Research Institute
University of Idaho
Moscow, Idaho

March 1977

ACKNOWLEDGMENT

I wish to express my gratitude to the Water Resources Research Institute, University of Idaho, for funding of this study and particularly to Professor C. C. Warnick for his assistance and encouragement.

Special acknowledgment is extended to Dr. Calvin Clyde, major professor, and to Dr. Marvin Jensen, ARS, thesis director, for his assistance, advice and for making available the necessary equipment and facilities at the Snake River Conservation Research Center, Kimberly, Idaho.

I am also grateful to Dr. Joel Fletcher, Dr. Robert Oaks, and Dr. Frederick Post for serving as members of my doctoral committee.

Acknowledgment is also extended to Mr. Robert Worstell, ARS, for his cooperation in the laboratory and field work and to Mr. Yung Chi Chung and Mr. Pedro Hernandez for their contribution to the laboratory studies.

Finally, I express my deep appreciation to my wife, Carol, for her continued devotion and encouragement during the course of my graduate studies.

Charles E. Brockway

TABLE OF CONTENTS

TABLE OF CONTENTS (continued)

TABLE OF CONTENTS (continued)

LIST OF TABLES

LIST OF FIGURES

LIST OF FIGURES (continued)

ABSTRACT

Investigation of Natural Sealing Processes

in Irrigation Canals and Reservoirs

by

Charles E. Brockway, Doctor of Philosophy

Utah State University, 1976

Major Professor: Dr. Calvin G. Clyde
Department: Civil and Environmental Engineering

Laboratory and field studies of physical, organic, and chemical factors affecting the variations in seepage rates due to natural processes in canals and reservoirs under prolonged submergence were performed.

Effective reduction of hydraulic conductivity due to sediment migration in three sand sizes with three sediment sizes was examined in laboratory columns. Sediment migration measured non-destructively by gamma ray scanning was compared with corresponding changes in hydraulic conductivity. A simplified equation relating the deposit ratio, σ, or volume of sediment retained at any point in the column to the hydraulic conductivity was developed.

Procedures for estimating changes in hydraulic conductivity of Portneuf silt-loam soils of southern Idaho due to soil-water-chemical effects were developed. Using measured hydraulic conductivities during percolation of mixed salt solutions, changes attributable to clay swelling under field operating conditions were estimated. Results showed that measured changes in saturated hydraulic conductivity in disturbed soil columns during percolation of normal filtered irrigation water

could not be accounted for by clay swelling. Since steps were taken to eliminate microbiological activity the measured reductions in conductivity were attributed to plugging of soil pores by particles physically or chemically dispersed or dislodged from aggregates.

Measurements of saturated hydraulic conductivity of undisturbed soil cores from the bottom of an operating canal showed reductions with time similar to disturbed samples. The top 20mm of the columns exhibited decreases to 20 percent of initial conductivity over a 30 day period and measurements of cores with the top 20mm removed had conductivities 25 times as great as those cores with the top layer intact.

Ponded seepage rates, inflow outflow rates and estimates of seepage rates from in-situ conductivity tests were made on an operating canal. Comparisons showed that estimates of seepage for proposed canals in silt loam soils can be as much as five times greater than actual operational losses.

Soil moisture tension and moisture content below an operating canal were monitored and indicated seasonal declines with major fluctuations over an irrigation season. Hydraulic gradients in the top 8cm of the canal bottom increased to five times the initial gradient over the season whereas the gradients in the lower layers remained relatively constant. Similar measurements on a section of canal where the top 8cm had been scraped from the canal bottom showed similar responses indicating that the presence of an initial sealing layer does not affect the seasonal change in seepage.

Sedimentation, microbiological activity, soil-water-chemical effects, and physical dispersion of the silt fraction can effect hydraulic conductivity of soils beneath canals and reservoirs. For the Portneuf

silt-loam soils, the effect of clay swelling due to changes in the chemical content of percolating water causes minimal reduction in hydraulic conductivity. Physical dispersion of the silt fraction in the top layer of the soil is the primary cause of conductivity reduction. Accumulation of sediment on the canal bottom causes long term decrease in seepage rates, however, the relative magnitude of the reduction is less than that caused by dispersion. The role of microbiological activity in seepage reduction is apparently significant under some situations but not in others. Hydraulic conductivity measurements of Portneuf silt-loam soil under sterile and non-sterile conditions showed no apparent differences. Data from these experiments is not sufficient to evaluate the relative effect of microbiological activity on seepage rate changes in operating canals and reservoirs.

(121 pages)

NOTATION

VARIABLE	DESCRIPTION
A	a seepage factor depending on the geometry of the canal cross section - dimensionless
B	canal water surface width - L
C	emperical factor relating ponding and well permeameter tests
C_o	total salt concentration of ambient solution - dimensionless
c	capillary tension - L
CEC	cation exchange capacity - dimensionless
d	soil or sediment particle
d_1	original effective particle size in sedimentation test - L
d*	adjusted interlayer spacing, $\mathring{A}$
ESP	exchangeable sodium percentage - dimensionless
ESP*	adjusted ESP - dimensionless
fmont	percentage of montmorillonite in total soil by weight - dimensionless
g	gravitational acceleration LT^{-2}
H	depth of water in canal - L
I	intensity of transmitted gamma ray - dimensionless
I_o	intensity of incident beam - dimensionless
i	hydraulic gradient - dimensionless
i_o	initial hydraulic gradient - dimensionless
J	the reciprocal of the constant in Kozeny's equation
K	hydraulic conductivity - L/T
k	intrinsic permeability - L^2
N	number of bacteria per unit gram of soil necessary to cause the reduction in hydraulic conductivity of 1 cm/day
n	emperical constant in clay swelling - hydraulic conductivity relationship - dimensionless

NOTATIONS (continued)

VARIABLE	DESCRIPTION
P	pressure - F/L^2
Q	seepage rate - L/T
Q'	seepage rate per unit length of canal - L^2/T
q	seepage rate, macroscopic velocity or specific discharge L/T
S	specific surface area of soil particles - L^{-1}
s	distance along soil column
SAR	sodium absorption ratio - dimensionless
T	tortuosity - dimensionless
t	time
V	approach velocity or rate of infiltration - L/T
v	volume - L^3
W_p	canal wetted perimeter - L
x	thickness of material, L, or swelling factor - dimensionless
y	relative soil hydraulic conductivity $\frac{Ki}{Ko}$ - dimensionless
α	mass absorption coefficient - dimensionless
γ	specific weight of the pore fluid - F/L^3
μ	dynamic viscosity - FTL^{-2}
ϕ	porosity - dimensionless or hydraulic potential - L
ϕ_L	linear porosity
ρ	mass density FT^2/L^4
ρbs	bulk density of soil FT^2/L^4
σ	deposit ratio (volume of sediment per unit volume of porous media) - dimensionless
ν	kinematic viscosity - L^2/T

CHAPTER I

INTRODUCTION

In the design of irrigation distribution systems or storage facilities, the decision on whether or not to install impermeable lining has been made based on estimates of seepage rates from soil types and limited field or laboratory permeability tests. Seepage estimates based on limited permeability tests of undisturbed or disturbed soil can be considerably in excess of the long term operating seepage rates. Ponding tests on recently completed canal sections or test sections have shown seepage rates larger than those measured after one or several seasons of operation. Also, pre-season seepage measurements on operating canals often show seepage rates higher than post-season rates.

More precise estimates of seepage rates on operating systems could influence decisions on lining of open systems, use of pipe systems or decreases in design capacity. With the increased demands on water supplies in irrigated areas, every means of reducing undesirable seepage losses should be explored and especially the enhancement of natural sealing phenomenon which may be active.

Long term or seasonal changes in seepage rates have been noted on operating canals in distribution systems and in recharge ponds associated with groundwater replenishment projects. These changes may be caused by any one or more of the following factors. First, and perhaps the most significant in most cases is the development of impeding layers or layers of low hydraulic conductivity on the wetted perimeter of channels caused by gradual siltation or clogging of soil pores. Evi-

dence of the effects of silt in irrigation channels and recharge ponds have been cited by several investigators.

Measurements of initial seepage losses in two sections of the All-American Canal in California prior to operation were 2.1 and 2.5 percent per mile, Foster (1941). After nine months of operation, losses naturally decreased to 0.2 and 0.5 percent per mile. Canal discharges increased over the nine month period and canal wetted perimeter increased, however the net decreases in seepage were 16 and 51 percent in the two sections. These decreases were attributed primarily to silting of the canal bottom.

Warnick (1949) measured the variation of hydraulic conductivity with depth in soil cores from canals which indicated that the top 0.1 foot of the cores possessed conductivity as low as 25% of that of the deeper soil. Many studies have been conducted on the effects of artificial sediments; primarily bentonitic clays on the seepage from irrigation canals. These studies have been primarily concerned with the penetration of suspensions of flocculated and unflocculated montmorillonitic clays in sands and the associated changes in hydraulic conductivity, Shen (1958).

A second factor which may decrease seepage rates from canals and reservoirs particularly under prolonged submergence is the activity of microorganisms in the surface layer of soil. Early studies by Allison (1947) with sterile and non-sterile laboratory soil columns showed reduced conductivity of columns innoculated with soil microorganisms. Reduction in seepage rates with time as reported by Muckel (1959) in groundwater recharge studies have been attributed to the activity of microorganisms. Johnson (1958) showed that temporary decreases in

bacteria counts in soils from recharge ponds could be achieved by chlorination with subsequent increases in infiltration rates. Evidence of the possible action of microorganisms in sealing of irrigation canals has been shown by observed changes in soil moisture tension beneath a canal as influenced by herbicide application, Brockway and Worstell (1969).

The third factor which can influence seepage rates in canals or reservoirs is the chemical interaction of the soil and the infiltrating water. Field or laboratory tests performed on soils with water containing different amounts of dissolved solids from that which will ultimately be transported can lead to errors in predicted seepage losses. For instance, short-term permeability tests on soils high in exchangeable calcium and magnesium with water high in sodium may yield larger values for hydraulic conductivity than would actually occur after equilibrium between the soil and water is reached. In many instances, field projects report actual seepage losses as much as five to ten times that predicted from standard laboratory soil tests. Studies by Qwirk and Schofield (1955), Gardner (1945) and McNeal and Coleman (1966) have shown the dependence of soil hydraulic conductivity on exchangeable sodium percentage and salt concentration of the percolating solution.

The objectives of the study summarized in this dissertation were: 1) to identify the role of the three described factors in sealing of canals and reservoirs; 2) to evaluate the expected magnitude of each effect on soils, and in particular the Portneuf silt-loam soil in Southern Idaho; and 3) to derive relationships for guidelines in estimating the magnitude of the sealing effect in future developments.

CHAPTER II

REVIEW OF LITERATURE

General

Development of a rational relationship between the discharge velocity of flow through porous media and the driving force was first published in 1856 by Henry Darcy based on his studies of "les fontaine publiques de la ville de Dijon". The equation, commonly known as Darcy's law is:

$$q = Ki = K \frac{dh}{ds} \tag{1}$$

which indicates that the macroscopic velocity or specific discharge, q, is linearly related to the driving force or gradient, $\frac{dh}{ds}$, by a proportionality constant K, commonly called the coefficient of permeability. Recognizing the analogy between the Darcy equation and the equation governing the flow of electricity the proportionality constant has been referred to as the hydraulic conductivity. Darcy's law treats the flow through porous media macroscopically and avoids the difficulties of analyzing the microscopic hydrodynamics of flow through the tortuous branching pores of the granular skeleton of the porous medium. However, Hubbert (1956) among others has derived the Darcy equation from the general Navier-Stokes equation for viscous flow by neglecting the inertia terms. This analysis shows that Darcy's law is therefore valid only for microscopic pore velocities such that the Reynolds number is in the laminar flow range. It can be shown that it is highly unlikely that the range of validity of Darcy's law will be exceeded under natural flow conditions, Muscat (1946).

The hydraulic conductivity normally refers to the flow of water through porous media and usually denotes the saturated conductivity. Because the energy loss of fluid flowing through a porous media is a viscous effect, the hydraulic conductivity is a function of the density and viscosity of the pore fluid. The intrinsic permeability, k, which is a function only of the structure of the media is related to the hydraulic conductivity by:

$$K = k \frac{\gamma}{\mu} \tag{2}$$

where γ = the specific weight of the pore fluid

μ = dynamic viscosity

Darcy's law is valid for partially saturated systems; however, K is not constant but is a function of the degree of saturation of the media, Sheideggar (1957), Richards (1931). Richards (1931) outlined the relationships between the unsaturated hydraulic conductivity, sometimes called capillary conductivity, and the water content of the media.

The generalized expression of Darcy's law is:

$$q_i = -K_i \text{ grad } \phi_i \tag{3}$$

where q_i = the macroscopic velocity, sometimes called seepage velocity

K_i = the hydraulic conductivity

ϕ_i = the hydraulic potential or peizometric head

The equation of continuity applied for steady flow to any finite element of the fluid media requires that the divergence of the mass flow equal zero, thus

$$\text{div } q = 0 \tag{4}$$

where q is the seepage velocity

Combining equation (3) and (4)

$$\text{div } (-K \text{ grad } \phi) = 0 \tag{5}$$

and expanding

$$K \text{ div grad } \phi + \text{grad } K \text{ grad } \phi = 0 \qquad (6)$$

If the media is homogenous; $\frac{\partial K}{\partial x}$, $\frac{\partial K}{\partial y}$, and $\frac{\partial K}{\partial z} = 0$

and therefore grad K = 0

equation (6) becomes

$$K \text{ div grad } \phi = 0 \qquad (7)$$

div grad ϕ is the Laplacian Operator, $\nabla^2 \phi$ and equation (7) becomes:

$$\frac{\partial^2 \phi}{\partial x^2} + \frac{\partial^2 \phi}{\partial y^2} + \frac{\partial^2 \phi}{\partial z^2} = 0$$

Flow Systems Beneath Canals

Analytical solutions

Water movement from an irrigation canal to the water table has been the concern of investigators from almost every country where irrigation is practiced. Analytical treatments of flow systems by means of conformal mapping has been treated thoroughly by Polubarinova-Kochina (1962) for various canal cross-sections. In general, the expression for seepage rate from canals with deep water tables as developed by V. U. Vedernikov and reported by Polubarinova-Kochina is:

$$Q' = K (B+AH) \qquad (8)$$

where Q' = seepage rate per unit length of canal - ft^2/day

K = saturated hydraulic conductivity - ft/day

B = canal water surface width - ft.

H = depth of water in canal - ft.

A = a factor depending on the geometry of the canal cross section

Using the same approach Muskat (1946) developed similar equations, one of which with an A value of 2.0 is applicable to canal cross sections

of approximately semicircular shape with seepage to an infinite water table, and has been used extensively by the U. S. Bureau of Reclamation. This equation currently used by the Bureau of Reclamation is:

$$Q = \frac{K(B+AH)}{C\ W_p} \tag{9}$$

where Q = seepage-$ft^3/ft^2/day$

K = the hydraulic conductivity in ft/day

W_p = the canal wetted perimeter in ft

C = an emperical factor relating ponding and well permeameter tests

A = determined graphically from functions presented by Harr (1962)

The hydraulic conductivity, K, is measured in the field with well permeameters prior to construction using the auger hole method or by ponding of a test section along the proposed canal right-of-way.

Additional analytical treatment of flow systems is presented by Polubarinova-Kochina and Muskat for seepage from canals underlain at shallow depths by bedrock or more pervious stratum. Approximate analytical solutions for saturated seepage considering capillarity are given by Harr (1962) and Polubarinova-Kochina (1962) who reported on work done by B. K. Risenkampf (1938). Approximate solutions for the case of a clogged layer on the canal wetted perimeter are presented by Polubarinova-Kochina.

Studies by Glover (1963) suggest recognition of the role of capillary tension in a silted canal and an approximate expression of the form:

$$q = SB(d+c)$$

when q = seepage loss per unit length of canal in ft^2/sec.

c = capillary tension in ft. of water

d = depth of water in canal in ft.

B = top width of the canal surface in ft.

S = a surface loss coefficient determined from field tests and equal to the seepage loss in cubic feet per second per square foot of wetted perimeter if subjected to a head of one foot of water - ft/sec. ft.

However, the surface loss coefficient has yet to be evaluated.

Numerical and analog solutions

The advent of high speed computers has caused the increased use of numerical methods, principally finite difference techniques, for studying the flow systems beneath canals. Flow systems which include non-homogenous and anisotropic porous media can be examined as well as partially saturated conditions. Programs developed by Risenaur, Nelson and Knudsen (1963) and applied by Risenaur and Nelson (1965) to seepage determination from lined and unlined canals utilize the functional relationship of hydraulic conductivity to capillary pressure head to examine partially saturated flow systems and the effect of depth to the water table on seepage rates. The computed seepage rate from a 4.6m (15 ft) wide, 1.5m (5 ft) deep canal in a gravelly sand with a depth to water table of 11.9m (35 ft) was 2.4m^3/day·m (26.1 ft^3 day·lin. ft) of canal, while the corresponding saturated flow estimated using the Muskat equation is 2.0m^3/day·m (21.8 ft^3/day·lin. ft). For this canal with a compacted earth lining of 0.3m (1.0 ft) thickness on the bottom and 0.2m (0.7 ft) thickness on the sides and with a conductivity of 20 percent of the normal soil, the reduction in seepage was from 2.4m^3/day·m (26.1 ft^3/day·lin. ft) of canal to 1.6m^3/day·m (16.8 ft^3/day·lin. ft). Figure 1 shows the marked effect on the

moisture content caused by the lining. A moisture content of 0.33 is saturation which indicates that for the lined conditions the flow system is almost entirely unsaturated. Similar flow characteristics could be expected for a canal in which the conductivity of the wetted perimeter is reduced by sedimentation, or microbiological activity.

Jeppson (1969) and Jeppson and Nelson (1970) have examined steady state flow systems of water through porous media using inverse methods and finite difference procedures. Capillary pressure-permeability relationship were used and these procedures applied to evaluate flow from canals. They found for reasonable values of hydraulic conductivity that the region of saturated flow beneath the canal was relatively small.

An extremely versatile three dimensional model developed by Freeze (1971) uses line successive overrelaxation techniques (LSON) to solve the non-linear partial differential equations. This program which is applicable to small scale flow problems such as canal seepage systems is also capable of solutions of regional groundwater flow problems and handles transient conditions for non-homogenous anisotropic aquifers.

Bouwer (1965) using electric analog techniques has analyzed flow systems below canals for three conditions including an investigation of seepage from canals with a thin, slowly permeable layer at the wetted perimeter to simulate clogged material or chemical sealants. Estimates of seepage reduction by sealants or clogging were made utilizing estimates of the hydraulic impedance of the slowly permeable layer.

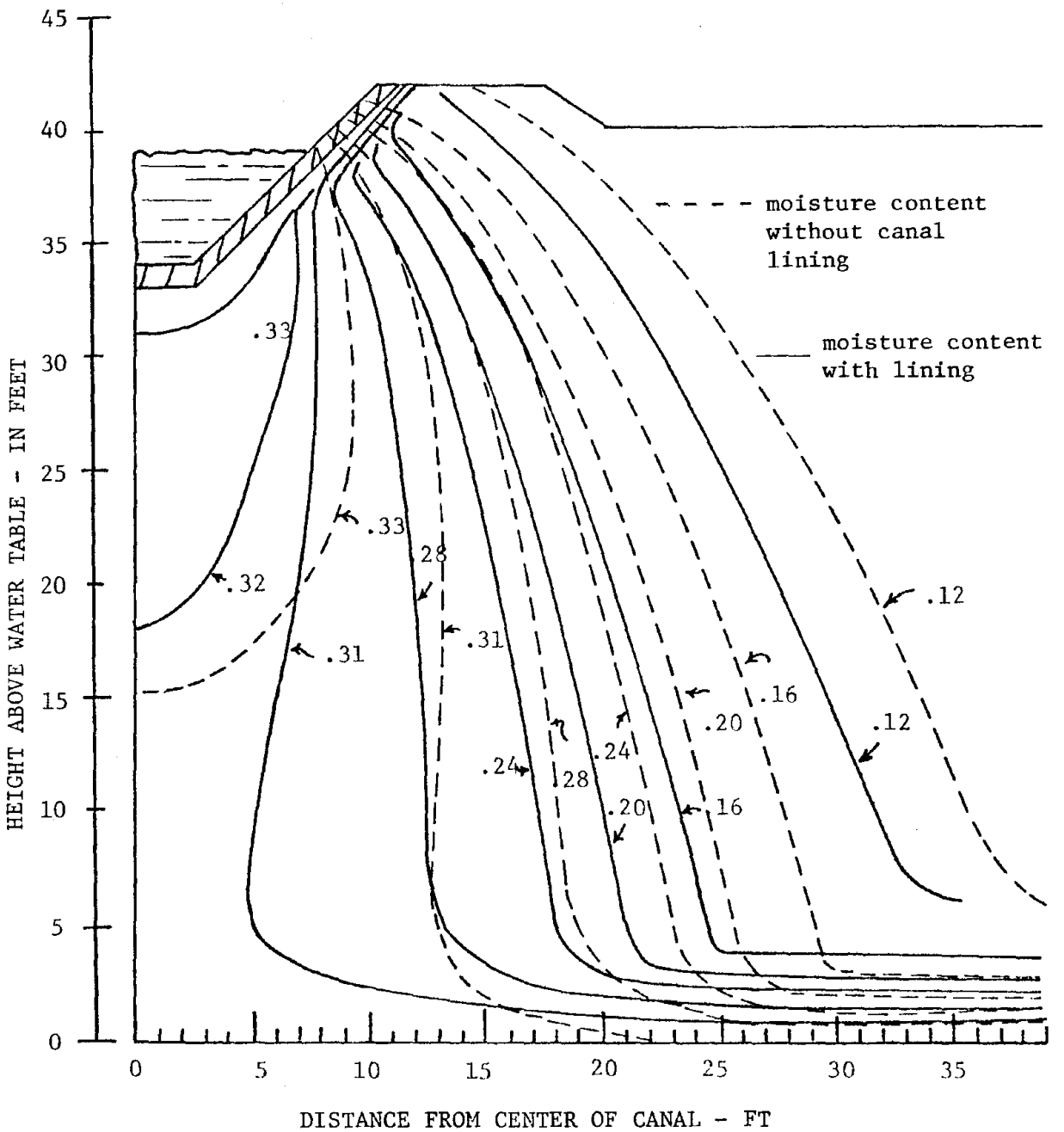

Figure 1. Effect of lining on moisture distribution below a canal, from Risenaur and Nelson (1965)

Field measurements

Tiedemann and Coffee (1966) have reported perhaps the most complete measurements of the flow system beneath an operating canal utilizing both tensiometers and nuclear moisture probes. However, with their installation they were unable to measure throughout the complete cross-section. Hendricks and Warnick (1959, 1960, 1961) reported on considerable work utilizing open piezometers for in-situ measurement of hydraulic conductivity as well as evaluating the flow pattern below operating canals. However, they were able to evaluate only the saturated areas of the flow system since negative pressures could not be measured.

Field measurement of soil moisture tension below canals had indicated the region of saturated flow is shallow as predicted by numerical techniques, Jeppson (1969).

Factors Affecting Hydraulic Conductivity

The expertise and techniques for accurately predicting the quantities of seepage flow from canal and configuration of flow systems are available. However, the limiting factor in predicting seepage rates is the measurement or estimation of the hydraulic conductivity applicable to the soil or soils in the cross section. Laboratory determination of hydraulic properties of field soils using 'undisturbed' cores is generally not satisfactory. In-situ measurements using auger-hole tests or infiltrometers must be used and the reliability of hydraulic conductivity values measured by these techniques is sometimes questionable. Where possible, ponding tests along the proposed canal right-of-way are desirable since the determination if K is eliminated and direct seepage rates are determined.

In any case whether or not seepage rates are estimated from hydraulic conductivity measurements on ponding tests prior to canal operation, the long term operational seepage rates can change by significant amounts from the initial values.

Some of the many factors which can influence either short term or long term changes in hydraulic conductivity of field soils are:

1. Temperature of seeping water
2. Barometric pressure
3. Sedimentation
4. Biological activity
5. Soil-water-chemical reactions

The effect of temperature changes on the hydraulic conductivity of the canal embankment and thus on the seepage rate is primarily due to expansion and contraction of entrapped gases. The hydraulic conductivity should increase with increasing water temperature since the viscosity decreases with increasing temperature. However, expansion of entrapped gases as temperature increases, reduces the effective porosity and thus decreases the conductivity.

Laliberte, Corey and Brooks (1966) showed that for changes in porosity of 5 percent, the saturated permeability can change as much as 50 percent on a sandy loam soil. The percentage change in permeability due to changes in porosity is greater for finer textured soils and less for sands. Pillsbury (1950) found that with acid washed inert sand separates using boiled distilled water that variation of saturated permeability with temperature was a wholly viscous effect. Robinson and Rowher (1959) measured the effect of temperature changes in the soil and water on seepage rates in seepage rings for three soils. They

showed that seepage decreases as temperature increases and that correcting the measured seepage for fiscous effects of temperature compensated for the estimated change caused by expansion of air bubbles in the soil.

The effect of changes in barometric pressure on seepage rates in operating canals is probably minimal compared to changes caused by other factors. Robinson and Rohwer (1959) measured barometric pressure during seepage tests in outdoor seepage rings and reported no apparent correlation with observed seepage rates. Changes in barometric pressure should affect the volume of gases in the pore matrix and thereby affect the conductivity.

However, the change in barometric pressure over an irrigation season is normally less than 40mm Hg, (measured data, Kimberly, Idaho 1967) so that the percentage change of the volume of air in the voids should be less than 5 percent. If the entrapped air in a saturated media is 10 percent of the voids then a 5 percent change in entrapped air volume would cause a change in porosity of only 0.5 percent and the net effect on the hydraulic conductivity caused by pressure changes should be minimal. Gupta and Swartzendruber (1964) measured hydraulic conductivity of washed quartz sand to boiled deionized water and evaluated the change in volume of the sample with a change in applied pressure, $\Delta v/ p$, throughout the period of measurement. The quantity $\Delta v/ p$ was found to be a highly sensitive indicator of entrapped air in the samples. They concluded that flow associated reductions in hydraulic conductivity were not caused by changes in volume of entrapped air.

Sedimentation in canals produces decreases in seepage rates and deliberate introduction of silt into operating canals has been practiced in several areas, USBR (1914, 1963), Reeves (1954), Hart (1963).

The use of bentonitic clay suspensions for seepage reduction has been studied in depth by Shen (1958) who found that both flocculated and unflocculated suspensions would not penetrate a dune sand matrix. Consequently, the deposited layer, although effective in reducing seepage, cracked and became ineffective after a drying period. Warnick (1949) found that naturally deposited sediments in irrigation canals in Southern Idaho could be effective in reducing seepage to about one fourth of the loss that occurred immediately after construction. Hydraulic conductivity measurements on undisturbed soil cores from the bottom of canals indicated that the gradients in the surface layers were as much as four times the hydraulic gradient in the underlying sands.

Sedimentation Effects

Since numerous investigations have shown that flow systems in the regions immediately below operating canals are most often partially saturated, the region of significance for this study is the first few inches of soil beneath the canal. The effect of natural and artificial sedimentation on the hydraulic conductivity of the impeding layer is dependent on the rate of sediment accumulation, the penetration of sediment into the soil pore matrix and the effect of the deposited layer on the conductivity of the soil. Deposited layers of bentonite clay reduce seepage rates, however, they are susceptible to erosion, drying and cracking which reduce their effectiveness to one or two seasons of operation. More permanent effects are achieved when sediment penetrates the soil pore spaces for considerable distances. It is therefore important in any artificial sedimentation program that the mechanics of sediment penetration be known and some idea of the

expected penetration for a given soil type and sediment gradation be evaluated.

The physical process occurring around the grains of a porous media during clogging by sediment, floc or other discrete particles is complex and difficult to evaluate. Stein (1961) investigated the mechanics of floc removal in a filter bed using a two dimensional model with lucite rods to represent spherical grains. He concluded that the primary process of removal was adherence or 'contact' of the particles with the grains and that sedimentation and coagulation within the pores is of minor importance. In essence then a 'sheath' of sediment is deposited on each grain resulting in an increase in the effective diameter of the grains and a decrease in porosity as the media becomes clogged. Stein's analysis recognized that the most important single filter parameter affecting headloss and velocity is the porosity, ϕ, of the media, Camp (1964).

Using this 'sheath' model for clogging and the Kozeny equations, Stein developed a relationship involving the deposit ratio (volume of sediment deposit per unit volume of media) any time after the start of filtration;

$$\frac{id^2}{K'} = \frac{(1-\phi+\sigma)^2}{(\phi-\sigma)^3} \cdot \frac{1}{\left[\sqrt{\frac{\sigma}{3(1-\phi)} + 1/4} + \frac{\sigma}{3(1-\phi)} + 1/2\right]} \qquad (10)$$

where $K' = \frac{JK^2\nu}{g} V$

ϕ = porosity at the start of the sediment run

d = effective grain size of media at start of run

σ = deposit ratio at any time during the run

i = hydraulic gradient at any time during the run

J = the reciprocal of the constant in Kozeny's equation

K = hydraulic conductivity

V = the approach velocity or rate of infiltration

ν = the kinematic viscosity

g = gravitational constant

Assuming that K' does not change during sedimentation the effect of d and K' were eliminated by expressing equation (10) in terms of the ratio of the hydraulic gradient to the initial hydraulic gradient.

$$\frac{i}{i_o} = \frac{(1-\phi+\sigma)^2}{(1-\phi)^2} \cdot \frac{\phi^3}{(\phi-\sigma)^3} \cdot \frac{1}{\left[\sqrt{\frac{\sigma}{3(1-\phi)} + 1/4} + \frac{\sigma}{3(1-\phi)} + 1/2\right]} \quad (11)$$

Equation (11) thus allows the computation of the deposit ratios by measurement of gradients at any time during a sedimentation period. Stein compared equation (11) with data from experiments on Ottowa sand and ferric chloride floc performed by Eliasen (1941) and found excellent agreement.

Filmer and Corey (1966) studied albumen molecules to simulate virus transport in water percolating through soils and concluded that retention was probably due to an absorption mechanism on particles. Behnke (1969) in experiments on artificial groundwater recharge suggests that clogging is a surface sealing process caused by gravitational settling and interstitial straining. He suggests that if the percolating water contains a range of particle sizes, the clogging process is initiated by gravitational grading. As the grain size at the top of the deposited layer becomes progressively smaller, interstitial straining begins to be the predominate mechanism of clogging.

Iwasaki (1951) showed that the time rate of change of the deposit ratio at a particular point and time in a filter is proportional to the rate of infiltration and the corresponding rate of decrease in volumetric concentration of particles in the water.

Biological Activity

The effect of microbiological activity in the soil layer forming the bottom and sides of a canal or reservoir can reduce the hydraulic conductivity of the media by significant amounts.

Allison (1947) presented considerable evidence for explanation of the causes for the shape of permeability curves for soils under prolonged submergence. Figure 2 shows the general S shaped permeability curve applicable to most soils. There is generally an initial decrease in permeability followed by a rapid increase to a maximum value and then a gradual decrease to some stable value after a long period of time.

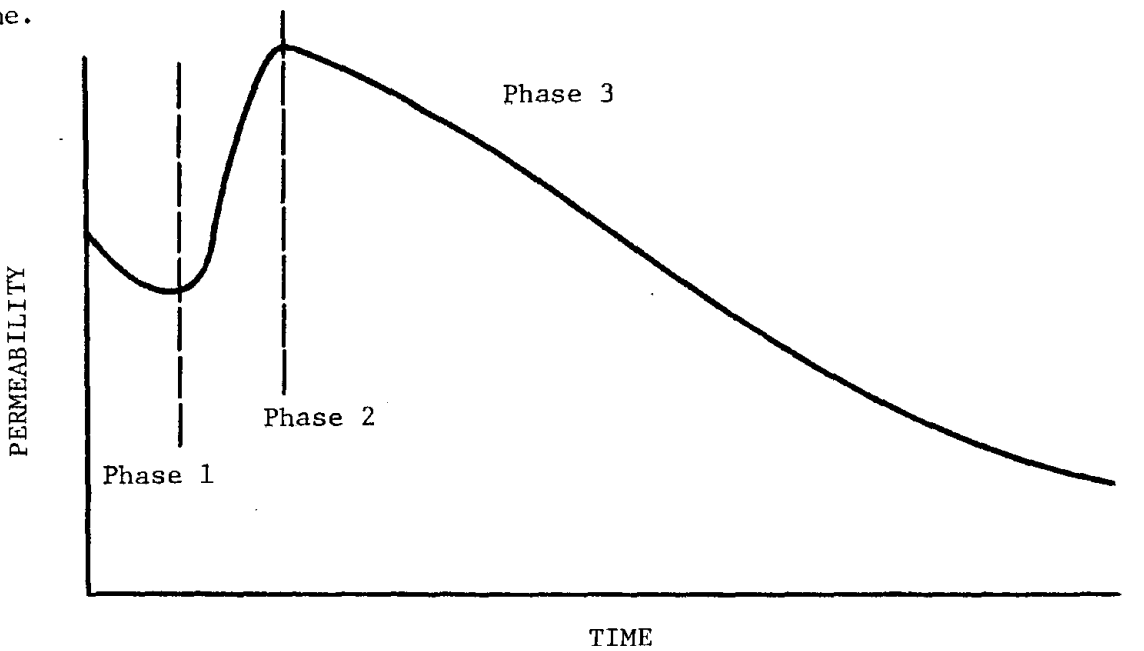

Figure 2. General permeability curve for soils under prolonged submergence

The S shaped curve was verified in laboratory studies with soil cores by Christiansen (1944), Allison (1947), and Pillsbury (1950) and confirmed in field tests by Muckel (1959). The shape of the curve is generally explained by three phases as follows:

In Phase I the decrease in permeability is believed to be caused by the swelling of soil particles and dispersion of the dry soil. This phase may be very pronounced for soils high in colloids or very small for highly permeable, coarse grained soils.

The increase in permeability in Phase II is likely due to the expulsion of entrapped gases by solution in the percolating water thereby increasing the pore space available for water movement.

During the third phase which starts after maximum permeability is reached the permeability decreases continuously at a decreasing rate to some stable value which may be only a small percentage of the initial permeability. This decrease has been attributed to biological activity. The decrease can be due to the clogging of soil pores with the products of microbiological growth, cells, slimes or waste products such as polysaccharides. Gupta and Swartzendruber (1962) confirmed the role of biological activity in permeability reduction of quartz sand.

Soil-Water-Chemical Reactions

The practical effects of the relationship of water quality and soil properties to seepage problems were indicated by Glenn (1968) who outlined the hazards of neglecting differences in water quality between laboratory tests and field operating conditions. Studies by Quirk and Schofield (1955), Gardner (1945), Reeve et al (1954), Bodman and Fireman (1950) and Martin and Richards (1969) have outlined the qualitative

effects on the hydraulic conductivity of changes in soils caused by percolation of salt solutions.

Changes in hydraulic conductivity of a soil or porous media are related to the cation exchange capacity of the media, the type of cation prevalent on the exchange sites and the character of the electrolyte concentration in the percolating water. Hydraulic conductivity is a function of the size, shape and tortuosity of the media matrix and any physical or chemical action within the matrix which changes this configuration will change the observed hydraulic conductivity.

For soils or media composed mostly of inert grains the chemical effect of percolating water is limited or negligible. Soils high in montmorillonitic clays exhibit large changes in conductivity when the electrolyte concentration of the percolating fluid is changed. Percolation of water with high sodium, low salt concentration generally results in soil sealing which can be detrimental on agricultural lands or beneficial in installations where low seepage rates are desirable.

McNeal and Coleman (1966), McNeal, Norval and Coleman (1966), and McNeal et al (1968) have evaluated the quantitative effects on hydraulic conductivity during percolation of mixed-salt solutions for groups of soils containing differing clay content and clay-fraction minerology. A procedure was derived to predict the effect on conductivity of mixed-salt solutions as a function of soil exchangeable sodium percentage (ESP), montmorillonite content of the soil, and total salt concentration of the ambient solution, McNeal (1968).

CHAPTER III

THEORY

Sediment Clogging

Estimating deposition

Regardless of the mechanism of particulate retention in a porous media, the most important parameter affecting the permeability at any point is the porosity. The deposit ratio, volume of sediment deposited per unit volume of soil, directly affects the porosity at any point in the mass and should be some function of the initial porosity, head loss, flow rate and permeability. Stein's equation, equation (11), successfully relates these factors but is somewhat cumbersome to evaluate and a simpler expression should be available. Many models have been proprosed for porous media to allow computation of saturated permeability values from geometric parameters namely, porosity or internal surface area. Treatment of the porous media as a series of uniform capillaries and applying the Hagen-Poiseuille equations or hydraulic radius analysis results in equations of the Kozeny (1927) type:

$$K = \frac{c\phi^3}{TS^2} \tag{12}$$

where K = hydraulic conductivity

c = cross section shape factor

ϕ = porosity

T = tortuosity

S = specific surface area of the solid pore boundaries per bulk volume

Much criticism has been directed at the Kozeny or Kozeny-Carman type equation as a means of quantitatively describing the permeability of saturated medium, Scheidegger (1957), Childs and Collis-George (1950). However, this equation, or modifications of it, continue to be used and cited for studies of flow through porous media, Wyllie and Gardner (1958). The use of the term tortuosity also has been questioned but continues to be used to account for the differences in flow path length between the media and the straight tube model.

Carman (1938) proposed a much used modification in which the value of C = 0.2 and the tortuosity T = 2.5 results in a simplified equation:

$$K = \frac{\phi^3}{5S^2} \tag{13}$$

If the particles are assumed to be spherical then the specific surface is related to the porosity by

$$S = \frac{6(1-\phi)}{d} \tag{14}$$

where d is the particle diameter.
Substituting equation (14) into the Kozeny-Carman equation gives the hydraulic conductivity for any time period:

$$K = \frac{d^2\phi^3}{180\ (1-\phi)^2} \tag{15}$$

The ratio of the hydraulic conductivity at some time, t, to the original hydraulic conductivity, K_1, is:

$$\frac{K}{K_1} = \frac{d^2\phi^3(1-\phi_1)^2}{d_1^2\phi_1^3(1-\phi)^2} \tag{16}$$

where d, ϕ, and K, are the effective particle size, porosity and hydraulic conductivity at time t.

With the assumption that sediment accumulation is by uniform buildup around spherical particles in a spherical space, the relationship between effective grain sizes at any time t, can be expressed as:

$$\frac{d}{d_1} = \left(\frac{1-\phi}{1-\phi_1}\right)^{1/3} \tag{17}$$

Substituting this expression into equation (16) gives

$$\phi_1^3 = \phi^3 \cdot \frac{K_1}{K} \left(\frac{1-\phi}{1-\phi_1}\right)^{4/3}$$

The porosity at time t, is $\phi_1 = \phi - \sigma$ where σ is the deposit ratio, volume of sediment per unit volume of porous media, at time t. Substituting into equation (17) yields:

$$\sigma = \phi\left(1 - \sqrt[3]{\frac{K_1}{K}} \left(\frac{(1-\phi+\sigma)}{1-\phi}\right)^{4/9}\right) \tag{18}$$

If the initial values of K and ϕ are known and the hydraulic conductivity is measured at any time during the sedimentation run, the deposit ratio, σ, can be determined by solving equation (18) with a trial and error procedure. However, since the deposit ratio, the volume of sediment per unit volume of porous medium, is very small, the last term in equation (18) can be considered equal to 1 and the simplified equation is

$$\sigma = \phi\left(1 - \sqrt[3]{\frac{K_1}{K}}\right) \tag{19}$$

Equation (19) can also be derived from the Hagan-Poiseuille flow theories applied to porous medium, Chung (1970).

Equation (19) is considerably easier to apply than Stein's equation as indicated by Camp (1964) to determine the amount and location of accumulated sediment during a run and it should be equally valid. Utilizing

this procedure in sedimentation tests on laboratory columns, the relative effect of sedimentation on conductivity reduction can be evaluated.

Measurement of sediment using gamma rays

Evaluation of sediment migration and deposition within the porous media to verify computed deposit ratios calculated from equation (19) or Stein's procedure, equation (11), can be accomplished using gamma ray scanning techniques. Gamma rays are quanta of electromagnetic wave energy similar to but of much higher energy than ordinary x-rays. When they pass through any substance, some amount of radiant energy will be absorbed or transformed into heat. The absorptive power of material varies with the character of the substance and the wave length of the incident energy.

If I_o is the original (incident) intensity of the gamma ray, I is the intensity of the gamma ray passing through a material of thickness, x, ρ is the density of the absorbing material, and α is the mass absorption coefficient, then the relation is, in general,

$$I = I_o e^{-\alpha x \rho} \text{ or } \ln \frac{Io}{I} = \alpha x \rho \tag{20}$$

The term on the right may be expanded to include a combination of absorbers; for instance, soil, water and the walls of the container. Equation (20) then becomes

$$\ln \frac{Io}{I} = \alpha_s \, x_s \, \rho_{bs} + \alpha_w \, x_w \, \rho_w + \alpha_c \, x_c \, \rho_c \tag{21}$$

where the subscripts, s, w, c, and bs denote soil, water, container material and bulk soil in the column. The total thickness of water in the porous medium is x_w and is equal to linear porosity, ϕ_L, multiplied

by a soil thickness ($s_w = \phi_L x_s$). If the pores in the porous medium are randomly arranged, the linear porosity is equal to volume porosity, ($\phi=\phi_L$). During sediment runs, the sediment will be retained in the soil column non-uniformly with the density and porosity being changed correspondingly. If the subscript "1" is used to express the data during the run, equation (21) will be

$$\ln \frac{I_o}{I_1} = \alpha_s x_s \rho_{bs_1} + \alpha_w \phi_1 x_s \rho_w + \alpha_c x_c \rho_c \tag{22}$$

The relationship between the porosity and density is

$$\phi_1 = 1 - \frac{\rho_{bs_1}}{\rho_s} \tag{23}$$

where ρ_s is soil particle density so that

$$\rho_{bs_1} = \frac{1}{x_s \left(\alpha_s - \alpha_s \frac{\rho_w}{\rho_s}\right)} \left(\ln \frac{I_o}{I_1} - \alpha_w x_s \rho_w - \alpha_c x_c \rho_c\right) \tag{24}$$

The density during the sediment run, ρ_{bs_1}, can be calculated from equation (24) and ϕ_1 calculated from equation (13). The deposit ratio is then equal to $\phi - \phi_1$.

By scanning a soil column before a sedimentation run and after or during a run, the deposit ratio can be calculated as follows. Substituting $(1 - \phi)\rho$ for ρ_{bs} in equation (21) the gamma ray intensity through the soil column prior to sedimentation is

$$I = I_o e^{-\alpha_s x_s (1-\phi) \rho_s - \alpha_w \phi x_s \rho_w - \alpha_c x_c \rho_c}$$

and after sedimentation is

$$I_1 = I_o e^{-\alpha_s x_s (1 - \phi + \sigma)\rho_s - \alpha_w (\phi - \sigma) x_s \rho_w - \alpha_c x_c \rho_c}$$

The ratio I/I_1 is given by

$$\frac{I}{I_1} = e^{(\alpha_s x_s \sigma\rho_s - \alpha_w \sigma x_s \rho_w)}$$

and

$$\sigma = \frac{1}{(\alpha_s \rho_s - \alpha_w \rho_w)x_s} \ln \frac{I}{I_1} \qquad (25)$$

Equation (25) is more convenient to use than equation (24) since several constants have been eliminated.

Soil-Water-Chemical Effects

Changes in hydraulic conductivity of soils when the chemical composition of the percolating water is changed are caused primarily by the effects on the clay and fine silt fractions of the soil. Most pronounced effects are observed when soils are leached with water having a low salt concentration as compared with the salt concentration of the percolating water with which the soil was in equilibrium. The observed decreases in hydraulic conductivity are caused either by swelling of clay particles or by dispersion of clay platelets. In either case the effective diameter of soil pores is decreased, either by swelling or by clogging by dispersed particles, and the hydraulic conductivity is decreased.

In any soil, the coarse particles, gravel, sand and coarse silt, act as discrete particles and are generally considered chemically inert as far as any reaction with percolating water is concerned. Chemical and physical-chemical reactions take place at the surface of particles therefore the response of the soil to percolating fluids is primarily determined by the type and amount of fine clays and medium to fine silt which have high specific surfaces. The clay mineralogy of the soil,

along with the solution properties determine the relative hydraulic conductivities of the soil. A classification of clay types with general information on hydration characteristics is shown in Table 1.

Table 1. Clay classification according to type and hydration characteristics

	Group Names	Ratio of number of silica to alumina layers	Hydration Characteristics
Layer-type lattice (typical shape is plate-like)	Kaolinite	1:1	Compact sheets, no internal (structural) hydration.
	Montmorillonite	2:1	Expands and contracts markedly with adsorption of water between clay sheets.
	Vermiculite	2:1	Expansion restricted.
	Illite	2:1	Hydration between packets of sheets.
	Chlorite	(Ordered stacking of alternate layers of different types)	Some hydration.
Chain-type lattice (typical shape is rod or needle like)	Fibrous clay	(Not appropriate).	Open porous structure; can absorb water internally without expansion.

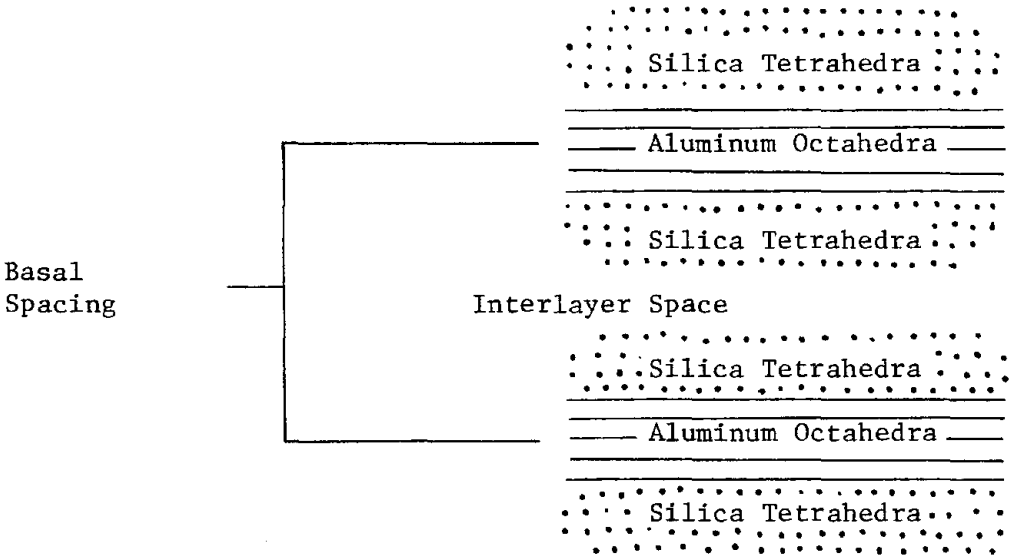

Figure 3. Idealized montmorillonite clay structure

The idealized clay structure where only silica is present in the outer layer and only aluminum is present in the inner layer results in a neutral cyrstal with no charge. Isomorphous substitution such as Mg^{+2} for Al^{+3} results in a net negative charge and substitution of Al^{+3} for Si^{+4} in the outer layer also gives a net negative charge. Any element with the same ionic size may substitute and depending on the ionic charge may result in an imbalance of charge on the crystal. Any imbalance of charge results in attraction of cations or dipoler water molecules into the interlayer spaces to neutralize the charge. The type of cation, H^{+1}, Ca^{+2}, Mg^{+2}, K^{+1}, NH^{+4}, or Na^{+1} largely determines the type and properties of the clay.

Kaolinite clays are 1:1 layer silicates with small interlayer spaces, tight H^{+} bonds and no shrinkage.

In mica type clays (illite) which are 2:1 layer silicates, the interlayer spaces are occupied by K^{+1} which has the right coordination to fit in the lattice of silica and oxygen very tightly. The result is

that very little water enters the interlayer spaces and therefore shrinkage is minimal. The only reactive surfaces on the illite type clays are the edges of the crystals.

Vermiculite structure is similar to illites except that the interlayer spaces are occupied generally by Ca^{+2} or Na^{+}, and the interlayer spacing is somewhat larger but not as large as montmorillonite. Swelling of vermiculite is somewhat restricted.

Montmorillonite is a 2:1 layer silicate with relatively large basal spacing, 18Å or larger. The interlayer spaces are generally occupied by Na^{+1}, Ca^{+2}, or Mg^{+2} and because of the interlayer spaces hydration is prevalent and swelling and shrinking very marked.

The ions in the interlayer spaces and on the edges of the crystals remain in a state of dynamic equilibrium with similar ions in the surrounding soil solution. However, if the ionic concentration of the surrounding solution is changed, the attached cations may or may not be 'exchanged'.

The charged clay surfaces with their associated exchangeable cations also react with water molecules which become oriented in the strong electric field near the charged surfaces. The resulting layers of oriented water molecules give characteristic properties of plasticity, cohesion, and shrinkage to clays and soils containing large amounts of clay.

The unbalanced negative charge left by isomorphous substitution is measured in meq (millequivalents) of charge and is equal to the number of meg's of cations necessary to neutralize the excess charge. This parameter is the cation exchange capacity (CEC) of the soil.

The principal cations normally found on the exchange complex of

soils in arid regions and on the soil solution are calcium and magnesium. If the soil solution becomes concentrated through evaporation or plant uptake, the solubility limits of calcium and magnesium may be exceeded and subsequent precipitation of calcium and magnesium carbonate and calcium sulfate may occur. Under these conditions sodium becomes the dominant cation in the soil solution and a part of the exchangeable calcium and magnesium is replaced by sodium.

The percentage of the exchange capacity of the soil which is occupied by sodium is termed the exchangeable sodium percentage (ESP) and calculated as:

$$ESP = \frac{\text{Exchangeable sodium (meq/100 g soil)}}{\text{Cation exchange capacity (meq/100 g soil)}}$$

The most commonly used indicator of agricultural water quality and sodium hazard is the sodium adsorption ratio (SAR) developed by the U. S. Salinity Laboratory (1954). The SAR is calculated by

$$SAR = \sqrt{\frac{Na^{+}}{\frac{Ca^{++}+Mg^{++}}{2}}}$$

where Na^{+}, Ca^{++}, and Mg^{++} are the concentrations in meq/liter of the respective ions.

There is a good correlation between the SAR of the soil solution and the ESP of the soil. This relationship between the soluble ions in solution which will remain in equilibrium with a given exchangeable sodium level in the soil has proven to be a good index of one phase of irrigation water quality. This index indicates how and to what extent a given water containing excess sodium might change the permeability and structural stability of the soil. Generally the higher the SAR the greater the potential for adverse affects on permeability and other indices of soil structure.

Since soil hydraulic conductivity depends both on the clay mineralogy of the soil and the chemical composition of the percolating water, some indices to be used as parameters in developing quantitative relationships must be chosen.

Studies by McNeal et al (1968) and Quirk and Schofield (1955) indicate that the ESP of the soil is a more responsive parameter of the exchange complex than the SAR and that the total salt concentration is a relevant parameter of the percolating solution. A good inverse correlation between the hydraulic conductivity of soils high in 2:1 layer silicates and the swelling of extracted soil clays in comparable solutions was found. McNeal (1968) developed a procedure for predicting the effect of mixed salt solutions on soil hydraulic conductivity based upon this relationship between clay swelling and hydraulic conductivity.

The empirical function relating clay swelling and hydraulic conductivity decreases can be expressed as a family of curves, each one representing a given exchangeable sodium percentage (ESP) for a given soil, McNeal (1968).

The empirical function is:

$$1 - y = cx^n / (1 + cx^n) \qquad (26)$$

in which:

y = relative soil hydraulic conductivity $\frac{K_i}{K_o}$. Dimensionless.

x = a swelling factor. Dimensionless.

c,n = constants for a given soil within a specified range of ESP values. Dimensionless.

Values of n in equation (26) have been found to depend primarily on the soil ESP. As a first approximation, acceptable n values are as shown in Table 2.

Table 2. Values of n for different soil ESP

	ESP<25	25<ESP<50	ESP<50
n	1	2	3

The values of c and x can be predicted from a knowledge of soil mineralogy and other soil properties. In practice, however, a common montmorillonite fractional content of 0.10 (10% montmorillonite on a whole soil basis) can be assumed for all soils. Any differences between the actual and assumed montmorillonite contents of the soil can then be incorporated into a multiplicative constant c':

$$c' = c\left(\frac{f_{mont}\ \text{actual}}{f_{mont}\ \text{assumed}}\right)^n \tag{27}$$

where f_{mont} = percentage of montmorillonite on a whole soil basis. The procedure can thus be used on soils for which no mineralogical information, or at best only qualitative information, is currently available. If enough information is available c' should be determined and used instead of c in equation (26).

Soils swell because they adsorb water. The mobility of soil-adsorped water is less than that of nonadsorbed water. As a result, swelling reduces the width of pore channels available to macroscopic flow. The magnitude of swelling depends upon the electrolyte concentration and composition of ambient solution. A modified 'domain' model w as used to develop the function for the swelling factor, x, in equation (26). In this model the interlayer swelling of montmoriollonite in mixed salt solution is described by assuming that Na-Ca montmorillonite consists essentially of homoionic regions containing either

Ca-clay or Na-clay with only the latter swelling as the salt concentration of the ambient solution is decreased.

$$x = (f_{mont})\ (ESP^*)(d^*3.6x10^{-4}) \tag{28}$$

where f_{mont} = montmorillonite fraction in total soil by weight; dimensionless

ESP* = adjusted ESP of soil, dimensionless

d* = adjusted interlayer spacing, Å

The adjusted ESP* = soil ESP - $(1.24+11.63\ \ln C_o)$ where C_o is the total salt concentration of the ambient solution in meq/l.

The adjusted interlayer spacing d* = 0 for $C_o > 300$ meq/l

and $d^* = 356.4\ (C_o)^{-1/2} + 1.2$ for $C_o < 300$ meq/l.

The constant is derived by using the average surface area of pure clay montmorillonite of 800 x 10^4 cm^2/g, the internal surface area of montmorillonite of 90% and using two surfaces per unit of interlayer spacing.

$$\frac{800x10^4 cm^2/g)(90\%)(10^{-8} cm/Å)}{(100)(2\ surfaces)} = 3.6x10^{-4}$$

In order to obtain C values for a soil the relative hydraulic conductivity can be measured first with a high salt-high SAR solution which should represent the maximum conductivity of the soil and also establish equilibrium between the ESP of the soil and the SAR of the solution. The soil can then be leached with a high SAR-low salt solution and hydraulic conductivity measured. With the latter solution appreciable interlayer swelling of the montmorillonite in the soil should have occurred. The calculated relative hydraulic conductivity values and calculated interlayer swelling can be substituted into equation (26) for values of n of 1, 2, and 3 to determine c values to be used

at various levels of soil ESP. Equation (26) with the calculated c values can then be used to predict relative hydraulic conductivity of the soil for any mixed salt solution for which an estimate of soil ESP is available.

Utilizing these relationships, the magnitude of the hydraulic conductivity which might be expected in a proposed irrigation canal could be evaluated if the chemical constituents of the proposed irrigation water were known. Also in existing canals where observed decreases from original values have occurred, the magnitude of the reduction in hydraulic conductivity due to soil-water-chemical reactions can be determined.

It should be pointed out that this procedure based on measured decreases of hydraulic conductivity will not differentiate between reductions caused by interlayer swelling which decreases flow path size and dispersion of soil clay and fine silt particles which move into conducting pore spaces. Both swelling and dispersion increase as sodium saturation increases and as salt concentration of the ambient solution decreases, Bodman and Fireman (1950) and McNeal, Norvell and Coleman (1966).

CHAPTER IV

PROCEDURE AND EQUIPMENT

The investigation was pursued in three phases. Laboratory studies on the prediction of sediment retention and the effects of sedimentation on hydraulic conductivity were examined in one phase. Soil-water chemical effects were studied in another phase and observations of microbiological effects were incorporated in both of the first two phases. Field experiments to evaluate in-situ changes in hydraulic conductivity in operating canals constituted the third phase.

Sediment Studies

Laboratory apparatus for this phase of the study included permeameters, constant head water supply system (Marriotte siphon), magnetic stirring devices for sediment suspensions, tensiometers, manometer board, gamma ray facility and other auxiliary equipment.

Apparatus

The permeameters were designed to measure hydraulic conductivity under both saturated and partially saturated flow. Water and sediments were introduced into the columns from the top. Tensiometers were used for measuring the pressure head and a porous plate was placed at the bottom to prevent air entry under tension, however, in this study, unsaturated hydraulic conductivity was not measured.

The columns were constructed of plexiglas plastic material and consisted of three sections, a top cap, a bottom cap, and a cylinder

connected with rubber gaskets and bolts as shown in Figure 4. The cylinders were 4.6cm (8-1/2 in) long made of 8.3cm (3-1/4) internal diameter clear plastic with .63cm (1/4 in) walls. Three 6.4cm (2-1/2 in) long, .47cm (3/16 in) diameter porous glass tensiometers were installed at approximately 6.7cm (2-5/8 in) intervals; twenty-liter glass carboys equipped with small glass air and outlet tubes were set on magnetic stirring devices and used as constant-head water supplies. The air tube was connected to an air filter which consisted of a 4.4cm (1-3/4 in) diamater plastic tube packed with sterilized cotton and Ascarite (sodium hydroxide coated with asbestos) as a CO_2 scrubber. Figure 5 shows a general view of the hydraulic conductivity measurement facilities.

The gamma ray facility included a gamma ray source (Isotope, Am-241, 100 millicuries), a detector (Model DS8-21, Nuclear-Chicago), a counter (main part: Model 33-10B, anti-walk, single channel analyzer, Radiation Instrument Development Laboratory) and an adjustable frame to focus the gamma ray source on any desired location. All equipment was housed in a constant temperature room, Figure 6.

Materials

Three size fractions of sand were prepared as porous media. A 50μ-150μ fraction was obtained from a blow sand area north of the Snake River near Kimberly, Idaho and 150μ-350μ and 350μ-500μ fractions obtained from sand from the "C" Canal of the Minidoka Irrigation District near Rupert, Idaho. The size fractions were obtained by dry and wet sieving and the material was then oven dried at 110°C for three days. Grain-size distribution curves from the mechanical analysis are shown

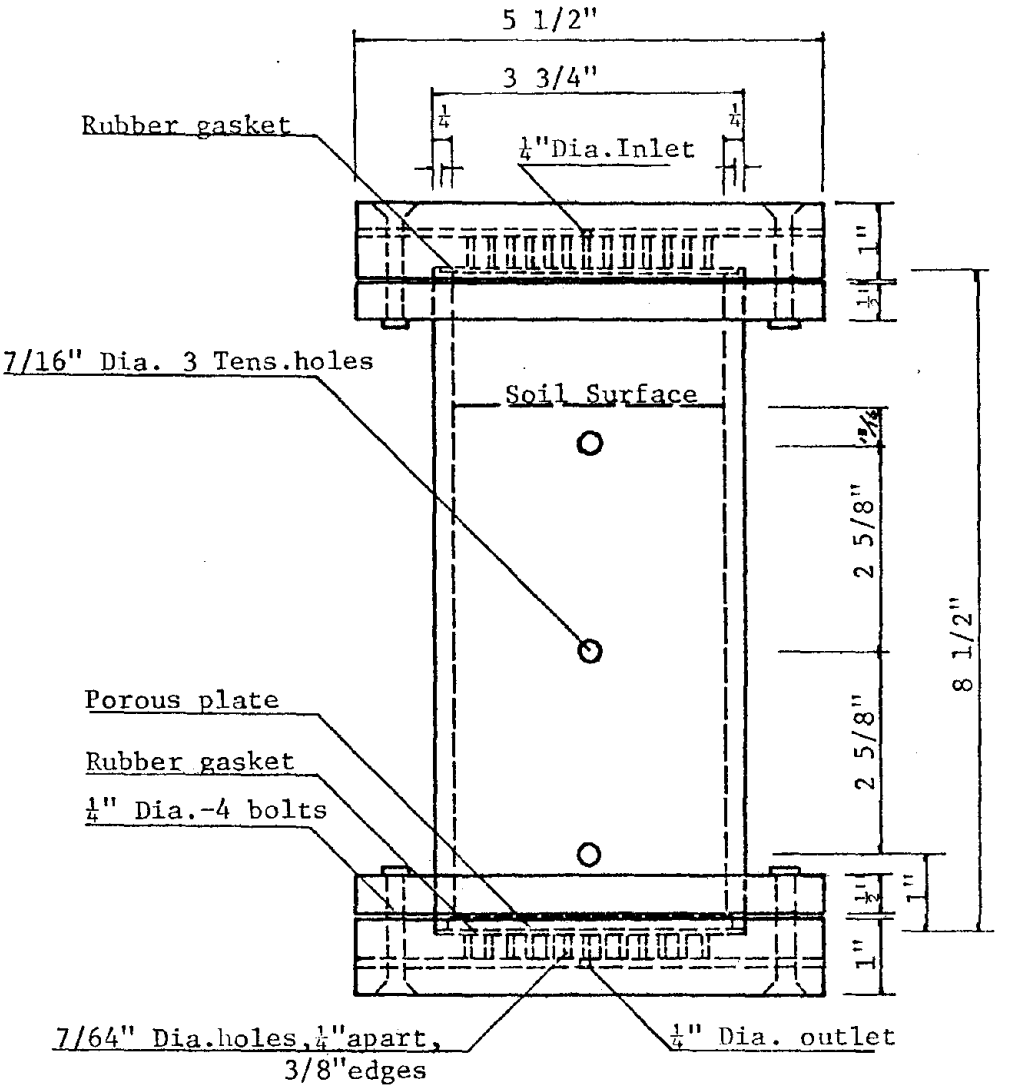

Figure 4. Permeameter construction

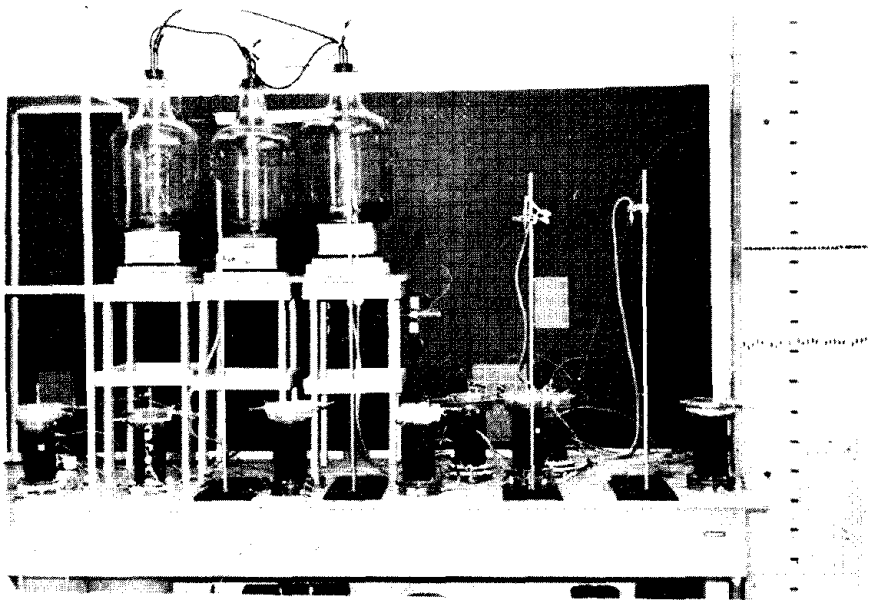

Figure 5 General view of hydraulic conductivity apparatus

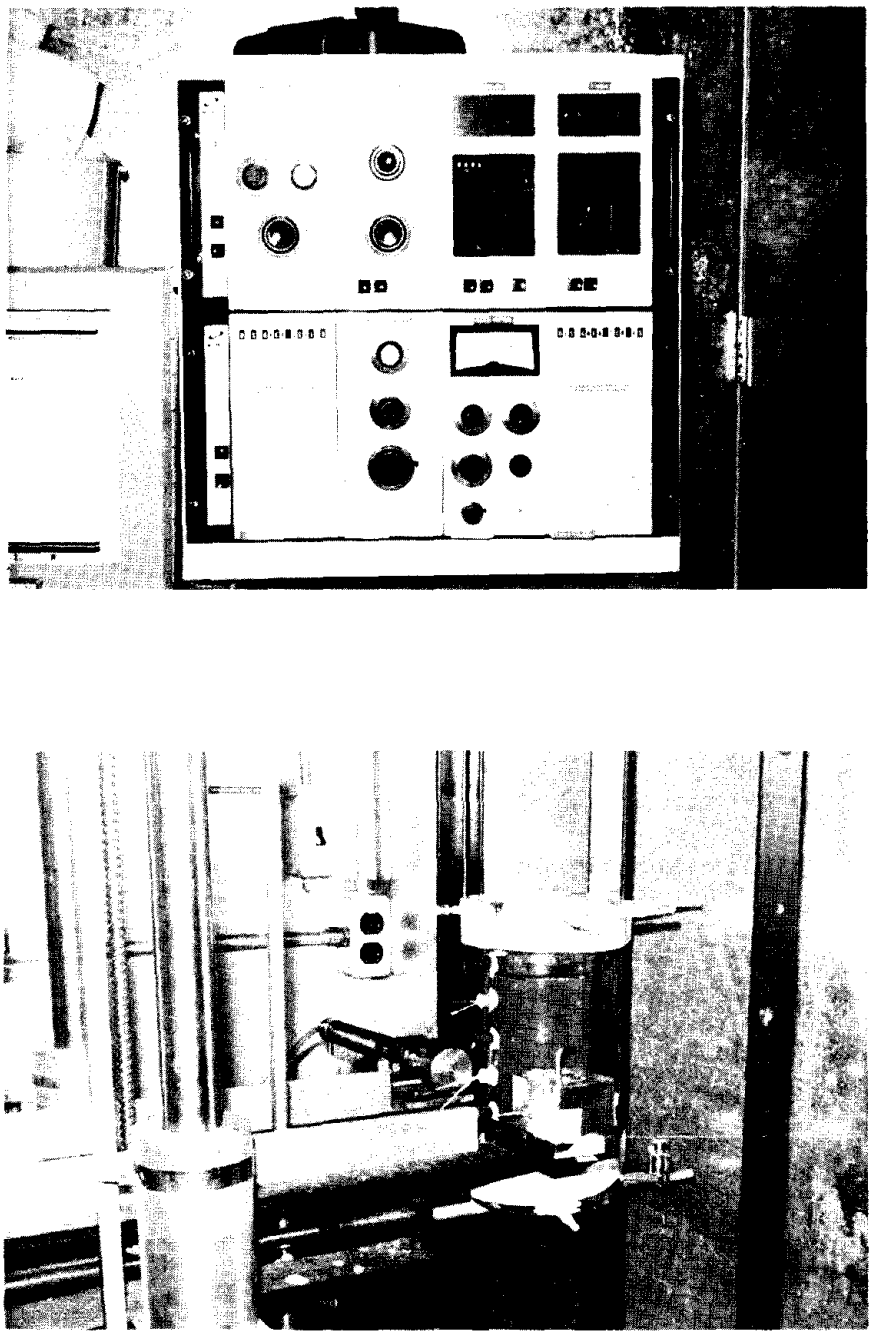

Figure 6 General view of gamma ray facility

in Figure 7. The particle density of each fraction was determined by pycnometer methods.

A milled fire clay obtained from the Denver Fire Clay Company was used as the sediment for this study. The material was fractionated into three size fractions, <2 , 2μ-5μ, and 5μ-10μ, with an elutriator, Beavers and Jones (1966).

Nine permeameters, three of each sand size, were packed with dry sand using a mechanical column packer with a rotating foot and vibrating base. The packer was fabricated from designs, suggested by Jackson, Reginato and Reeves (1962). Each column was scanned with the gamma ray apparatus and intensity measured at several locations to check for uniform density and the column was repacked if necessary. Tensiometers were installed by inserting the porous glass tubes horizontally into the pilot holes formed in the sand and secured to the permeameter wall with silicone rubber cement.

The nine columns designated by letter A through I with three size ranges of sediment were run in the laboratory. Table 3 shows the combinations of sand and sediment and corresponding column designations for each series of tests.

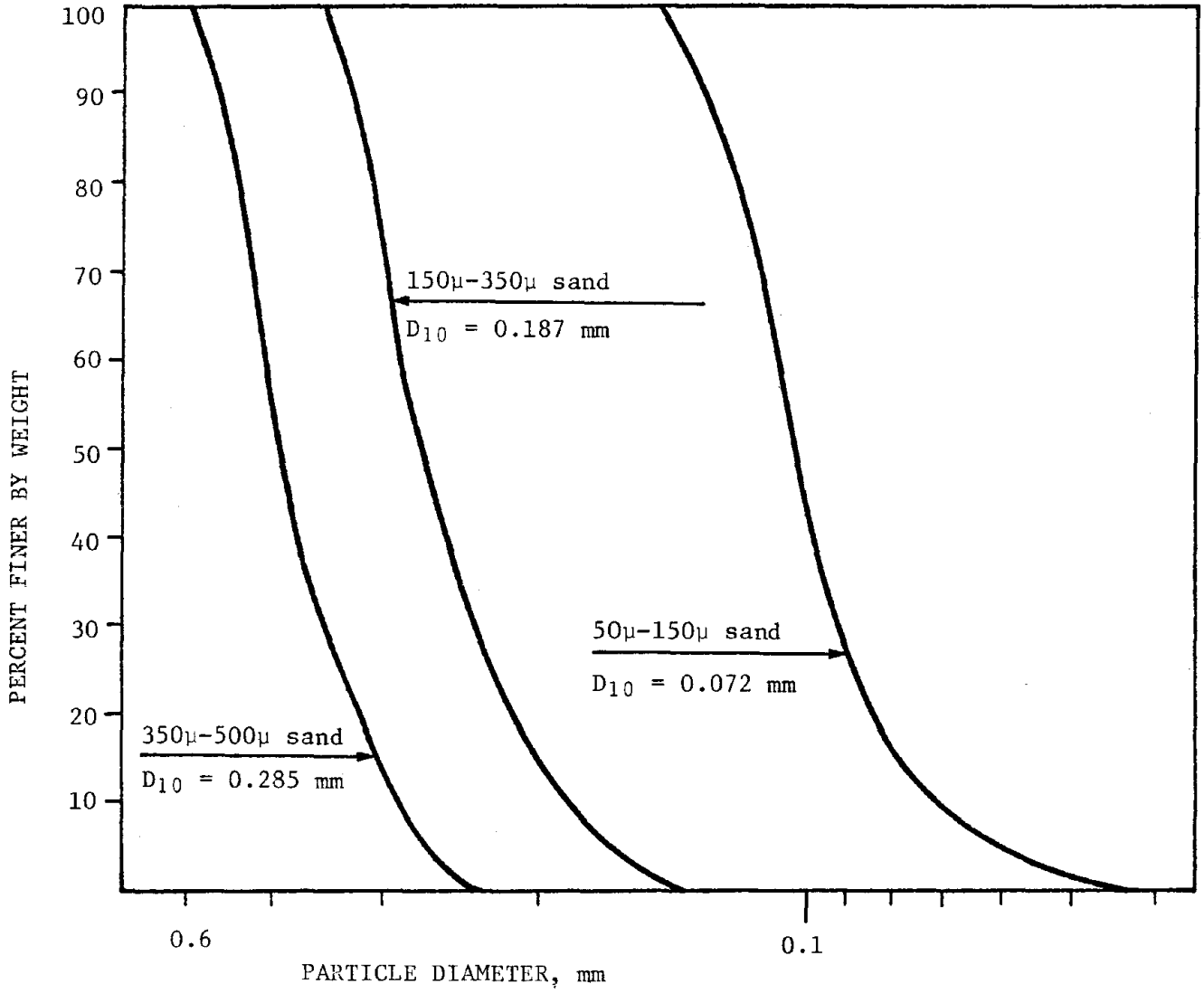

Figure 7. Grain-size distribution curves for sand

Table 3. Sand and sediment sizes - sedimentation tests

Series	Sand size μ	Sediment <2μ	2μ-5μ	5μ-10μ	Growth Inhibitor
I	50-150	A	B	C	Toluene
II	150-350	D	E	F	Phenol, Xylene
III	350-5-0	G	H	I	Commercial Germicide

Air was displaced from each permeameter by introducing carbon dioxide from the bottom. Distilled water was allowed to enter through the bottom of the permeameter and slowly saturate the media. Dissolved carbon dioxide was then leached out by reversing the flow into the permeameter.

Sediment and hydraulic conductivity

The saturated column was set in a frame and the gamma ray source was adjusted vertically and laterally to the desired location. The scanner settings, window, threshold, discriminator, range, and counting period were selected and fixed. Gamma ray intensity was measured at selected vertical intervals throughout the columns and the average count or intensity for the total column was calculated. In order to decrease Compton scattering and eliminate possible operational error, it was necessary to restrict the measurement to the highest energy peak of the gamma ray source and to lengthen counting periods if possible.

The experiments were conducted in an approximately constant temperature room, $22^{\circ}C \pm 1$. The temperature and the humidity were continuously recorded by a hygrothermograph. To determine hydraulic conductivity,

throughout the column, the hydraulic head was measured at each tensiometer location (see Figure 4), effluent was collected in a graduated cylinder and elapsed time was recorded for each determination. The electrical conductivity of the influent and effluent were measured. The discharge was increased by adjusting the level of the outlet until the differential between any two adjacent tensiometers was sufficiently large to allow an accurate determination of hydraulic conductivity.

It was observed that the sand surface started to seal periodically when the columns were run with distilled water. This also occurred with solutions of toluene, phenol, and other chemicals. A disproportionately high loss of head across the soil surface was indicated clearly by the manometers and the soil surface had a gummy appearance. Soil samples were taken from the top soil surface of columns E and F and series of microbiological tests were performed. (see the last two items in this chapter).

The hydraulic conductivity measurements were continued until the hydraulic conductivity remained constant and the electrical conductivity of the influent and effluent were the same. The last approximately constant hydraulic conductivity was used as the initial hydraulic conductivity, K.

After the initial hydraulic conductivity had been established, the glass carboys were filled with a solution of 500 ppm of sediment in distilled water with growth inhibitor added. The magnetic stirring device maintained the sediment in suspension. Hydraulic conductivity measurements were made at frequent intervals and visible phenomena were noted. The initial effluent in runs A and B appeared turbid so the sediments in the effluent were collected and separated in a centri-

fuge so that total sediment remaining in the column could be determined. The experiments were continued until the flow rates were lower than 1 ml/min.

The final hydraulic conductivity was determined using the procedure similar to that for the initial determination using distilled water. The purpose of this procedure was to observe the effect on hydraulic conductivity of sediment migration in the soil at the low flow rate. The experiments were stopped after a few days observation.

After the sediment runs, gamma ray attenuation was measured in the soil columns at the same locations as the initial measurements.

Calculation of sediment migration by gamma ray techniques

Before using equations (24) or (25) the mass absorption coefficient for all materials used and the original intensity of gamma ray sources must be known. The absorption coefficient depends on the radioactive energy source and varies widely with different materials. This constant is completely dependent of the environment, chemical combination, pressure, or temperature. Original intensity for a given material depends on the radiant source only. By scanning several pieces of the same material whose density and dimensions are known and plotting ln I, counting number, against x, thickness of material, straight lines with slopes, $-\alpha$, are produced. All lines for different materials intersect at one point on the ordinate which is zero thickness. This value of I is the original intensity, I_o, of the radiant source at a selected counting period. In this study, pieces of plexiglas, aluminum and steel were selected as materials to evaluate I_o (see Appendix A).

Before applying this technique for the measurement of the sediment

accumulation during the run, studies were carried out, using small short plastic columns containing dry or saturated soil with or without sediment to determine that the volume porosity could be substituted for linear porosity and that the equations derived for calculation of the amount of the sediment in the soil column were valid. These same columns were used to evaluate the mass absorption coefficients for dry soil and distilled water (see Appendix B).

The original intensity of the gamma ray source, I_o, and mass absorption coefficients, α, for all the materials used were calculated by using equation (21) and the results were as follows:

I_o = 298,000 counts (counting period 10 seconds)

α for plexiglas = 0.15993 cm^2/g

α for steel = 1.09612 cm^2/g

α for aluminum = 0.22007 cm^2/g

α for distilled water = 0.16821 cm^2/g

α for soil (sand) = 0.23743 cm^2/g

α for distilled water with 235 ppm toluene = 0.18476 cm^2/g

The deposit ratio, σ, is given by equation (25) as

$$\sigma = \frac{1}{(\alpha_s\rho_s - \alpha_w\rho_w)x_s} \ln \frac{I}{I_1}$$

in which the corresponding parameters for the experimental soil columns were:

α_s = 0.23743 cm^2/g for sand

ρ_s = 2.7294 g/cm^3 for 50μ–150μ sand

α_w = 0.18476 cm^2/g for distilled water with 235 ppm toluene

ρ_w = 0.99763 g/cm^3 for distilled water at temperature 22.7°C

x_s = 8.255 cm

Substituting these constants into the above equation and simplifying,

$$\sigma = \frac{}{3.828} \ln \frac{I}{I_1}$$

In the experimental columns the intensity, I, prior to the sediment run was measured as well as the intensity, I_1, after the sediment run. Substituting these values in the above equation, the amount of the sediment remaining in the soil at any depth was calculated.

Microbiological activity at the soil surface

For the purpose of minimizing the microbiological activity in the soil during the sediment run, several growth inhibitors were used in the distilled water. Growth still occurred on the soil surface as indicated by high head loss across the soil-water interface. Samples were taken from the soil surface of two columns, E and F, for microbiological tests. Tests were made for bacteria and algae. Soil samples of 0.2 g from column E and 0.15 g from column F were added to water blanks and three dilutions, 1/10,000, 1/100,000, and 1/1,000,000 were obtained. Three nutrient agar plates were made from each dilution. The media were incubated at a temperature of 34°C for one week. Bacteria numbers and other data are shown in Table 4.

The number of bacteria per unit gram of soil necessary to cause the reduction in hydraulic conductivity of 1 cm/day is:

Column E

$$N = \frac{39,000,000}{2,229} = 17,600$$

Column F

$$N = \frac{877,000}{502} = 1,750$$

Measurements indicated that all of the growth was bacterial, and

Table 4. Bacteria counts and hydraulic conductivity: surface layer of columns

Column	Bacteria Number per g of soil	Hydraulic Conductivity (cm/day) Initial	Final	Reduction	Period of run (days)	Solution	Condition
E	39,000,000	2326	97	2229	8	4 days:0.1% phenol 0.86% $CaSO_4$ 4 days:0.15% phenol	Without light
F	877,000	518	16	502	14	4 days:0.086% $CaSO_4$ 10 days:0.1% phenol 0.086% $CaSO_4$	With

no algae were present. In these two columns the number of bacteria per unit gram of soil necessary to cause the reduction in hydraulic conductivity of 1 cm/day differs by a factor of ten.

In the study of flow-associated reduction in the hydraulic conductivity of quartz sand by Gupta and Swartzendruber (1962), major reductions in hydraulic conductivity did not occur for numbers of bacteria below 400,000 per gram of sand. Above this number, drastic reduction did occur and, within a range of 400,000 to 700,000 bacteria per unit gram of soil, the ratio of hydraulic conductivity (K final/K initial) dropped sharply from near unity to nearly zero. Following their results using an initial K_1 value of 1.2 cm/min. the number of bacteria in the upper layers of sand causing a reduction in hydraulic conductivity of 1 cm/day is calculated as:

$$N = \frac{700,000 - 400,000}{1.2 \times 1,440} = 174$$

This value is considerably lower than the numbers found in this study showing that the reduction depends on other than the number of organisms.

The results show that 0.1% phenol solution is not effective for inhibiting microbial growth during the run for the conditions of room temperature 22°C and distilled water. High loss across the soil-water interface is caused by microbial growth.

Media especially prepared for algae showed no growth in tubes which had been incubated for one month.

Sterilization of soil columns

Several methods for sterilizing soil columns and inhibiting microbial growth in the soil were tested, such as propylene oxide under

vacuum and pressure treatment, 0.0235% toluene solution, 0.1% phenol solution, 0.2% xylene with emulsifier and 0.2% commercial instrument germicide. The commercial material was manufactured by the Lehn and Fink Industrial Products Division of Sterling Drug, Inc. and sold as an instrument germicide for cold disinfection of surgical and dental instruments. The propylene oxide treatment was used to sterilize a soil column before the run. This procedure of sterilization was effective, however, the plexiglas permeameters were softened by the chemical so this procedure could not be used. The results of experiments with other chemicals to inhibit microbial growth are outlined in the next section.

Soil-Water-Chemical Effects

Characteristics of Portneuf silt-loam soil

Soil samples for investigation of changes in chemical water quality on hydraulic conductivity were obtained from a section of the Unit A Main Canal of the A & B Irrigation District near Paul, Idaho. This canal with a capacity of 6.8 m^3/s (240 cfs) and a bottom width of 2.4 to 4.3m (8 to 14 ft) was chosen because of the deep soil profile and the fact that extensive field tests on seepage and water use had been performed by the University of Idaho and U. S. Bureau of Reclamation on this system.

Samples and a soil profile log to a depth of 1.72m (5.6 ft) were obtained from the right bank of a cut section of canal where the operating water depth was about 1m (3.3 ft). The canal is built in a Portneuf silt-loam soil. The primarily silt-loam soil with layers of moderate

to highly consolidated silt-loam through the profile is consistent through the area.

Three soil layers were chosen for study to determine differences in channel and hydraulic properties. The layers are designated as A(0.-61m); B(.61-1.07m); and C(1.07-1.60m). These layers do not correspond to the A, B, and C horizons in the soil profile description. The Portneuf silt-loam soil occurs throughout southern Idaho and many of the large canals and reservoirs have been constructed in these soils. The loessal soil covers large areas of the basalt plains and is generally light brownish grey to pale brown in the A and B horizons to light grey in the C horizon. These soils are generally noncalcareous in the A horizon but weakly to strongly calcareous on the lower horizons. A lime-silica hardpan generally occurs at less than 1.0m (3.3 ft) depth. The soil chemical properties and mechanical analysis of the three soil zones and a mixed profile are given in Tables 5 and 6.

Table 5. Chemical properties of Portneuf silt-loam soil

Layer	pH[1]	Exchangeable Cations, meq/100g			meq/100g	ESP	EC[2]	Cations[3] (Sat. Ext.) meq/l		
		Ca + Mg	Na	K				Ca + Mg	Na	K
A	7.7	14.4	1.43	0.29	16.0	8.94	0.91	6.1	1.75	.19
B	7.9	9.9	1.12	0.20	11.3	9.91	0.73	6.0	0.98	.15
C	8.2	8.2	1.17	0.19	9.6	12.2	0.85	6.5	0.94	.15
Mixed M	7.9	9.2	1.44	0.20	10.9	13.2	0.77	6.5	1.54	.16

1 pH of saturated soil paste.

2 Electrical conductivity of saturation extract at 25°C in millimhos/cm.

3 EC and Ca + Mg are from analyses of Portneuf soil from SRCRC, Kimberly, Idaho.

Table 6. Particle size analysis - Portneuf silt-loam soil

	Sand	Silt	Clay
Layer	750μ	2.50μ	<2μ
A(0-.61m)	16.4%	62.0%	21.6%
B(.61-1.07m)	17.4	69.0	13.6
C(1.07-1.60m)	20.4	72.0	7.6

Minerological analysis of the Portneuf silt-loam soils in southern Idaho have been performed by the University of Idaho Soils Department. The clay fraction minerology expected for the Portneuf silt-loam used in these studies is shown in Table 7. The analysis shown is for a Portneuf silt-loam near Pocatello, Idaho area, however, major differences between these soils and the same series near Paul, Idaho are not expected[1/].

Hydraulic conductivity with high and low salt solutions

Plexiglass perameters, 8.5cm long and 3.2cm I.D. were fitted with 20 mesh copper screen at the bottom with a fibreglass matting over the screen. Portneuf silt-loam soil was packed to a depth of 2.6cm in each permeameter and dried <0.1mm soil was introduced through a funnel keeping the end of the funnel just above the top of the soil and rotating the end of the funnel around the permeameter to minimize particle segregation. The soil was covered with a 500 g weight and each permeameter dropped 200 times through a distance of 2.5cm. A layer of fibreglass

1/ Personal communications with Professor G. C. Lewis, Department of Soils, University of Idaho.

matting was placed on top of the compacted soil to prevent erosion by the impinging water during hydraulic conductivity tests.

Table 7. Clay fraction minerology - Portneuf silt-loam soil

	Percent	
	Course Clay	Medium and fine clay
Montmorillonite	7-10	38-40
Kaolinite	8-12	4
Illite	79-80	58-60

Air was displaced from the compacted soil by passing CO_2 through the column for 15 minutes. A high salt-high sodium solution (Solution No. 1, C_o = 500 meq/l, SAR = 100) was introduced and the maximum hydraulic conductivity of the soil measured. Twenty samples, 6 of layers A and B and 8 from layer C, were run simultaneously. A constant hydraulic gradient of 2.0 was maintained on each permeameter and hourly measurements of effluent volume were made until the rate was constant for four or six hours. Temperature was maintained at $24^{\circ}C \pm 1$ and temperature and humidity were continuously recorded.

Following the determination of the maximum hydraulic conductivity with solution No. 1, the same procedure was repeated using a low salt-high sodium solution (solution No. 2, C_o = 50 meq/l, SAR = 100). Both solutions contained 40 ppm $HgCl_2$ to inhibit microbiological activity.

Average relative hydraulic conductivity $y = K_i/K_o$ was calculated for each of three values of c using equation (26) and n values corresponding to three ESP ranges, Table 2. The c values were then used to

predict hydraulic conductivity decreases for each layer assuming salt concentration of 1, 5, and 10 meq/l for the Portneuf silt-loam soil.

Hysteresis effects

To examine the reversibility of the hydraulic conductivity decreases, hydraulic conductivities of nine columns (3 of each layer) which had previously been brought to equilibrium with solution No. 2 were run with three different solutions. Three columns were run with a high salt solution 0.5N $CaCl_2$, SAR = 0 , three with distilled water, and three with normal irrigation water. Each column was run for 5 days until equilibrium was achieved.

Variation of hydraulic conductivity with time - irrigation water

The variation with time of hydraulic conductivity of the Portneuf silt-loam soil was examined by measuring the conductivity of each layer with irrigation water over a two month period.

Cylindrical permeameters of 8.2 cm I D plexiglass, 19.5cm in length were fitted with sections of 20-mesh copper screen in the bottom and covered with fibre glass matting. The screen was supported 1.2cm above the bottom of the cylinder by a series of plastic strips radially oriented to channel the effluent water toward the center outlet pipe which was 0.6cm I D and 2.5cm long. Each cylinder was filled and compacted to approximately 7.4cm depth with sieved soil <2mm in the same manner as used previously. Table 8 shows the dimensions and bulk density of each sample.

The solution used for this series of tests was Snake River water obtained from an irrigation ditch near the Snake River Conservation Research Center Laboratory. Previous chemical tests have shown this

source to be of the same chemical quality as that pumped from the Snake River for use on the A & B Irrigation District. Table 9 shows a water analysis for the solution used in this series of tests.

Table 8. Soil column characteristics - soil-water-chemical effects

Layer	Column	Weight g	Length cm	Bulk Density $\rho(g/cm^3)$
A	1	541	7.40	1.38
	2	541	7.35	1.39
	ST1	541	7.30	1.40
	ST2	539	7.50	1.36
B	1	570	7.40	1.46
	2	570	7.35	1.47
	ST1	542	7.40	1.39
	ST2	567	7.50	1.43
C	1	574	7.40	1.47
	2	574	7.35	1.48
	ST1	571	7.50	1.44
	ST2	574	7.50	1.45
M	1	564	7.40	1.44
	2	564	7.35	1.45
	ST1	556	7.60	1.39
	ST2	566	7.50	1.43

Duplicate soil columns of the three layers, A, B, and C and a mixture of the three layers were instrumented, saturated with CO_2 and then wetted with the irrigation water solution. A constant head was maintained by use of a Marriotte siphon and saturated hydraulic conductivity measured periodically over a two month period during which the columns were run continuously. Room temperature was maintained at $24^{o}C \pm 1$.

The initial conductivity was considered to be the conductivity measured one hour after the columns were wetted.

Table 9. Chemical analysis - Snake River water

Conductivity, EC x 10^6 @ 25°C	455
SAR	0.46
Percent sodium	14.0
Suspended solids, ppm	70
Hydrogen-ion activity (pH)	8.3
Cations, meq/liter	
Calcium (Ca)	2.54
Magnesium (Mg)	1.23
Sodium (Na)	0.63
Potassium (K)	0.10
Anions, meq/liter or ppm	
Carbonate (CO_3)	0
Bicarbonate (HCO_3)	3.25
Sulfate (SO_4-S), ppm	14
Chloride (Cl)	0.61
Nitrate (NO_3-N), ppm	0.06

Four weeks after the beginning of measurements the top 4mm of soil from each column was removed and the measurements continued for another four weeks.

Variation of hydraulic conductivity with time - filtered irrigation water with sterile soil

Eight soil columns identical to those in the previous series were prepared except that the soil was autoclaved for 24 hours for sterilization. The irrigation water was filtered to remove suspended particles and 40 ppm $HgCl_2$ added to inhibit biological activity. Physical properties of these columns are outlined in Table 8, Columns ST1 and ST2. The hydraulic conductivity was measured for about three weeks until it had stabilized. The top 4mm of the columns in this series was not removed as in the previous series.

Undisturbed soil column studies

In order to determine whether the results of hydraulic conductivity measurements on disturbed columns and subsequent estimation of hydraulic conductivity decreases due to clay swelling were applicable to in-situ soils, several undisturbed soil cores were obtained from the Unit 'A' Canal. The 8.26cm (3 1/4 in) diameter cores were taken from the centerline of the canal using an auger type sampler, Hayden and Heineman (1967). The relative elevation of the bottom of the invert of the canal at this station would place it at approximately the same elevation as the B layer of soil used in the soil-water chemical effects experiments. A typical core taken at Station 148+00 was 18.5cm long taken through the soil surface on the canal invert and contained a distinct top layer of darker material about 2.7cm thick. Core No. 2

was 15cm long and was taken vertically at station 134+00 after removing the top 3cm of soil. Each core was wrapped in several layers of "Saran" wrap immediately after removal and stored in cardboard cylinders until used. Core No. 2 was run about one year after Core No. 1. These two cores were taken from typical profiles in the canal bottom and exhibited responses representative of all other cores.

Both cores were encased in shrinkable plastic tubing, Bondurant, Worstell, and Brockway (1969), instrumented with 3.2mm diameter porous glass tensiometers at three levels and saturated with CO_2. Columns were saturated with tap water and hydraulic conductivity determined with Snake River water taken from Station 0 + 00 of the Unit 'A' Canal. Saturated hydraulic conductivity only was measured in each section of the column until equilibrium had been reached.

CHAPTER V

RESULTS AND DISCUSSION

Sedimentation

Hydraulic measurements

Because of difficulties in retarding microbiological growth in Series II and III columns (see table 3), full sedimentation tests were performed on only three columns in Series I. Results of the Series I tests were as follows:

Column A. The flow rate prior to the introduction of sediment was 6.30 ml/min. The effluent appeared turbid during the early hours indicating that the sediment penetrated both the soil and the porous plate which was placed at the bottom of the column. After seven hours the flow rate decreased to 1.30 ml/min and at this time the effluent appeared clear indicating no sediment passing through the porous plate. When the flow rate was low (about 1 ml/min or lower), the calculation of hydraulic conductivity was not possible as almost the entire loss of head occurred at the soil surface and at the bottom across the porous plate, and the difference of pressure head across the second and third layers became negligible. High loss of head occurred at the surface and the bottom indicating that most of the sediments were retained at the soil surface and porous plate. After the sediment run, clear distilled water was run through for several days. No indication of sediment migration in the soil was possible because the head loss across the second and the third layers was near zero, and no sediment migration showed at the top layer.

Figure 8 shows the hydraulic conductivity for column A prior to sediment introduction. Conductivity stabilized after about 300 pore volumes of effluent had passed through the column. However, during the stabilization period the hydraulic conductivity of the top layer decreased to about 20 percent of the initial value. Figure 9 shows the effect on hydraulic conductivity of sediment introduction and flushing with distilled water on Column A.

Column B. The initial flow rate was 9.42 ml/min. The effluent appeared turbid until the flow rate decreased to 5.4 ml/min, approximately 3 hours from starting, indicating that during high flow rates some sediments still penetrated both the soil and the porous plate. During low flow rates no calculation of hydraulic conductivity was possible because of low head differentials. High loss of head still occurred at the surface and the bottom of the soil, but the loss of head across the porous plate and the bottom 2 cm of soil was not as high as in Run A, which indicated that sediments retained at the plate were much less than in Run A. During the distilled water run, the hydraulic conductivity at the top layer increased slightly indicating that some sediments originally retained in this layer were migrating down. At this time, the flow rate was apparently large enough to produce shear forces sufficient to dislodge some sediments and transport them along the column. No observation was possible in the second and third layers because the head loss across these layers was too small.

Figures 10 and 11 show the hydraulic conductivity for Column B prior to and during the introduction of sediment. Initial reductions in hydraulic conductivity prior to sedimentation were similar to Column A.

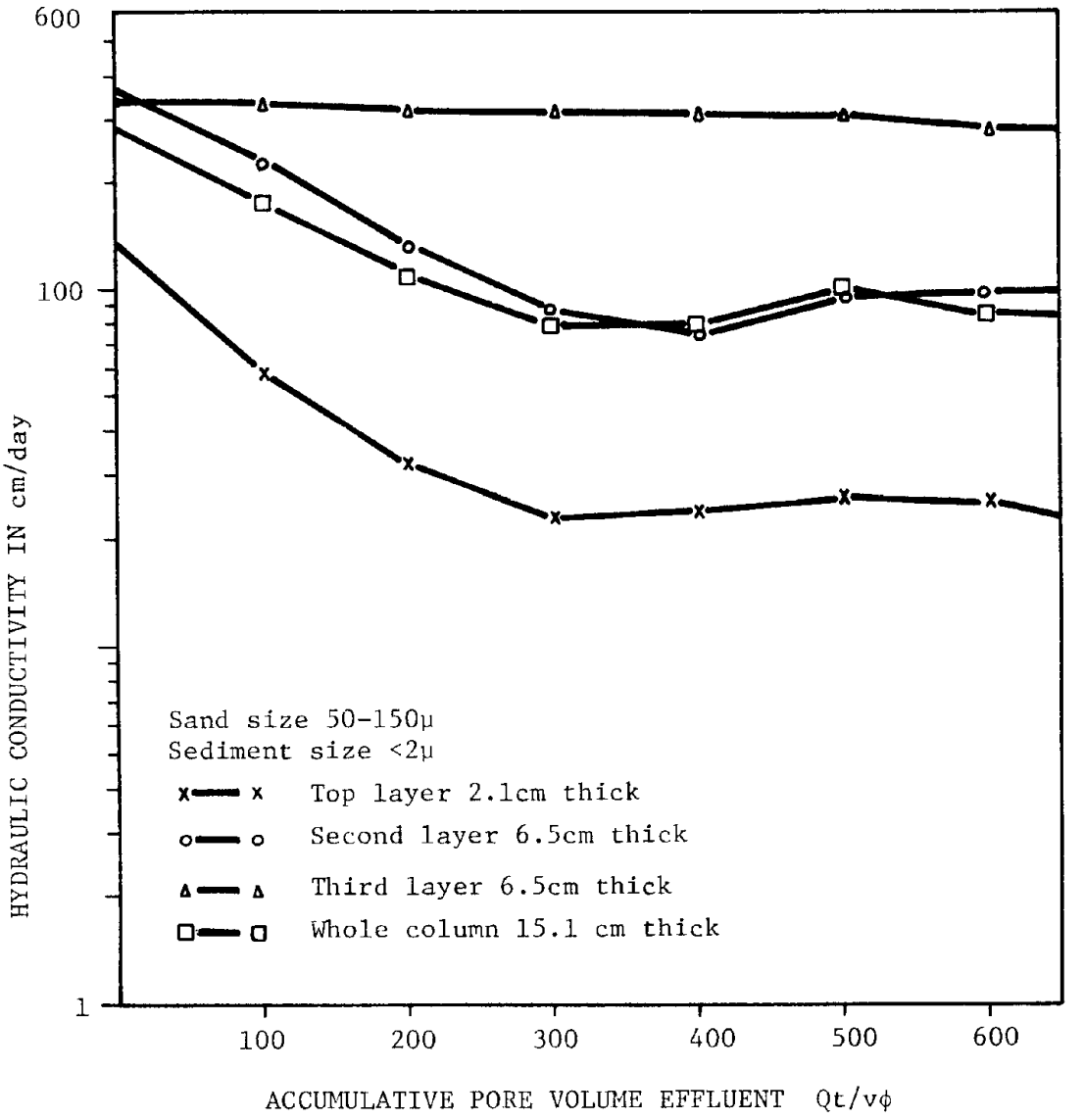

Figure 8. Variation of hydraulic conductivity with accumulated pore volume effluent - Series I Run A

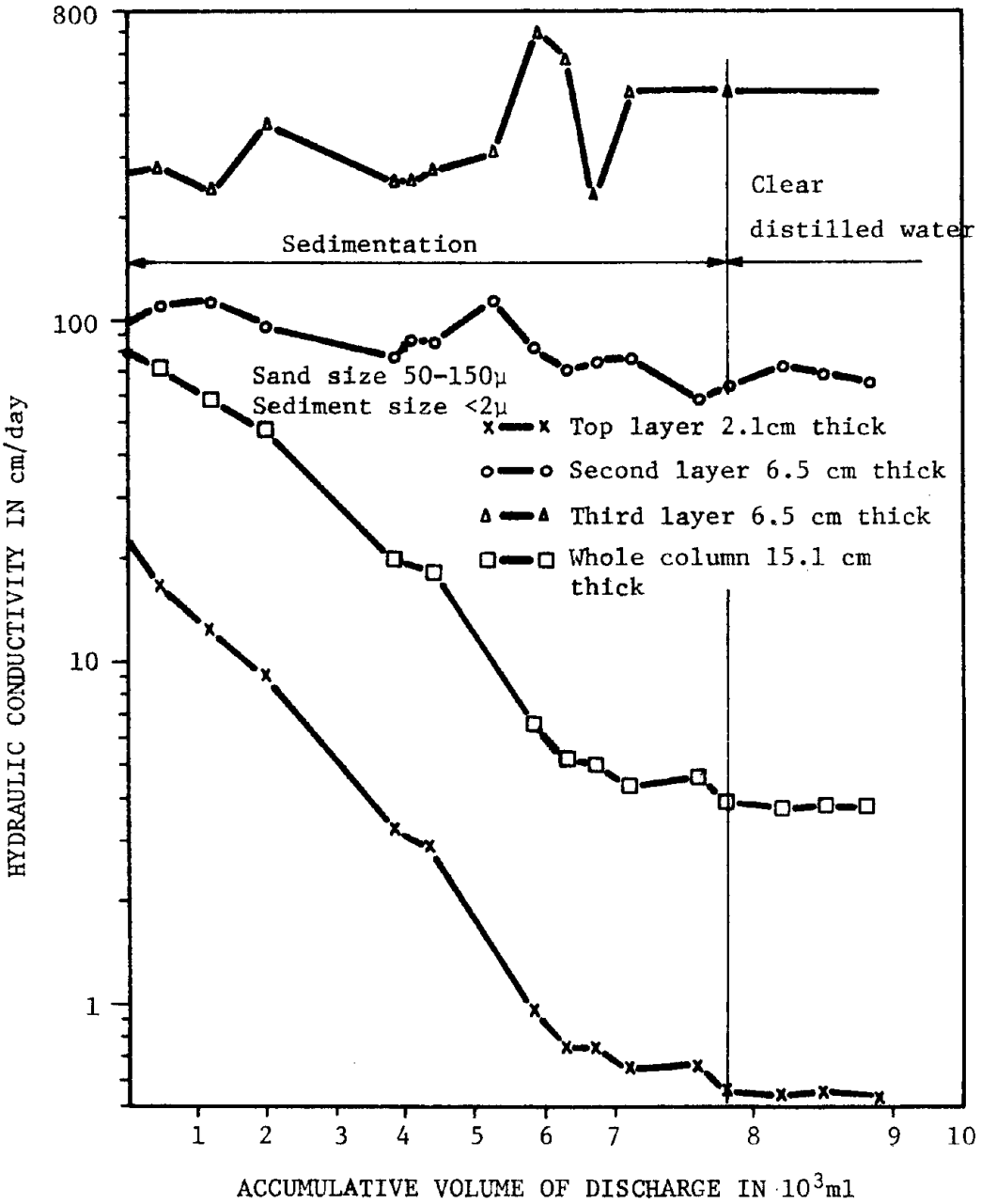

Figure 9. Variation of hydraulic conductivity with accumulated volume of discharge in sedimentation Series I Run A

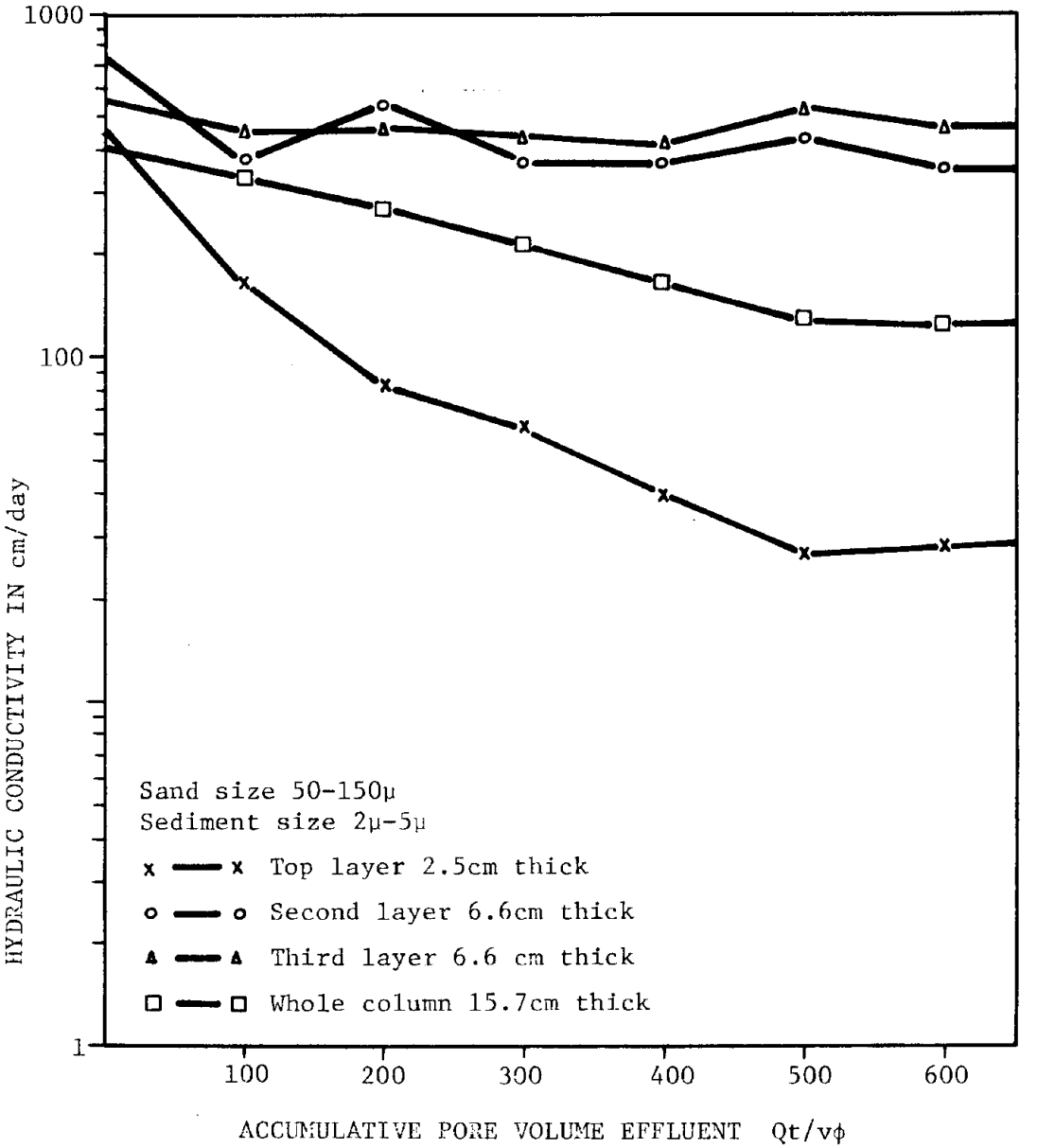

Figure 10. Variation of hydraulic conductivity with accumulated pore volume effluent Series I Run B

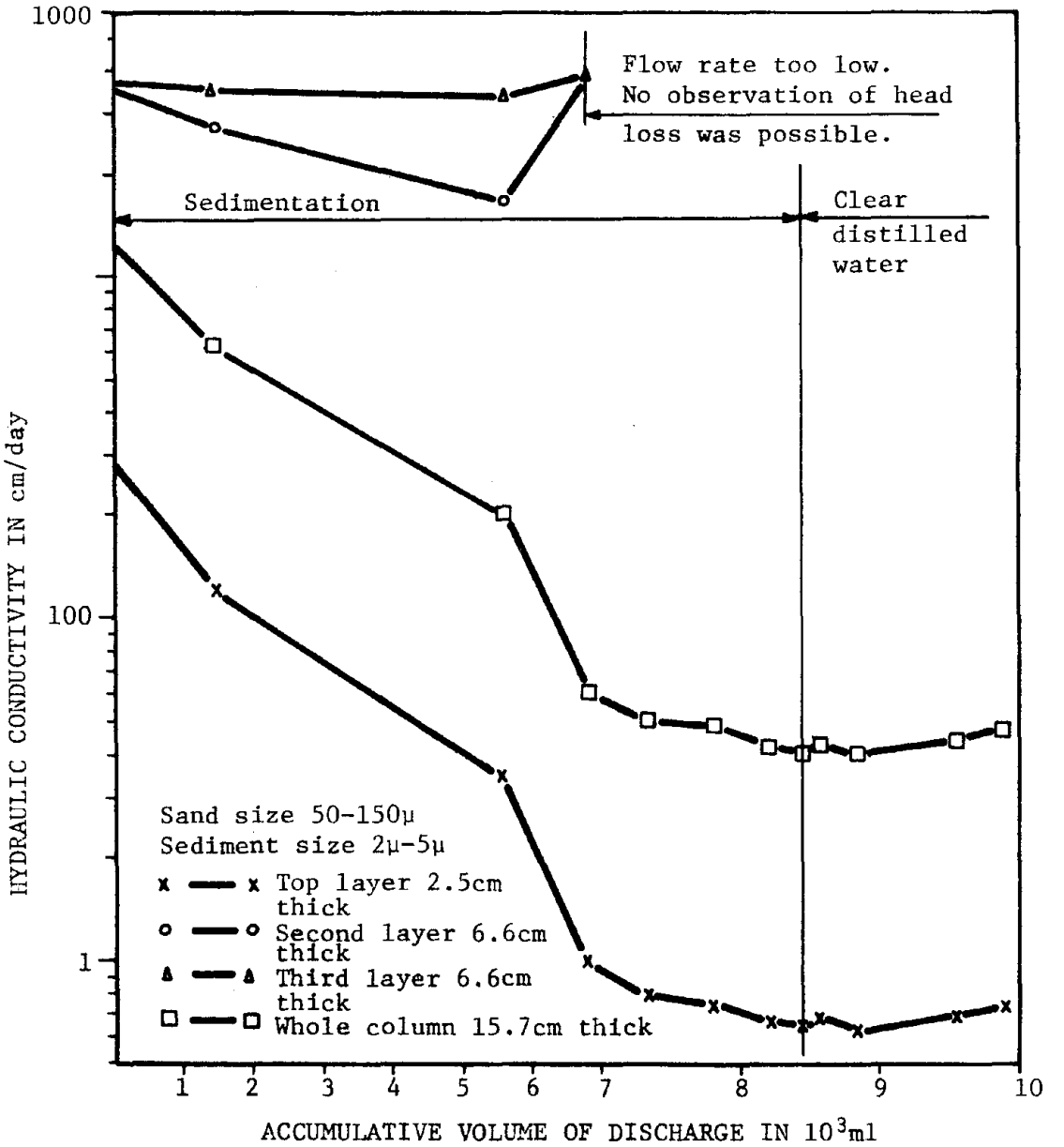

Figure 11. Variation of hydraulic conductivity with accumulated volume of discharge in sedimentation Series I Run B

Column C. The initial flow was 9.53 ml/min. The effluent remained clear at all times during the run, indicating no sediment passing through the porous plate. As in runs B and C, high head loss occurred at the surface. Head loss across the porous plate remained constant, proportional to the flow rate indicating no sediment retained at the plate. During the distilled water run, the hydraulic conductivity in the whole column increased slightly indicating some sediment migration in the soil.

Figures 12 and 13 are the results of hydraulic conductivity measurements on Column C.

Table 10 is a summary of hydraulic data for the sedimentation tests and Figure 14 shows a graphical comparison of hydraulic conductivity reduction in the total column due to sedimentation for columns A, B, and C.

Gamma ray scanning

Results of gamma ray scanning of the Series I columns before and after sedimentation are shown in Table 11. Table 12 shows a summary of sediment retention estimates in the Series I columns computed from hydraulic conductivity measurements and measured by gamma ray scanning. Figure 15 is a plot of measured sediment distribution in the soil columns determined by gamma ray analysis.

Several procedures for retarding microbiological growth were used including toluene, phenol, xylene, and a commercial germicide solution in the influent water. Results of the individual trials and procedures indicate that some solutions, namely .0235% toluene and .1% phenol either did not dissolve completely in the water and caused sealing of the soil surface or the concentrations were not adequate to retard

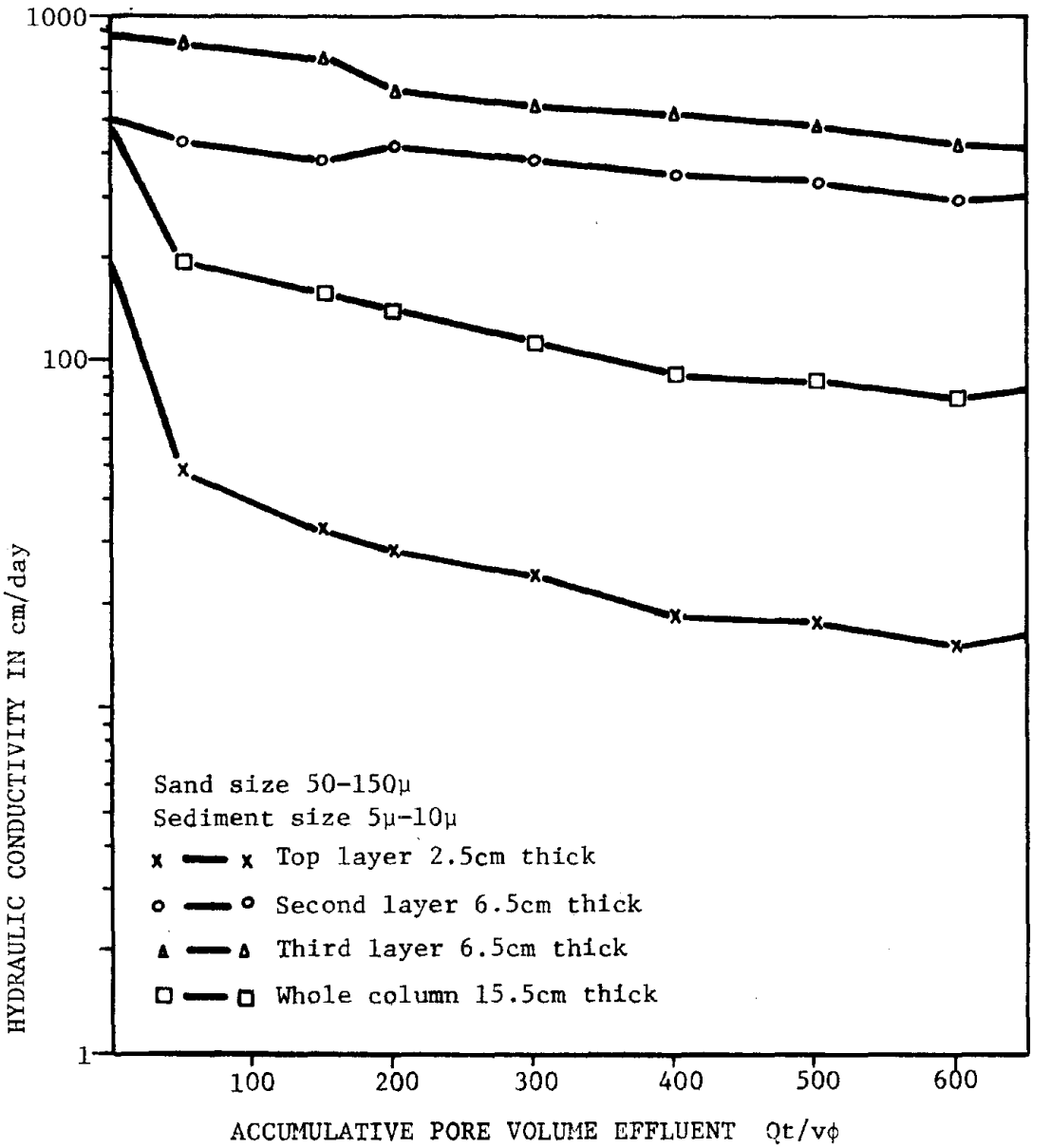

Figure 12. Variation of hydraulic conductivity with accumulated pore volume effluent Series I Run C

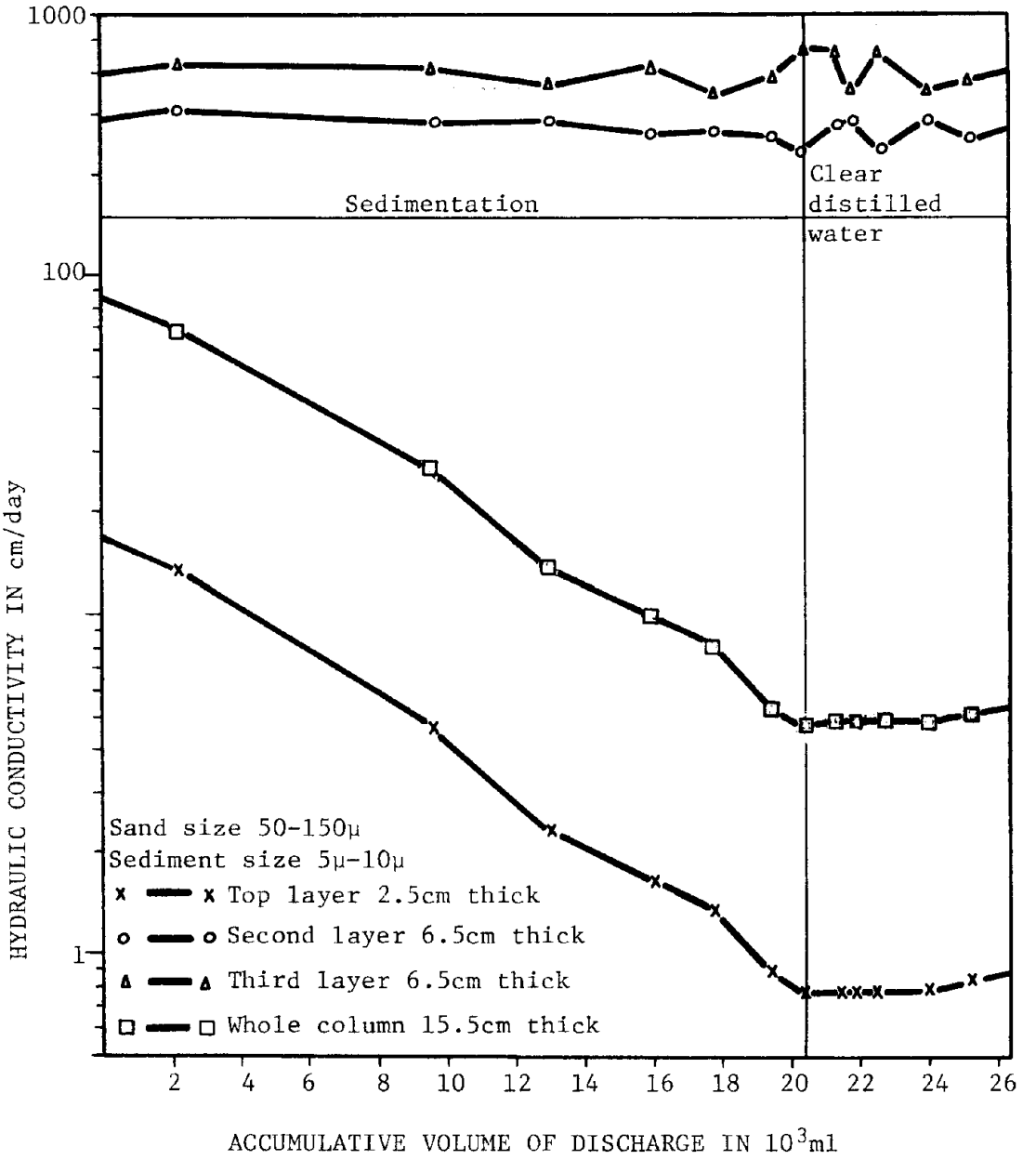

Figure 13. Variation of hydraulic conductivity with accumulated volume of discharge in sedimentation Series I Run C

Table 10. Summary of hydraulic data - sedimentation tests

	Run No. A	Run No. B	Run No. C
Sand size (μ)	50 - 150	50 - 150	50 - 150
Sediment size (μ)	<2	2 - 5	5 - 10
Sand particle density	2.7221	2.7221	2.7221
Dry bulk density	1.653	1.649	1.651
Porosity of soil column	0.3927	0.3942	0.3935
Initial hydraulic gradient	1.212 (2.16)**	0.735 (2.075)**	0.705 (3.10)**
Sediment concentration (ppm)	500	500	500
Sedimenting time (hrs)	192	144	145
Initial flow rate (ml/min)	6.30	9.42	9.53
Final flow rate (ml/min)	0.22	0.25	0.80
Hydraulic conductivity (cm/day):			

	A Initial	A Final	A Reduction%	B Initial	B Final	B Reduction%	C Initial	C Final	C Reduction%
top 2cm layer	21.66	0.56	97	27.98	0.64	98	15.82	0.88	94
next 6cm layer	97.56	87.58*	10	344.55	167.71*	51	295.75	260.29	12
next 6cm layer	272.86	252.45*	7	866.61	335.42*	9	429.94	390.43	10
whole column	80.69	3.95	95	124.11	4.12	97	79.40	5.40	93
Visible phenomena in effluent	Turbid effluent for 7 hours after start of sediment run			Turbid effluent for 3 hours after start of sediment run			No turbidity in effluent		

* This was the value measured when the flow rate was slightly greater than 1 ml/min
** Gradients in parentheses include the top soil surface

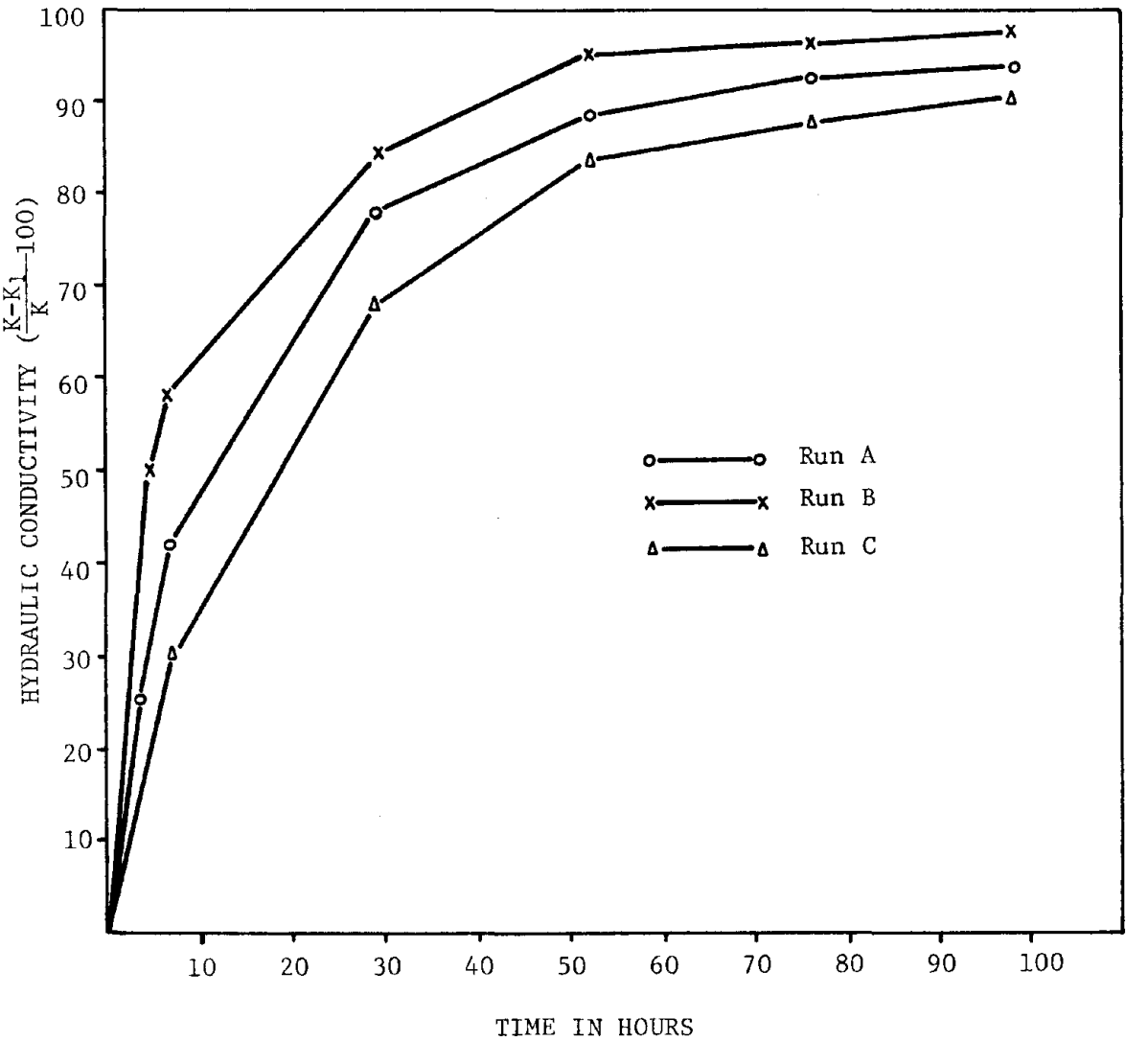

Figure 14. Comparison of hydraulic conductivity reduction between three experimental soil columns after sedimentation

Table 11. Gamma ray data on sediment columns

Settings of gamma ray scanner: Window 0.00, Threshold 035, Range 5 x 10^5 Discriminator 5.00, Counting period 100 seconds.
Counts (gamma ray intensity) = Average of 10 counting periods.

Room temperature = 22.7°C

Run	A		B		C	
Sand (μ)	50 - 150		50 - 150		50 - 150	
Sediment (μ)	<2		2 - 5		5 - 10	
Distance* (cm)	Sediment run Before	After	Sediment run Before	After	Sediment run Before	After
1	47052	47013	47264	44993	45684	44900
3	42106	40868	42910	40379	44286	42851
5	41236	40363	42562	40368	45489	43596
7	41818	40460	42545	40456	44924	42858
9	41222	40780	42576	40286	45624	42688
11	41725	40394	41968	40172	46702	45330
Average count of total column	42526	41468	43304	41108	45451	43704

* Distance is measured below the soil surface in the column.

microbiological activity at room temperatures. Xylene with emulsifier in concentrations normally used in operating canals for moss control caused both the surface and the porous plate at the bottom of the column to seal. A 0.2% solution of commercial instrument germicide caused the hydraulic conductivity of the sand column to remain constant but caused high head loss across the porous plate.

The results of sedimentation trials point out the significance of the ratio of sediment size to media size in influencing the penetration

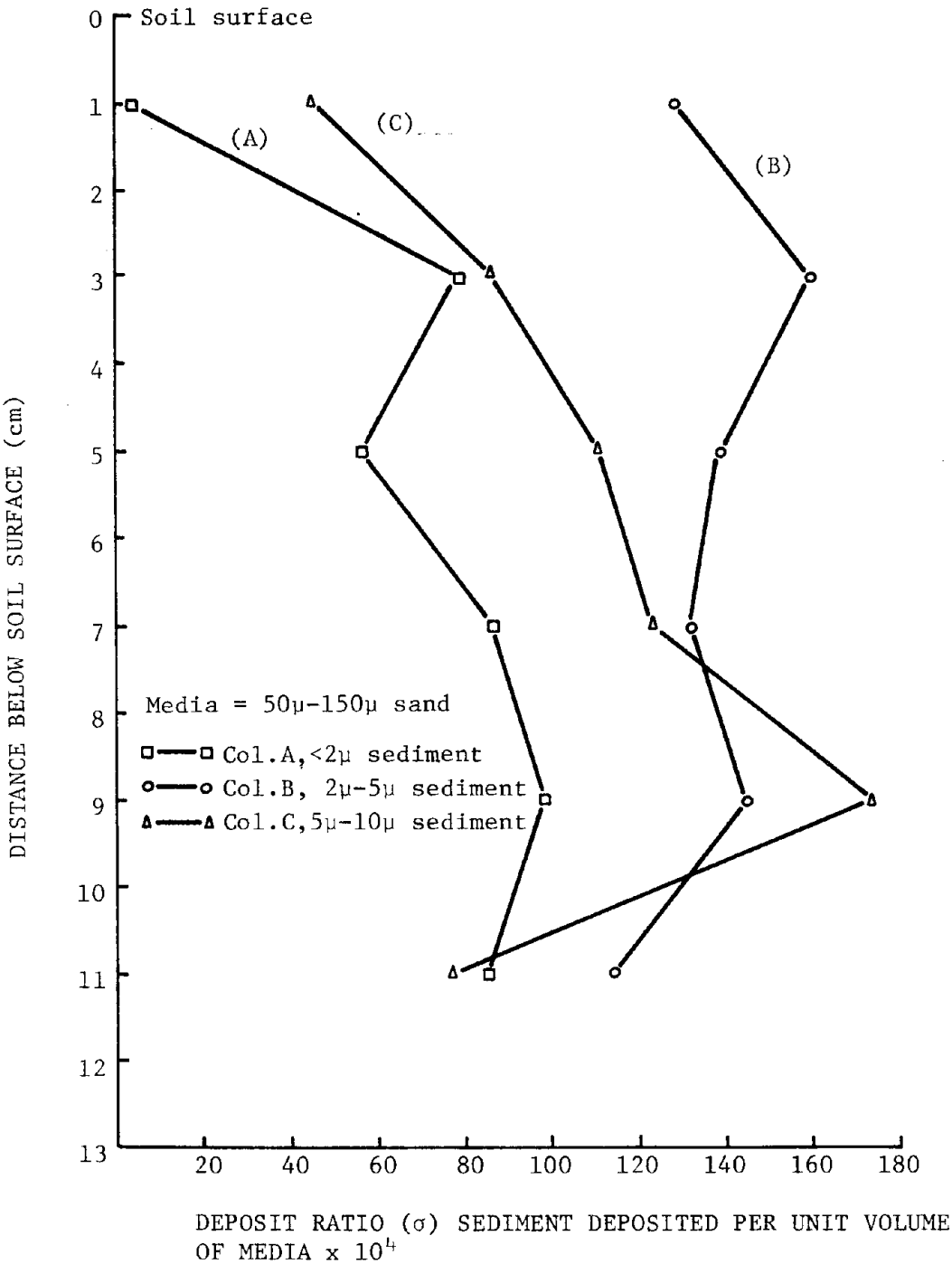

Figure 15. Distribution of the sediment retained in soil columns by gamma ray analysis

Table 12. Summary of sediment retention analysis

Item	Run No. A	B	C
Sediment size (μ)	<2	2 - 5	5 - 10
Total weight of sediment introduced into soil column	4.59	4.04	4.67
Percentage of total sediment remaining above soil surface (%)	24.62	51.24	67.88
Percentage of total sediment passing soil surface (%)	75.38	48.76	32.12
Weight of sediment retained in the soil column at 1cm to 11cm below the soil surface	0.94	1.80	1.50
Percentage of voids filled with sediment (%)	1.13	2.16	1.76
Head loss caused by sediment at the bottom of the soil and porous plate (cm/unit flow rate)	380	94	14
Deposit ratio by Eq. (11), Stein's Equation			
Average, 2cm to 8.5cm below soil surface	.0076	.0128	.0606
Average, 8.5cm to 15cm below soil surface	.0140	.0092	.0089
Deposit ratio by Eq. (25)			
Average, 2cm to 8.5cm below soil surface	0.0141	0.0842	0.0164
Average, 8.5cm to 15cm below soil surface	0.0101	0.0115	0.0124
Deposit ratio by gamma ray analysis (volume/unit of soil volume)			
Average value from 3cm to 9cm below the soil surface	0.0079	0.0143	0.0124
Average value from 9cm to 11cm below the soil surface	0.0091	0.0129	0.0126

and retention of sediment within the matrix. It is unfortunate that Series II and III columns could not be tested for sediment retention, however, results for Series I are gratifying.

In Column A it was observed that no sediment penetrated the bottom porous plate when the flow rate decreased to 3.0 ml/min indicating the dependency of sediment movement on pore velocity and resulting shear forces. Although 75% of the applied <2μ sediment in Column A passed into the sand, only .94 g or 27% of the sediment entering the sand remained in the top 11cm of the column, Table 12. The amount of sediment was sufficient to fill only 1.13% of the voids in this length of column. High head loss across the bottom of the soil column and porous plate also indicates the migration of most of the sediment to the lower areas of the column and retention on the porous plate.

Determination of the sediment deposit ratio by gamma ray analysis shows that only about half as much sediment was retained in this soil column as compared with runs B and C using larger sediment. Although the hydraulic conductivity of the entire soil column was reduced 95% from the initial value, most of the reduction was in the surface layer. Figure 12 shows that hydraulic conductivity of the top layer decreased significantly and the rate of decrease is greater than for the other columns indicating that the <2μ size sediment produces an effective sealing layer as it accumulates on the surface. In this run therefore the sediment introduced formed two main layers, one above the soil surface and one at the bottom above the plate. The <2μ sediment is too small for penetration and retention in the profile for the 50μ-150μ media. No migration of sediments was apparent at the top layer during

the final distilled water run, probably because the flow rate was too low (0.2ml/min) to move the sediments down.

In Column B sediment initially penetrated the porous plate and was retained at the surface and the bottom to form two main layers as in Column A. However, the sediment retained above the plate was much less than in Column A (See table 12). The initial flow rate in Run B was considerably higher than in Run A and the finer sediment may have flushed out through the plate leaving the coarser sediment above the plate. Larger amounts of sediment were retained in the soil in Run B than in the other two columns and the sediment distribution was very uniform throughout the column as indicated by the comparison of the deposit ratios calculated from the gamma ray measurements. Approximately one-half of the applied sediment entered the soil column and 2.16% of the voids were filled in the column between 1cm and 11cm below the surface. The hydraulic conductivity of the entire column was reduced 97% from the initial value and the second layer was reduced 51%. The hydraulic conductivity reduction was caused not only by sediments deposited at the surface but sediments retained in the soil at the second and third layers. Sediment migration from the top layer during the final distilled water run was evident from the increase of hydraulic conductivity in this layer. Low gradients at flow rates below 1.70 mℓ/min prevented the determination of hydraulic conductivity across the two lower layers of this column.

In Column C with 5μ-10μ sediment and 50μ-150μ sand, the effluent remained clear at all times. The head loss across the bottom 2cm of soil and the porous plate was negligible compared with the high loss in the other two columns (Table 12). Sediment therefore neither penetrated

the plate nor was retained in the bottom 2-1/2cm of soil above the plate. Gamma ray measurements showed some sediment retained at 11cm below the soil surface. The depth of penetration was 15cm below the soil surface at this flow rate as indicated with most of the sediment retained around 9cm below the surface. About one-third of the applied sediment entered the soil but the reduction of hydraulic conductivity in the entire column was 93%. Sediment migration was evident during the final run with distilled water in the overall column. The total amount of the sediment retained in the soil was more than in Run A but less than in Run B.

Soil-Water-Chemical Effects

Hydraulic conductivity with high and low salt solutions

Table 13 shows the results of hydraulic conductivity measurements on the Portneuf silt loam soils with high salt-high sodium solutions (K_o) and low salt-high sodium solution (K_i) relative conductivity (y) values, and c values calculated using equation 26. Calculated values of relative conductivity for each layer for a range of soil ESP values are shown in Figures 16, 17 and 18 for solutions with salt concentrations of 1, 5 and 10 meq/1. These curves were determined using c values computed from the experimental data, Table 13. Data points used for the curves in Figures 16, 17, and 18 are somewhat scattered, however, the apparently better fit for layer A with the high clay content reflects the greater applicability of this procedure to soils with higher montmorillonite content. The S shaped curves are typical of those found by McNeal (1968) and Rasmussen and McNeil (1973).

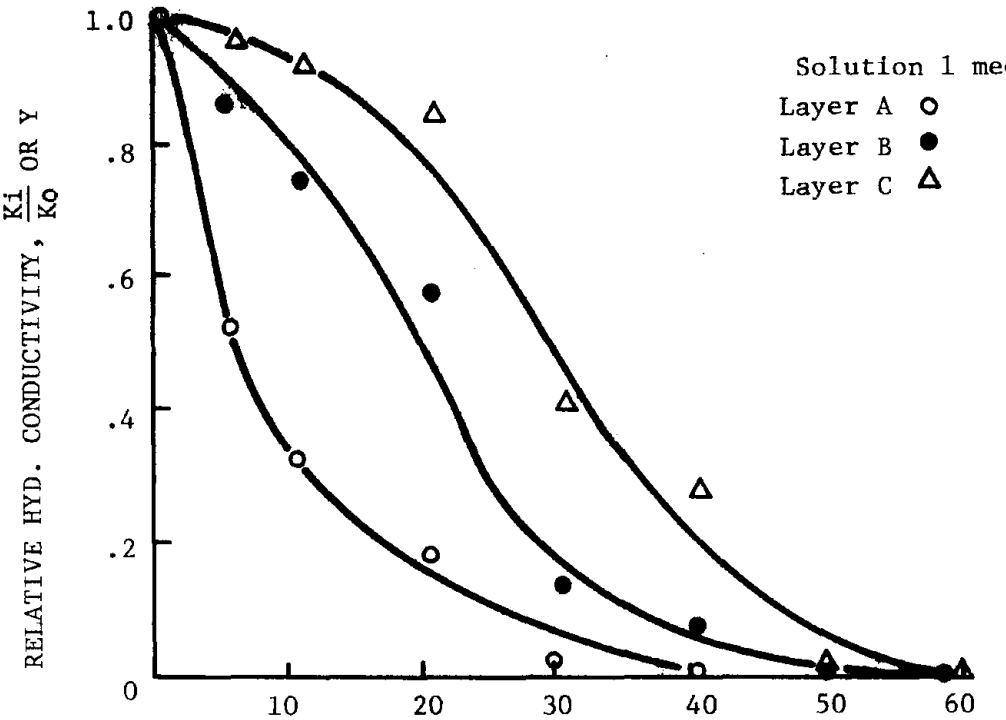

Figure 16. Relative hydraulic conductivity, 1 meq/ℓ solution

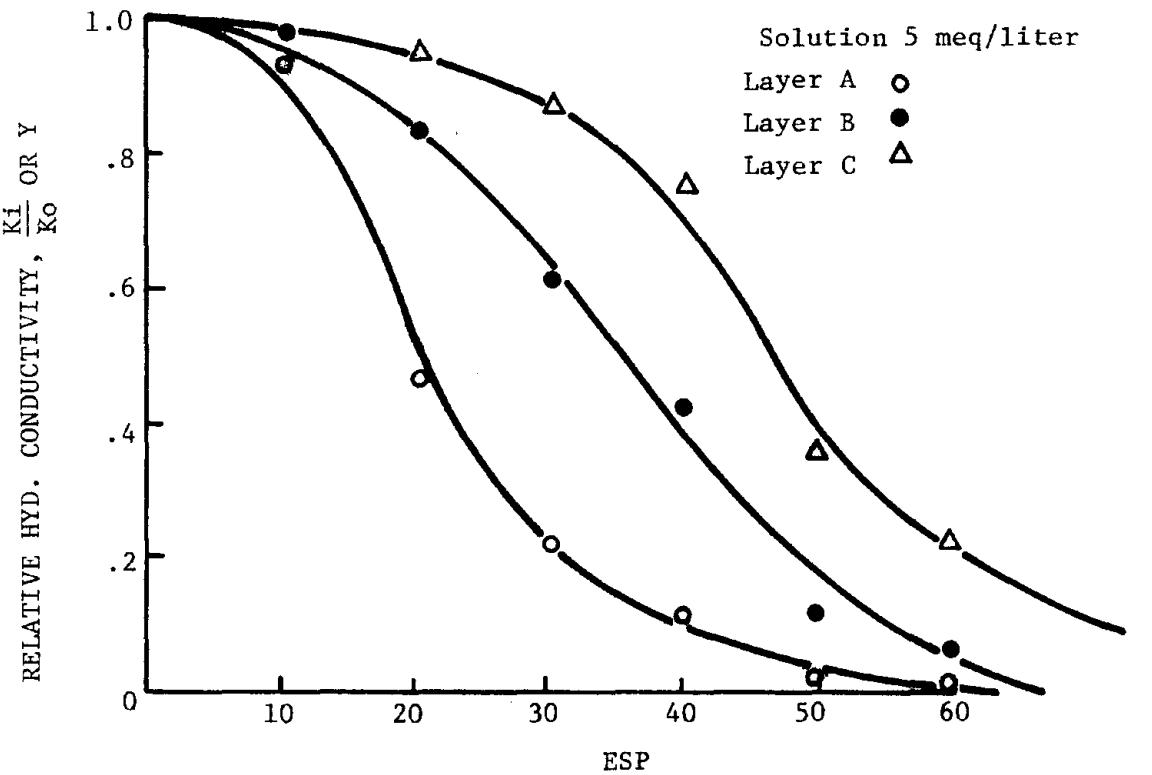

Figure 17. Relative hydraulic conductivity, y, vs. soil ESP for 5 meq/ℓ solutions

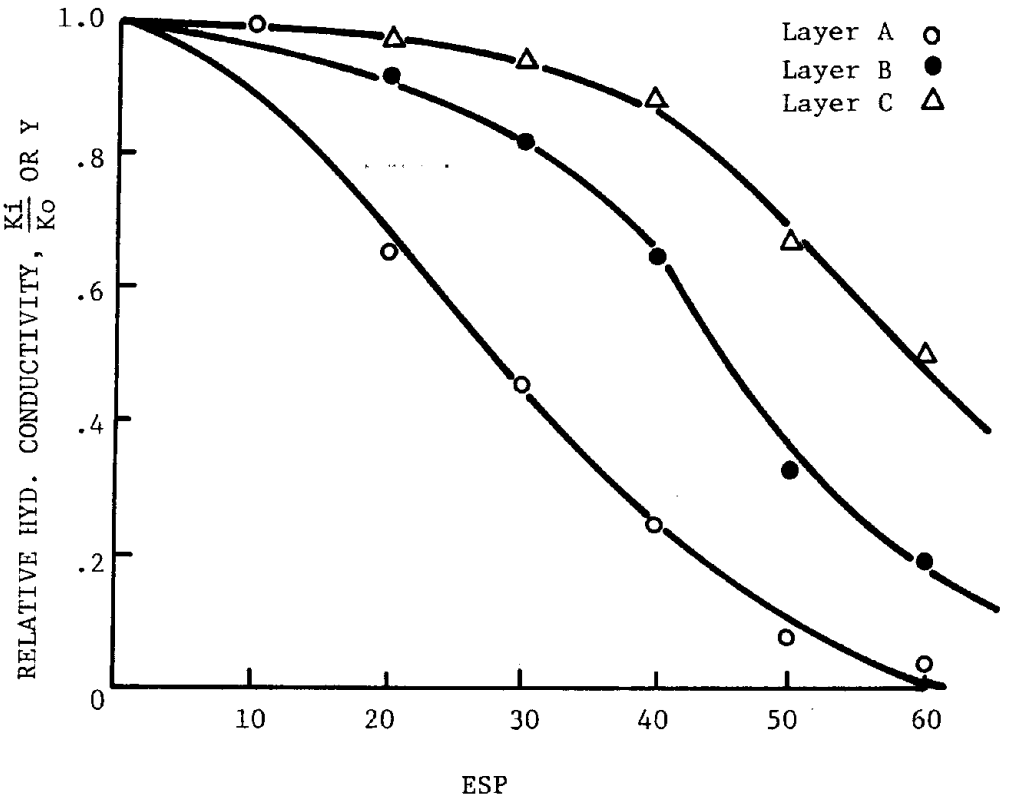

Figure 18. Relative hydraulic conductivity, y, vs. soil ESP for 10 meq/ℓ solution

Table 13. Absolute and relative hydraulic conductivities - high and low salt solutions

LAYER		A			B			C		
		K_o	K_i	y	K_o	K_i	y	K_o	K_i	y
REPLICATIONS	1	.988	.433	0.44	.446	.374	0.84	.964	.849	0.88
	2	.970	.416	0.43	.519	.410	0.79	.973	.908	0.93
	3	.493	.215	0.44	.489	.400	0.82	.944	.937	0.99
	4	.489	.215	0.44	.525	.447	0.85	1.17	1.10	0.93
	5	.578	.248	0.43	.629	.499	0.79	1.07	1.06	0.99
	6	.553	.238	0.43	.507	.412	0.81	1.10	1.06	0.96
	7	-	-	-	-	-	-	1.29	1.20	0.93
	8	-	-	-	-	-	-	1.30	1.28	0.98
$y_{avg.}$				0.43			0.82			0.95
C for	n = 1			18			3			0.7
	n = 2			248			43			10
	n = 3			3,424			589			137

K_o = Hydraulic conductivity measured with high salt-high sodium solution

K_i = Hydraulic conductivity measured with low salt-high sodium solution

y = Relative conductivity K_o/K_i

c, n = Constants in the equation relating clay swelling and hydraulic conductivity decreases (Equation 26)

Hysteresis effects

Percolation of 250ml of high salt-low sodium (0.5N $CaCl_2$, SAR = 0 through the samples previously equilibrated with low salt-high sodium solution caused no significant change in hydraulic conductivity after 5 days, Table 14. Salt free (distilled water) solution resulted in a one order of magnitude decrease in hydraulic conductivity from the final values obtained with the low salt-high sodium solution. Essentially the same results as with distilled water were found when Snake River irrigation water was percolated through the samples. Recovery of hydraulic conductivity upon reintroduction of high salt solution would be expected if the initial reduction were due to swelling of the clay fraction. Since this did not occur for the Portneuf silt-loam soil, the reduction cannot be attributed to clay swelling.

Table 14. Initial and final hydraulic conductivities obtained with the percolation of a high salt solution, distilled water, and Snake River Water

Layer	$CaCl_2$(.5N)		Distilled Water		Snake River Irrigation Water	
	K_o[1]	K_i	K_o[2]	K_i	K_o[2]	K_i
A	.160	.163	.215	.019	.248	.027
B	.247	.256	.374	.039	.400	.042
C	.96	1.04	.908	.092	1.06	.113

[1] K_o represents the initial hydraulic conductivity obtained immediately after percolation with $CaCl_2$(.5n). (Solution 11)

[2] K_o is the final low hydraulic conductivity obtained with solution II

Variation of hydraulic conductivity with time

Figure 19 shows the measured hydraulic conductivity of the Portneuf silt-loam soil with time using irrigation water under non-sterile conditions. Plotted points are the average value determined from two permeameters on each layer, A, B, C and the mixed profile, M. Changes in hydraulic conductivity for the A and B layers are similar, decreasing from 0.70 cm/hr to 0.17 cm/hr over a 54 day period or to a relative hydraulic conductivity of approximately 0.24. Removal of the top 4mm of the samples after 26 days caused no increases in the hydraulic conductivity of layer A and only a slight increase in layer B. The rate of decrease of both layer A and B after removal of the top 4mm remained essentially constant.

Layer C, Figure 19, shows a decrease from 1.20 to 0.46 cm/hr in 26 days at which time the top layer was removed. After removal of the top layer the hydraulic conductivity increased to 0.71 cm/hr but subsequently decreased after 54 days to 0.41 cm/hr and a relative conductivity of 0.34.

The mixed sample, M, exhibited decreases somewhat greater than layers A and B but less than layer C. A slight increase in hydraulic conductivity after removal of the top layer was measured.

The increase in hydraulic conductivity with removal of the top layer in layer C did not occur in layers A and B under the same non-sterile conditions. Therefore, it is not probable that microbiological activity in the top layer of the sample is responsible for the initial decreases. The clay content of layer C is lower than A or B whereas the silt content is highest and the ESP of this layer is the highest. Aggregate

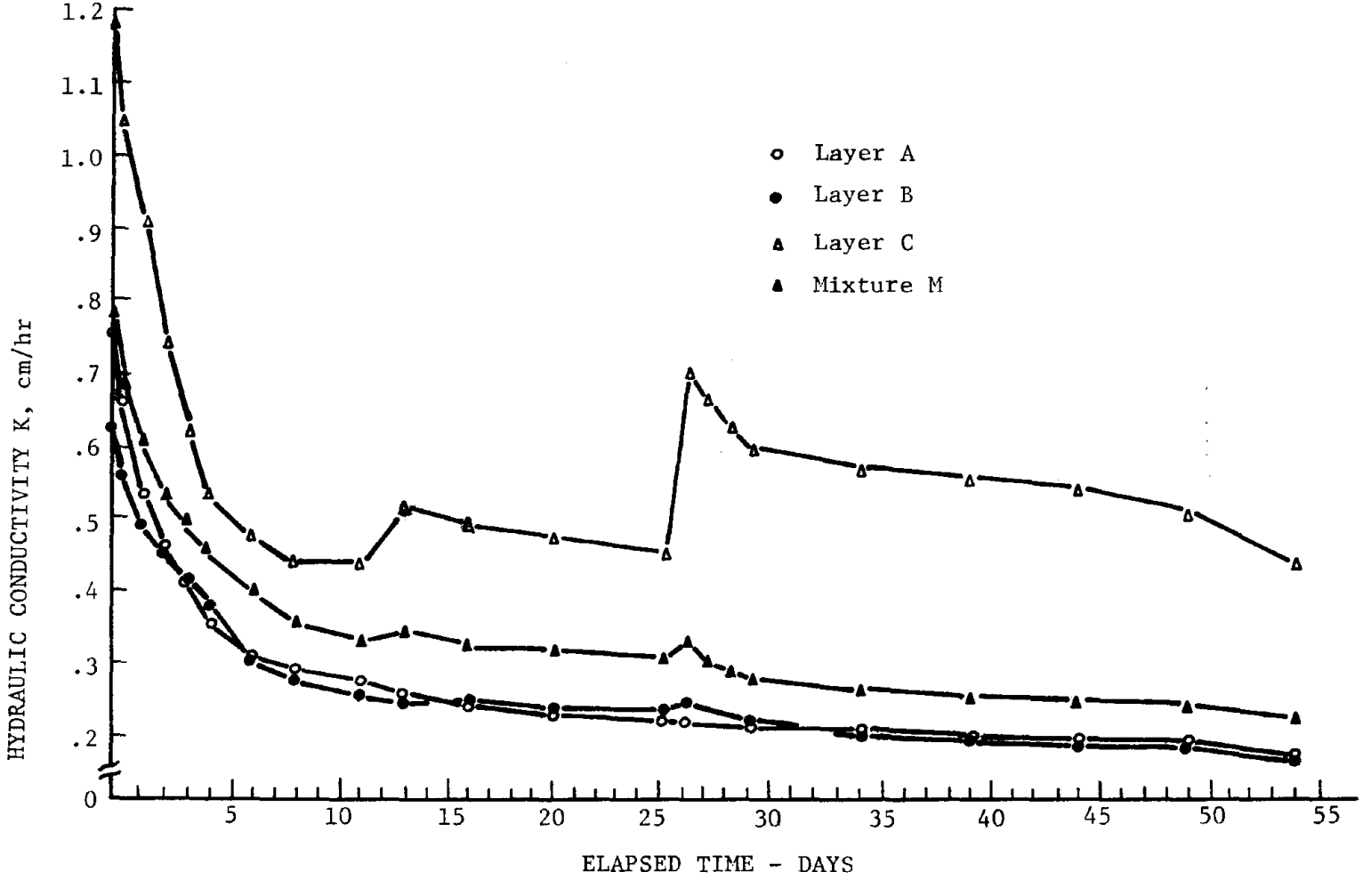

Figure 19. Hydraulic conductivity vs. time-irrigation water (non-sterile) Portneuf silt-loam soil

breakdown or physical dispersion in the surface layers of soil may account for behavior observed in layer C.

Variation of hydraulic conductivity with time for the three soil layers and mixed sample under sterile conditions is shown in Figure 20. In this set of experiments, the soil was autoclaved and the irrigation water used as influent was filtered and $HgCl_2$ added to retard microbiological growth. Plate counts using agar as a growth medium showed zero or very low numbers on samples from this series. For this reason, the samples were run for only 26 days and the top 4mm layer was not removed as in the series using non-sterile conditions. The hydraulic conductivity of layer A decreased from 0.82 to 0.36 cm/hr whereas layer B decreased similarly from 0.70 to 0.32 cm/hr. Layer C showed a greater decrease, 1.41 to 0.55 cm/hr than either layer A or B. The initial hydraulic conductivity of layer C was considerably higher than either layer A or B as was the case in the series using non-sterile conditions and is expected since layer C has the lowest clay content. The mixed sample, M, showed hydraulic conductivity values intermediate between A, B and C. During the percolation of filtered irrigation water through the samples the initial effluent was dark yellow in samples of the A layer, light yellow in samples of the B layer and very light yellow in samples of the C layer. After three days the percolation solution became clear. The discoloration is due to organic matter oxidation during autoclaving and was not observed in the previous series of experiments where the soil was not sterilized. Organic matter content of layer A, nearest the soil surface is probably the highest and had correspondingly the darkest effluent color. Layer C with a minimum amount of organic matter showed the least discoloration of the effluent.

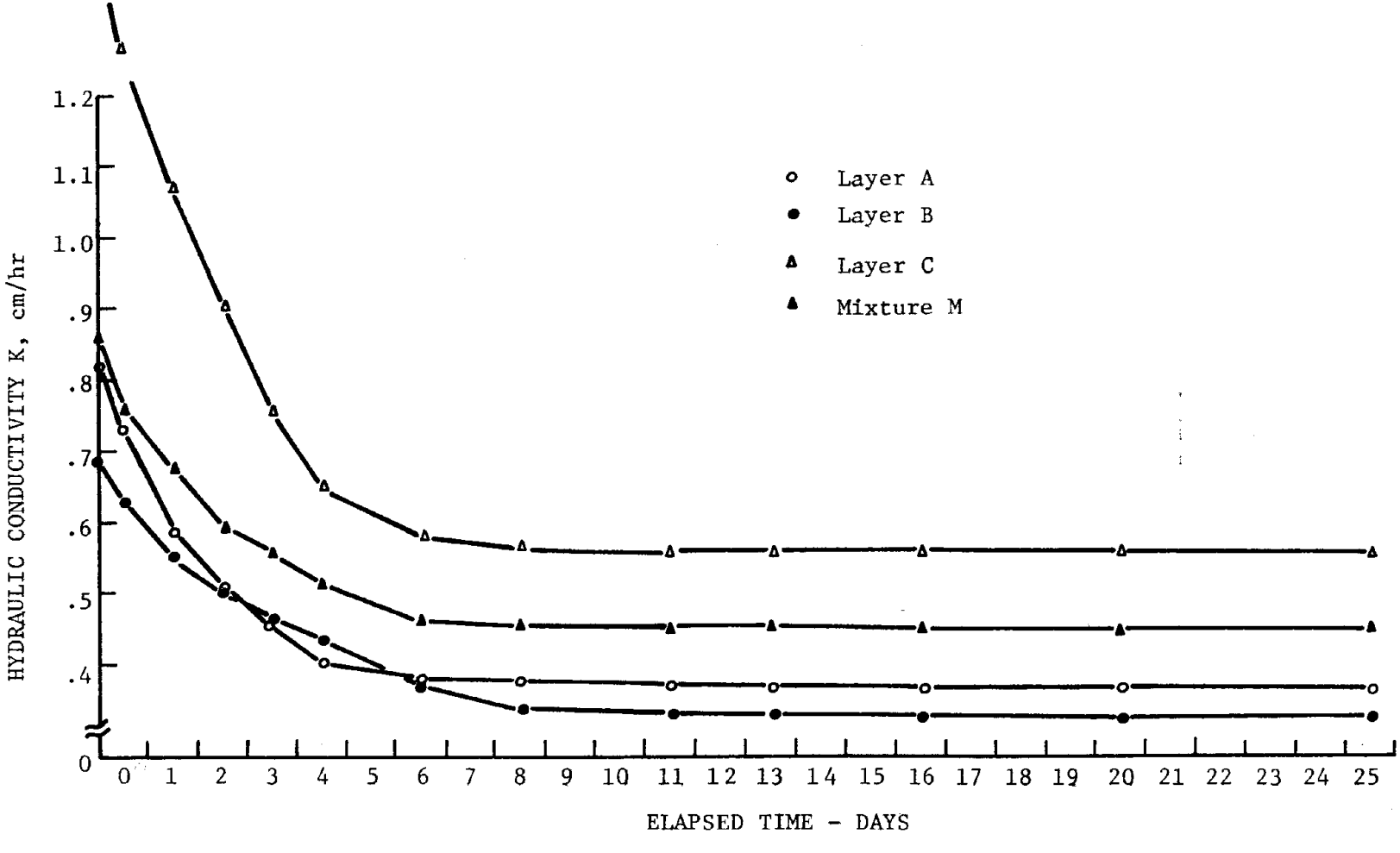

Figure 20. Hydraulic conductivity vs. time-irrigation water (sterile) Portneuf silt-loam soil

It is generally believed that microbiological activity, if it takes place, occurs in the upper few centimeters or millimeters of the soil surface. If the A layer has the largest organic matter content, the microbiological activity in that layer should be more pronounced than in layer B or layer C where organic matter is smaller. However, no appreciable increases in hydraulic conductivity were measured when the top 4mm of the column surface in samples A and B were removed whereas some increase was observed in Column C, Figure 19.

The surface layers in the experiments with sterile soil and irrigation water were not removed due to lack of time and the fact that the plate counts were negative. This would have provided additional information on the relative effects of physical dispersion versus microbiological sealing as a mechanism for permeability decreases.

Comparison of predicted and measured relative hydraulic conductivities

Using equation 26 or Figures 16-18 it is possible to estimate the expected decrease in relative hydraulic conductivity with irrigation water of each layer caused by clay swelling. These values can then be compared with the measured values obtained in the laboratory. The measured values of relative hydraulic conductivity for the three layers using non-sterile irrigation water are shown in Figure 21. The curves shown include only the first 26 days of the tests and are terminated just prior to the time the top layer was removed from each sample. Figure 22 shows the measured relative hydraulic conductivity using sterile irrigation water and sterile soil.

The measured total salt concentration of the irrigation water for both the sterile and non-sterile series of tests was 4.5 meq/liter.

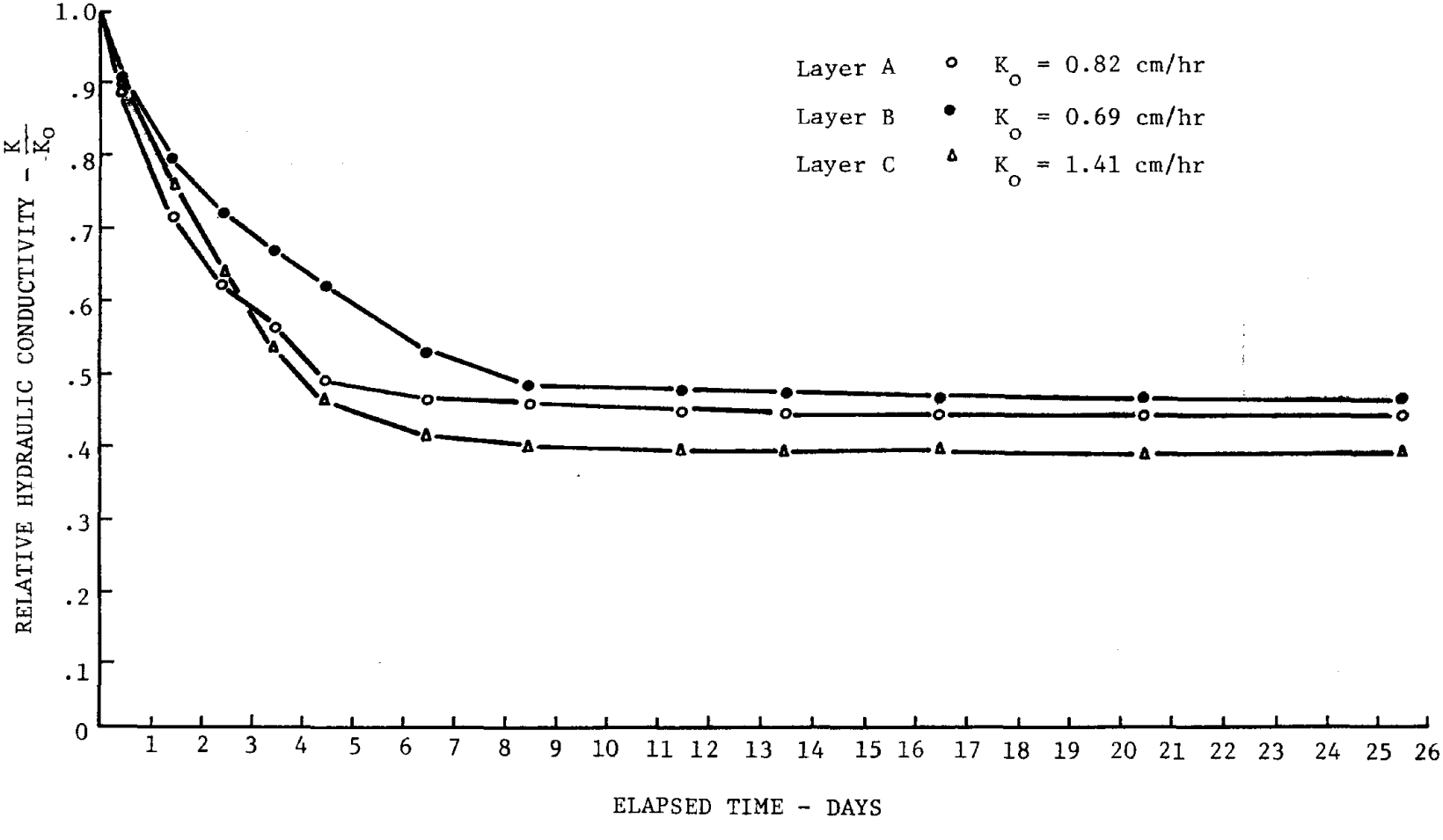

Figure 21. Relative hydraulic conductivity vs. time-irrigation water (sterile) Portneuf silt-loam soil

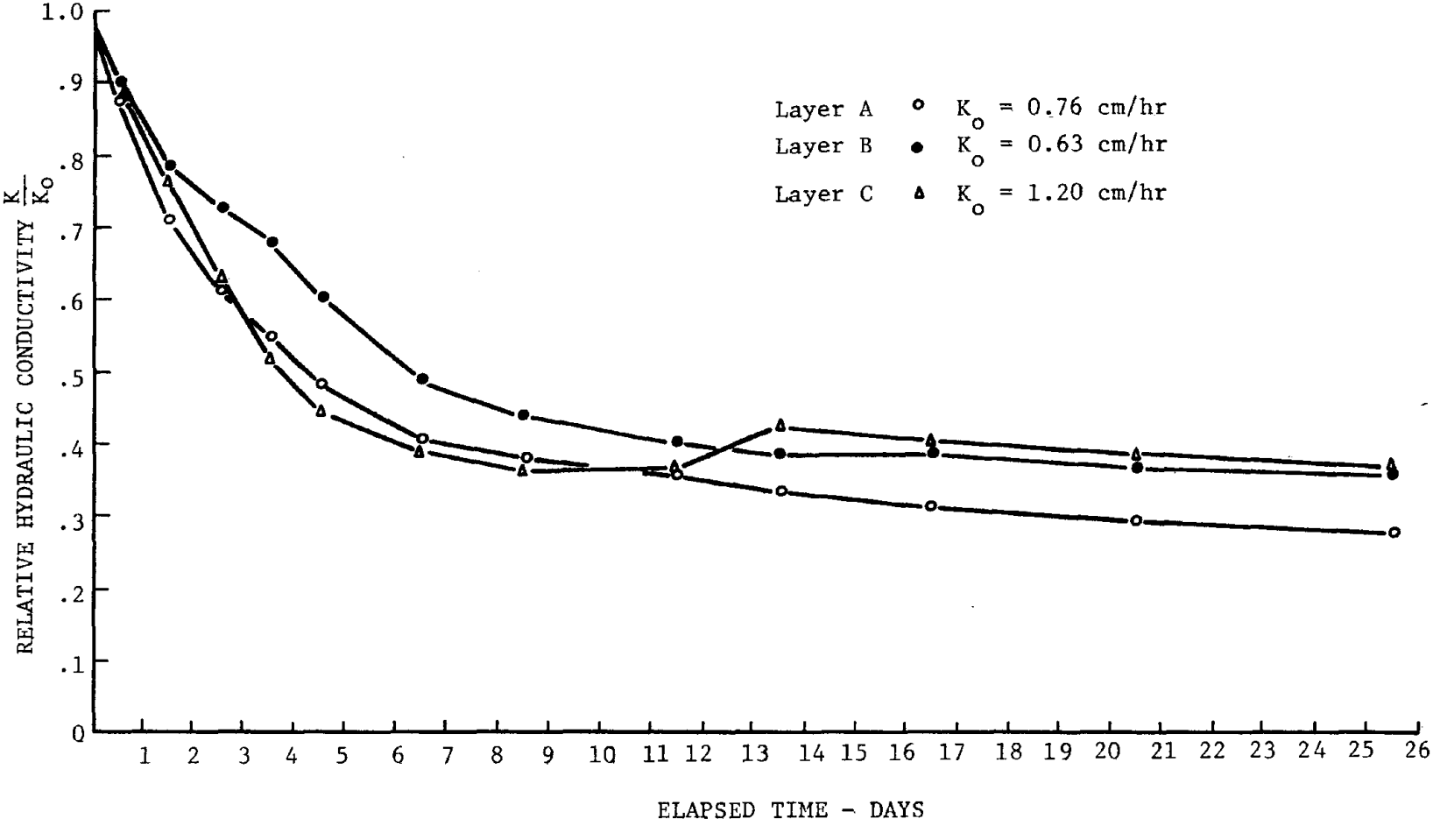

Figure 22. Relative hydraulic conductivity vs. time-irrigation water (non-sterile) Portneuf silt-loam soil

Using an an average ESP of 10 for the Portneuf silt-loam soils, the predicted relative hydraulic conductivity, as estimated from Figure 18, should have been 0.90 for layer A, 0.96 for layer B and 0.99 for layer C; therefore very little decrease in the relative hydraulic conductivity due to swelling of the clay fraction is expected. Figure 21 shows final relative hydraulic conductivities of 0.44, 0.47 and 0.39 for layers A, B and C respectively. These differences in predicted and measured conductivities are significant and cannot be attributed to differences in bulk density or experimental error. Clay swelling therefore cannot account for the measured decrease in hydraulic conductivity in the laboratory experiments and since microbiological activity in the series is limited, the differences must be attributed to other physical factors, namely dispersion of the clay and silt fractions. Physical dispersion of the clay or silt fraction in a soil is construed to mean the deflocculation or dislodgement of the fine particles from larger aggregates with subsequent migration into pores in the matrix.

Measured relative hydraulic conductivities for the three soil layers using filtered non-sterile irrigation water are shown in Figure 22. The measured relative hydraulic conductivities of 0.30, 0.38 and 0.39 for layers A, B, and C for the non-sterile systems are higher than the corresponding values for sterile systems except for layer C. One might attribute the greater relative decreases in hydraulic conductivity in the non-sterile system to microbiological effects, clogging of soil pores by sediments, or physical dispersion.

The effect of removal of the top 4mm layer of each sample after equilibrium is reached is shown in Figure 19. Removal of the top layer in samples corresponding to layer A did not cause appreciable changes in

hydraulic conductivity. A small increase (0.24 to 0.25 cm/hr) in hydraulic conductivity was noted for samples of layer B and a significant increase (0.46 to 0.71 cm/hr) in samples from layer C. Hydraulic conductivity of samples from the mixed profile, M, increased from 0.31 to 0.34 cm/hr. Table 15 summarizes the initial and equilibrium hydraulic conductivity values and computed relative hydraulic conductivities for the three soil layers under non-sterile and sterile conditions as shown graphically in Figure 19 and 20.

Table 15. Initial and equilibrium hydraulic conductivities with irrigation water

Layer	Initial K_o cm/hr		Equilibrium K_i cm/hr		$y = K_i/K_o$	
	Non-sterile	Sterile	Non-sterile	Sterile	Non-sterile	Sterile
A	0.76	0.82	0.23	0.36	0.30	0.44
B	0.63	0.70	0.24	0.32	0.38	0.47
C	1.18	1.41	0.46	0.55	0.39	0.39

The difference in behavior of samples from layer C compared to layers A and B is due either to greater physical dispersion in layer C samples or differences in clay content of the samples. However, the estimated change due to clay swelling was least for layer C and this was not observed in the measured relative hydraulic conductivities. Layer C with the highest silt content would be expected to disperse more readily although the differences in silt content are not great between the three layers, Table 6. Based on this series of experiments the contribution

of microbiological activity and soil-water-chemical reactions to long term reduction of hydraulic conductivity of Portneuf silt-loam soils is small compared to the migration and plugging of pores by physically dispersed particles.

Undisturbed Column Studies

Figure 23 is a plot of relative conductivity with time for three segments in Core No. 1. The top segment (0.43cm depth) contains a natural dark surface layer with finer silt particles approximately 2.7cm thick. Initial saturated hydraulic conductivity varied from .083 cm/hr for the top segment to .74 cm/hr for the segment from 8.9 to 13.7cm. The relative hydraulic conductivity of the top layer decreased to 0.20 after 35 days at which time equilibrium was reached. No appreciable decrease was evident in the two lower segments of the column.

The relative hydraulic conductivity of Core No. 2 with the top layer removed is shown in Figure 24. Initial saturated hydraulic conductivity of the top segment (0-3.0cm) was 2.2 cm/hr whereas the two lower segments had initial conductivities of .42 cm/hr and .53 cm/hr for the 3-8.5cm segment and the 8.5 to 14cm segment respectively. The relative hydraulic conductivity decreased to 0.15 for the top 3cm and to 0.2 for the lower segments.

The response of the saturated hydraulic conductivity of undisturbed cores to percolation of irrigation water under non-sterile conditions is similar to that of disturbed samples, Figure 19. Relative hydraulic conductivities were lower for the undisturbed cores (.15 to .20) than for the disturbed soil (.35 to .45). The differences in behavior of the hydraulic conductivity of the two cores is quite pronounced. The

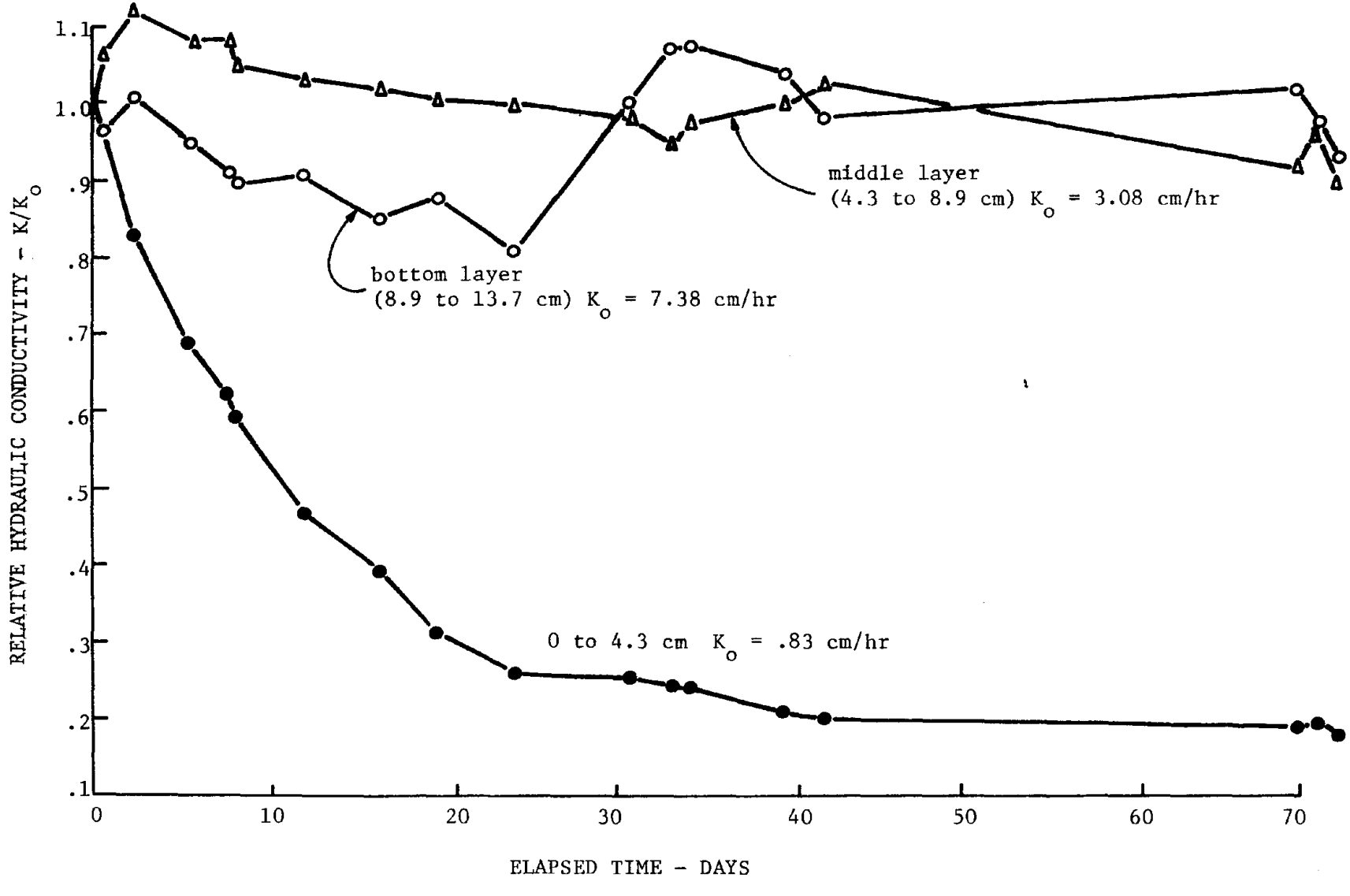

Figure 23. Variation of saturated hydraulic conductivity with time in undisturbed soil core No. 1

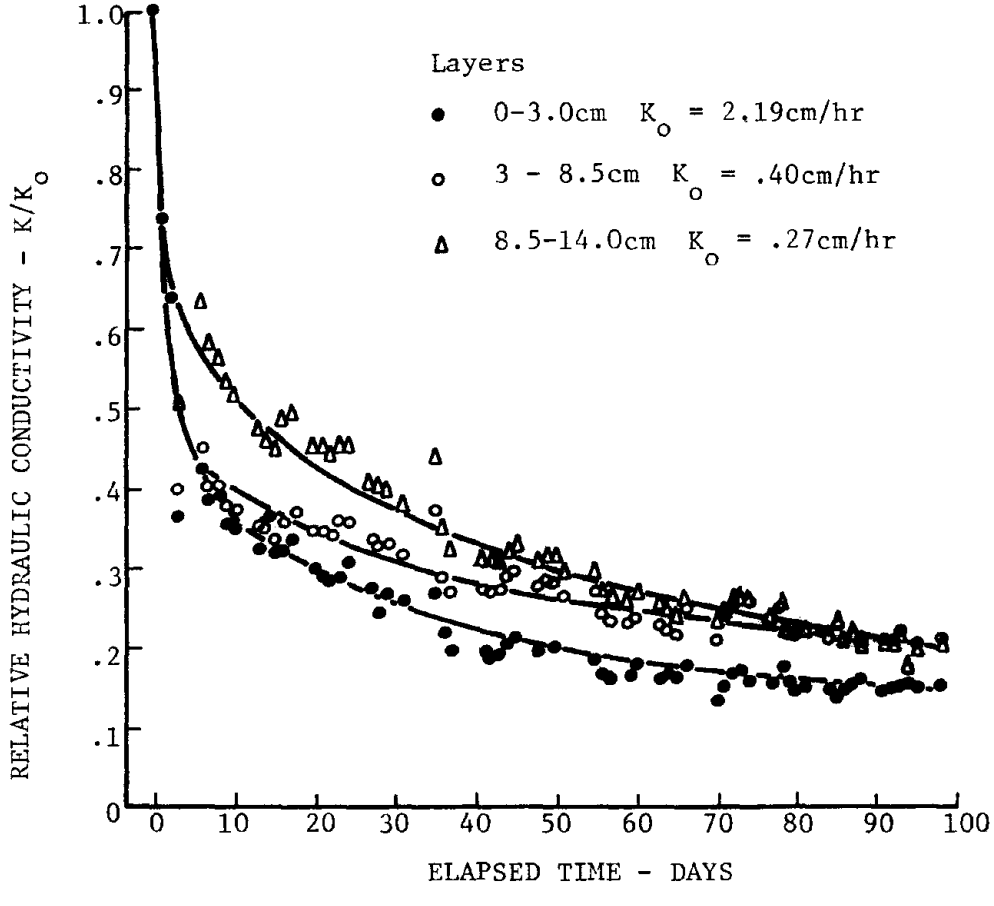

Figure 24. Variation of saturated hydraulic conductivity with time in undisturbed soil core no. 2

top layer of core No. 1 which contained the impeding layer had an initial hydraulic conductivity 2.5 fold lower than the top of core No. 2 from which the top layer had been removed. This was expected since the fine sediments and organic materials from previous years' operation were contained in the impeding layer. An equilibrium relative hydraulic conductivity of 0.2 for the top layer of core No. 1 after 35 days was typical of the cores tested. It should be pointed out that core No. 1 was obtained shortly after the canal was taken out of service in the fall of the year and was tested before any appreciable drying could take place except for the top and bottom surfaces. Core No. 2 was obtained at the same time as core No. 1 but was not tested for about one year. Even though the core was wrapped in "Saran" material, appreciable drying did take place.

The lack of decrease in hydraulic conductivity of the lower segments of core No. 1 is probably due to the fact that the condition of the soil matrix at the time of testing was nearly the same as at the end of the operation season at which time all decreases had occurred.

Decreases in hydraulic conductivity occurred for all layers in core No. 2 with essentially the same percentage reduction (90-85%) in all layers. The fact that the lower layers exhibited decreasing hydraulic conductivity in core No. 2 and not in core No. 1 could be due to the additional drying that occurred in core No. 2.

CHAPTER VI

FIELD TESTS

Considerable effort was expended in evaluating the magnitude of seepage losses in an operating canal and determining seasonal changes in the loss rates. Tests were conducted in the Main Canal of the Northside Pumping Division of the Minidoka Project. These experiments were conducted in cooperation with the U. S. Bureau of Reclamation and the Agricultural Research Service. The emphasis was placed on evaluating the magnitude of actual operational seepage losses as compared with predicted or pre-project losses and in determining probable causes of seasonal fluctuations in seepage losses.

Ponded Seepage Tests

Seepage loss measurements by ponding sections of canal are recognized as the most accurate means of measuring average losses in operating canals. Tests were therefore run during two seasons on the Main Northside canal. In all 2.6km (1.5 mi) of canal were ponded using standard ponding procedures in which the bank storage was satisfied before seepage rates were determined. Average ponded seepage rates were .20 to .25 cubic meters per square meter per day (0.60 to 0.75 cubic feet per square foot per day, cfd). All tests were performed in the fall after the irrigation season and should represent the minimum rate for the year.

Inflow-outflow seepage measurements

The U. S. Bureau of Reclamation performed loss measurements on a 7.34km (4.56 mi) reach of the Main Northside Pumping Canal by measuring inflow and outflow on a volumetric basis for 12 periods approximately two weeks long during two seasons. Those results are reported here as a comparison to the ponded rates determined for the 2.6km of the total reach. Figure 25 shows the operational loss rates for the canal for two seasons. Average rates were about .34 cubic meters per square meter per day (1.1 cfd) with the higher losses occuring at the start of the season. Assuming that the actual seepage rates are represented by the average ponded rate of .20cmd (0.67 cfd), the operational waste or loss accounts for .10 cmd (0.33 cfd) or 30% of the total transmission loss.

Well permeameter tests

Since one of the objectives of this study was to evaluate the magnitude of the effect of natural sealing on operational systems, a comparison of actual seepage loss rates with predicted rates was deemed worthwhile.

Twenty-eight shallow well pump-in tests were performed on the Portneuf silt-loam soils adjacent to the Main Canal during two seasons by the U. S. Bureau of Reclamation (1971). The average permeability of the 28 tests was 11 cm/day (.36 ft/day), the average water depth 1.46m (4.8 ft), and width 7.0m (23 ft). Using equation 9 as modified by the U. S. Bureau of Reclamation (Glover 1963) with a C factor of 3.5:

$$q = \frac{K\ (b+2d)}{3.5}$$

The computed seepage rate is 1.02cmd (3.35 cfd). This value is considerably greater than the ponded rate of .20cmd (0.67 cfd) and shows the possible errors in estimating operational seepage losses.

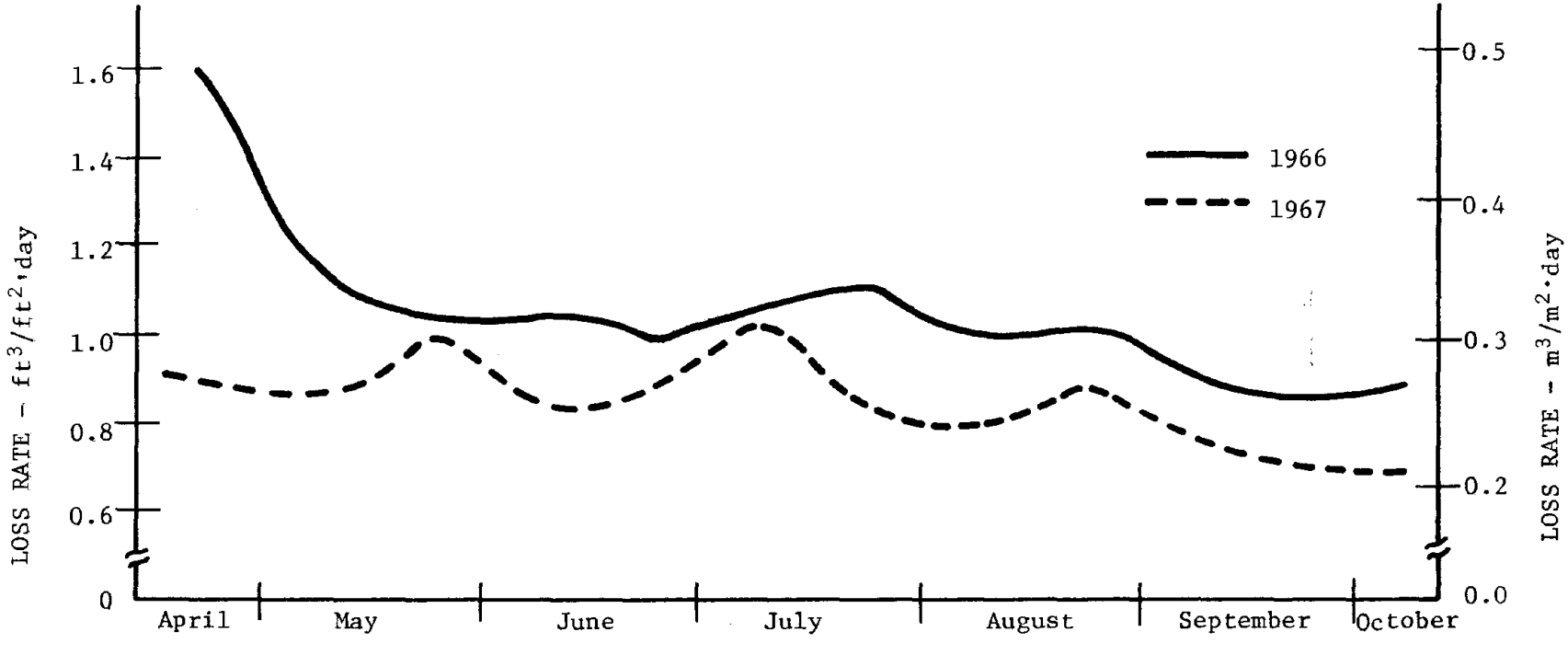

Figure 25. Average inflow-outflow loss rates - Unit A main canal - 1966-67

Soil moisture tension measurements

Since the flow regime below the Main Northside Canal was known to be partially saturated at shallow depths below the canal bottom, changes in soil moisture tension measurements were believed to be indicative of seasonal changes in seepage rates.

In order to determine the soil moisture tension and evaluate various field techniques, porous cup tensiometers and tensiometer readout equipment were installed below the operating canal. Several types of installations were attempted. At canal stations 132 + 90 and 133 + 13 nine ceramic tensiometer tubes, Figure 26, were installed in groups of three in the sides of pits at the canal center line and 1.5m (5 ft) right and left of center line, Figure 27. In each pit tensiometers were installed and small diameter nylon readout and flushing tubes were buried in ditches leading to the mercury manometers or pressure transducer readout equipment on the canal bank. At station 132 + 90 tensiometers were installed at .08, .30, and 6.61m (.25, 1.0 and 2.0 ft) below the canal bottom and at station 133 + 13 installed depths were .15, .30 and .61m (.5, 1.0 and 2.0 ft). At stations 132 + 75, and 133 + 48 three sets of two were installed by inserting the porous cups into the soil at the bottoms of one inch diamater piezometer tubes driven to depths of .38 and .69m (1.25 and 2.25 ft) in the canal bottom. Tensiometer leads were attached to mercury manometers fastened to the tops of the piezometers, Figure 28. Approximately 2.5cm of the surface of the bottom of the canal was removed for a distance of 1.5m (5 ft) upstream and downstream of tensiometers at station 133 + 48. The tensiometer installation at station 133 + 53 involved insertion of the porous cups vertically into the bottom of the canal to the appropriate depth.

Figure 26. Porous ceramic cup tensiometer

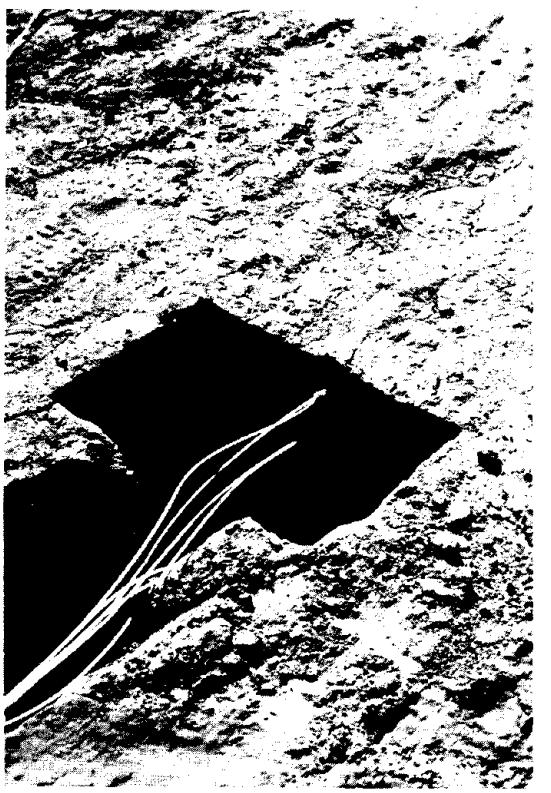

Figure 27. Tensiometer installation in canal bottom stations 133+90 and 133+13 Unit A main canal

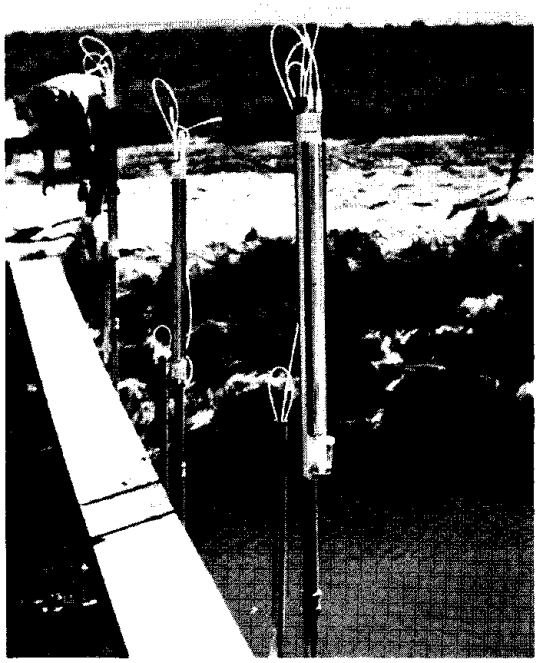

Figure 28. Mercury manometer for monitoring tensiometers installed in piezometer tubes

Readout tubes were buried in shallow trenches to manometers on the canal bank.

The tensiometer installations in the bottoms of piezometer tubes proved more reliable and easier to install and installation did not require that the canal be out of operation. Tensiometer installation at shallow depths in the canal bottom was not possible using piezometers since about .3 to .5m (1 to 1.5 ft) of insertion was necessary to maintain the stability of the piezometer tube. In the pit installations, tensiometers could be inserted to within 8cm (3 in) of the canal bottom. Tensiometers were monitored for all of one irrigation season and part of another.

Measurements of the soil moisture tension were made on each of the 39 tensiometers during the time the canal was operating. Readings were taken at least twice weekly on all tensiometers. Generally morning and afternoon readings were obtained and averaged to minimize any temperature effects.

Response of all banks of tensiometers during the season were similar. Figure 29 shows the potentials measured at station 132 + 90, 1.5m (5.0 ft) left of canal centerline. A partial ponding test was performed prior to the irrigation season and the canal dewatered for 15 days for removal of ponding test facilities before refilling. Potentials at all three levels below the bottom of the canal show typical responses at the beginning of the season with initial small increase in potential and gradual decreases over a two month period.

Several abrupt changes in elevation potentials beneath the canal occurred during the 1967 irrigation season at all tensiometer stations. After the initial increase in potential probably caused by displacement

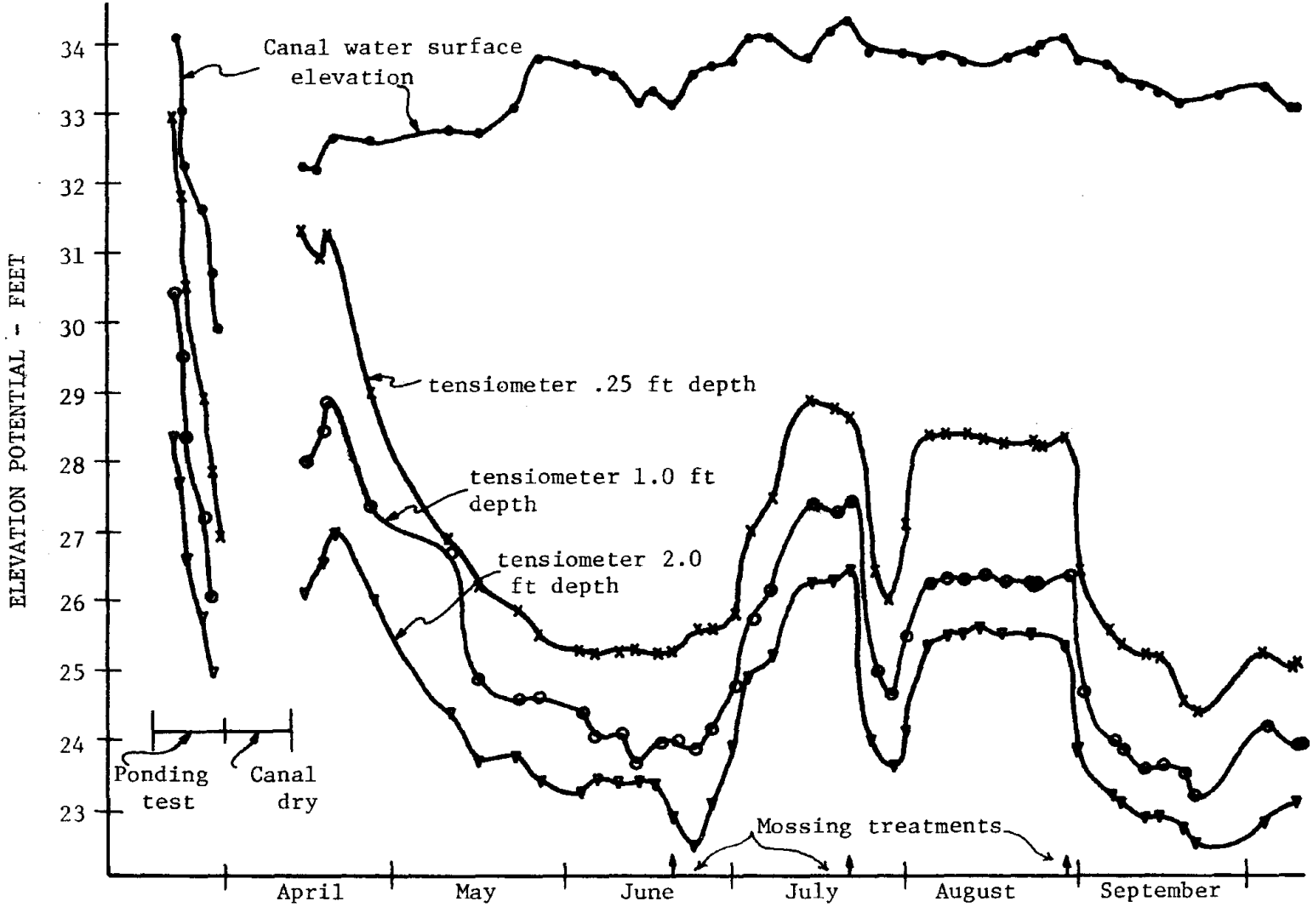

Figure 29. Soil moisture potentials - Unit A main canal station 132+90 5.0 ft left of canal centerline - 1967

of air in the voids, the potentials decreased at a decreasing rate and reached equilibrium in about 65 days. A somewhat abrupt increase in potential occurred at all depths after 66 days causing increases of over 1m (3 ft) of pressure during a 20 day period. A rapid decrease and corresponding rebound occurred between 86 or 96 days after filling and after 139 days the elevation potentials decreased abruptly to the equilibrium levels or lower. Causes of the rapid changes in elevation potential are not readily apparent. Meterological records at Twin Falls, Idaho, approximately 48km (30 mi) from the test section show no major changes in temperature or barometric pressure which could account for these responses. Water temperature in the Snake River at Milner from which the canal water is pumped showed minor fluctuations in temperature over the season and therefore it is not likely that temperature effects can account for the observed fluctuation in soil moisture tension.

During the 1967 irrigation season, the entire length of the Unit A canal was treated for moss with aromatic solvent "tear gas". The dates of these treatments were June 19, July 21, and August 29 as shown on Figure 30. The mossing treatments could have caused the rather abrupt changes in elevation potentials perhaps by destroying micro-organisms in the top layer of soil on the canal bottom. If the effect of mossing is to increase conductivity of the top surface layers by removal of algae or other organisms, the effective hydraulic conductivity of the surface layer should be increased resulting in a decrease in hydraulic gradient across the upper layer. Conversely, if the effect of the mossing treatment is to clog pores of the surface soil with residue of dead organisms, decreases in hydraulic conductivity would be expected with increases in gradient across the top layer. Figure 30 shows the average hydraulic

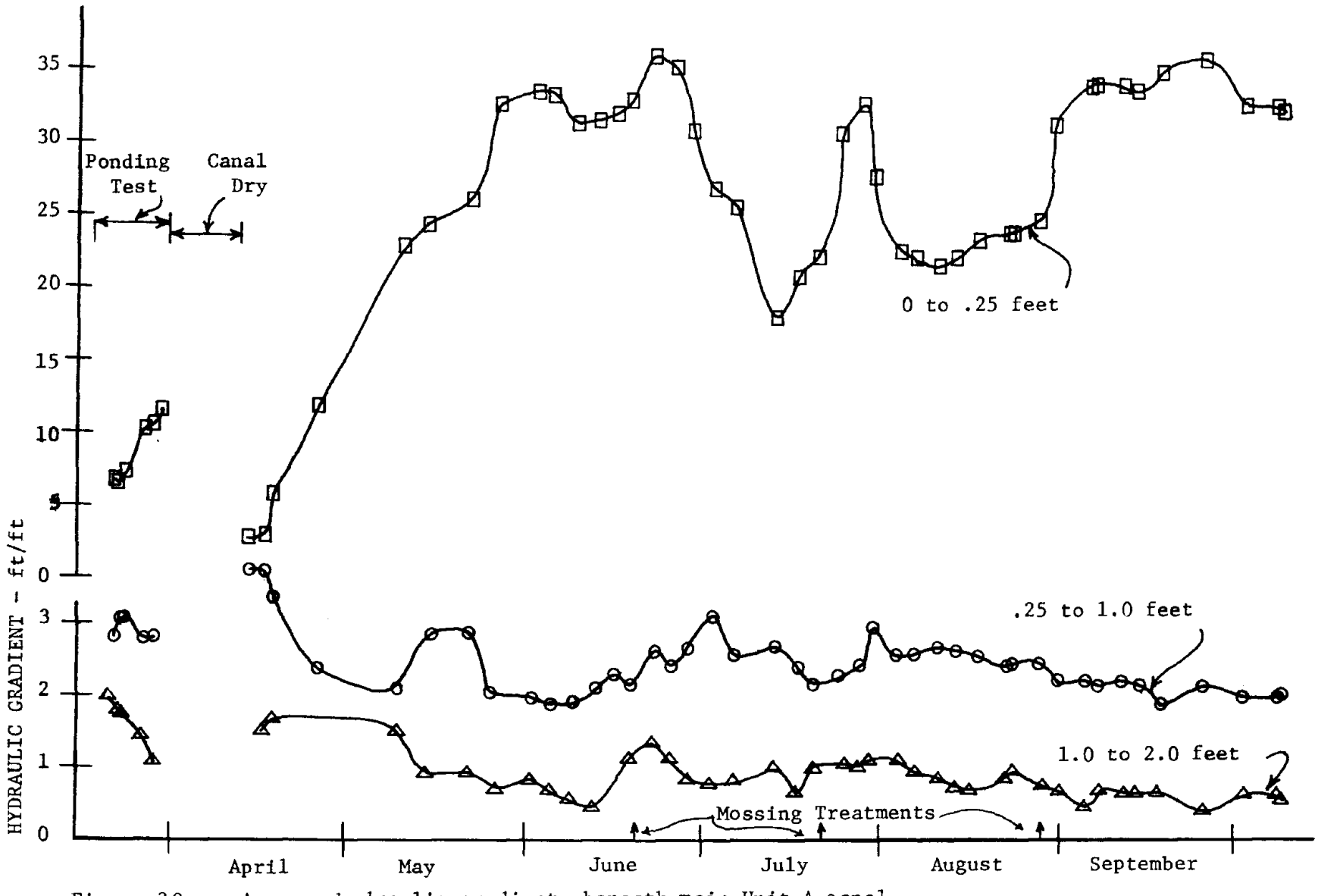

Figure 30. Average hydraulic gradients beneath main Unit A canal station 132+90 - 1967

gradient computed from the banks of tensiometers at station 132 + 90 during 1967. Gradients in the top surface layer 0 to .08m (0 to 0.25 ft) are 10 to 20 times as large as gradients at the lower elevations. This indicates that the surface sealing effect is the major restriction to seepage from the canal. The response of the gradients during the initial filling for the ponding test and then during filling for irrigation operation are similar with the surface layer gradient increasing and the gradients at the deeper depths tending to decrease. The gradual increase in the surface layer continued for forty days before peaking. This time period and response compares with the undisturbed soil core measurements in which the hydraulic conductivity of the top layer decreased for 35 days before equilibrium was reached, Figures 23 and 24. Also, the deeper layers of the undisturbed cores showed small decreases compared with the top layer, Figure 23.

The record of tensiometers at station 133 + 48 shows the differences in response of the hydraulic gradient as a result of removing the top layer prior to canal filling. At station 133 + 48 the top 2.5cm of material including the previous season's accumulation of sediment was removed for a 6.1m (20 ft) reach and tensiometers installed at depths of .38 and .69m (1.25 and 2.25 ft). Figure 31 shows a comparison of hydraulic gradients from 0 to .38m (0 to 1.25 ft) and .38 to .69m (1.25 to 2.25 ft) at station 133 + 48 with gradients from station 132 + 75 where the top layer was not removed. The responses are nearly identical except that the surface gradient at the scraped section is about .30m/m (1.0 ft/ft) greater than at the non-scraped section. The gradients at the deeper depths tend to unity which is expected. This response indicates that the same mechanisms affecting changes in hydraulic gradient are in effect with or without an initial sealing layer.

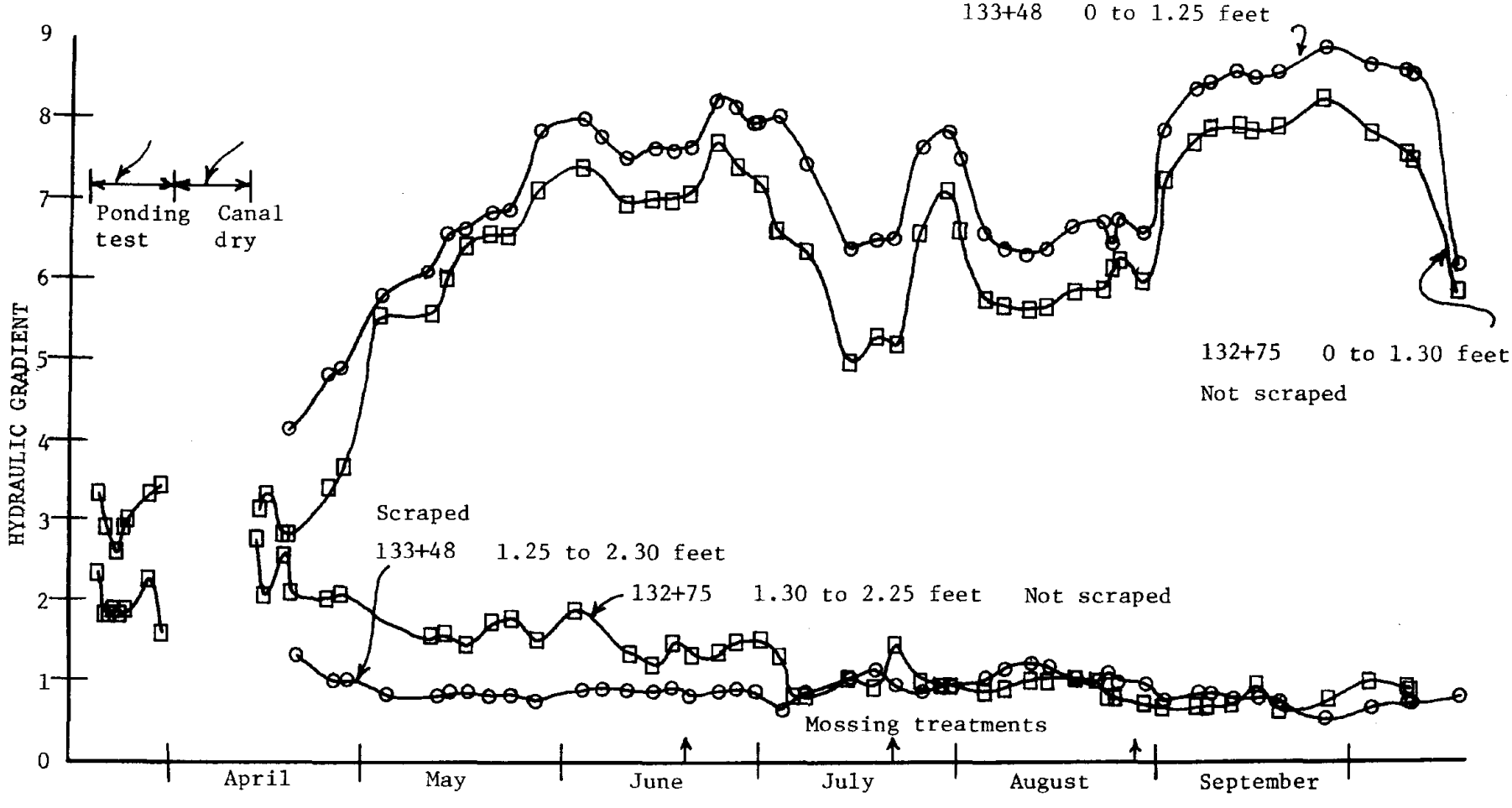

Figure 31. Average hydraulic gradients beneath main Unit A canal-stations 132+75 and 133+48 1967

Soil moisture measurements

To supplement the tensiometer measurements of the soil moisture movement beneath the Main Unit A canal, soil moisture content was measured at several stations. Neutron meter access tubes were installed in the center of the operating canal at station 132 + 86 and 133 + 48 and soil moisture measured to a depth of 1.30m (4.25 ft) below the canal bottom during four months of the 1967 irrigation season. Moisture measurements were made at seven points from .08 to .99m (.25 to 3.25 ft) below the canal bottom. Figure 32 shows a plot of selected soil moisture profiles at station 133 + 48 for the 1967 season. The moisture profiles are similar throughout the season with moisture content ranging from 42 to 46 percent at the lower depths and up to 52 percent at the .08m (.25 ft) depth. Measurements at depths less than .08m (.25 ft) depth below the soil surface were not possible because of the sensitivity of the probe near the soil-water interface.

Soil moisture measurements were taken at the two canal stations to examine the effect of removing the top one inch of the soil on the canal bottom and to compare the changes in elevation potentials with soil moisture changes. At canal station 133 + 48 the layer was removed prior to filling for a distance of 10 feet upstream and downstream of the access tubes whereas at station 132 + 90 the layer was not removed. There was no significant difference in the soil moisture levels or seasonal response of soil moisture at the two stations. Figure 33 shows the comparison of soil moisture and elevation potential at Stations 133 + 48 and 132 + 90.

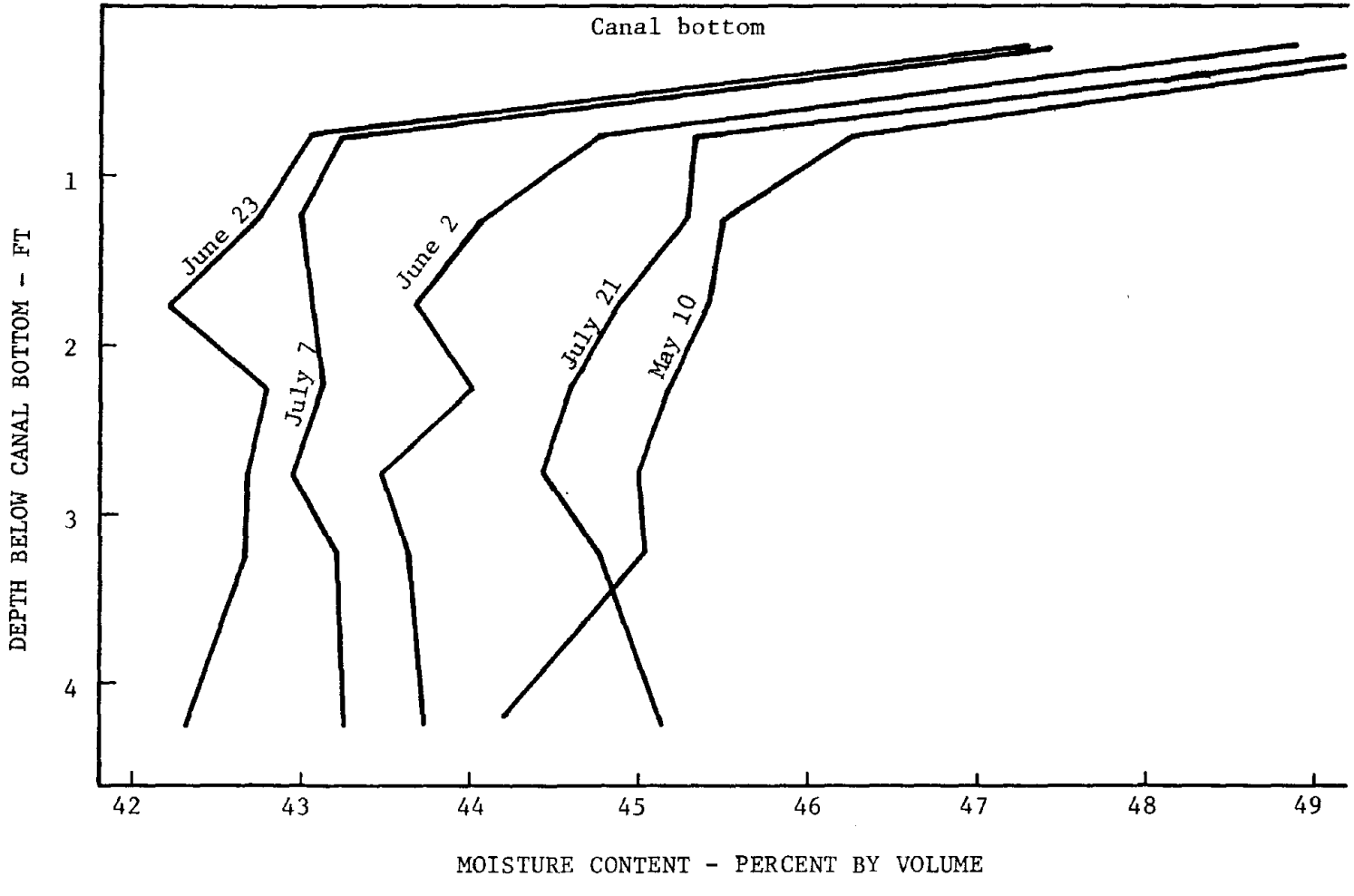

Figure 32. Soil moisture profiles below Unit A main canal station 133+48 - 1967

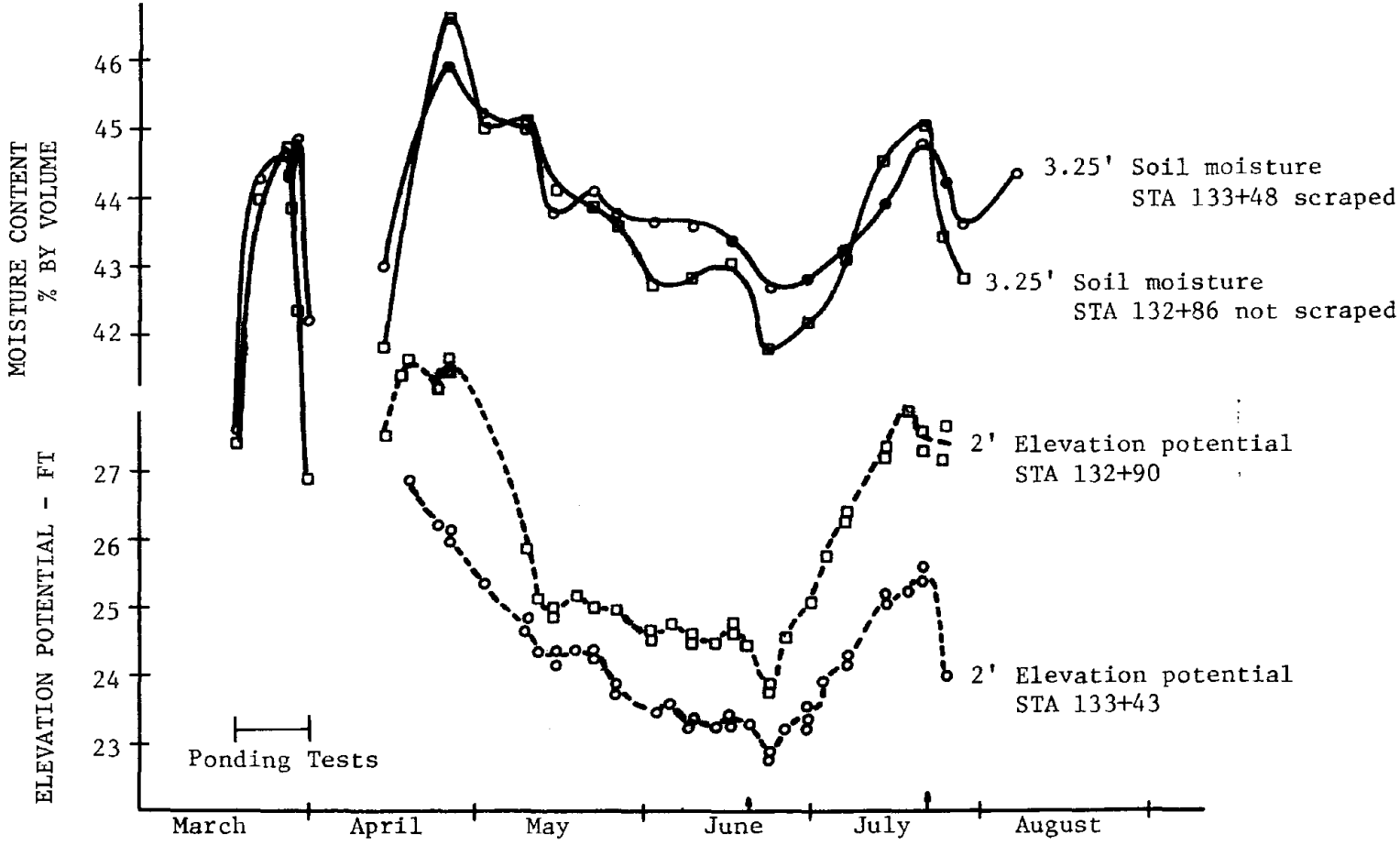

Figure 33. Comparison of soil moisture content and elevation potential Stations 133+48 and 132+90 Unit A main canal - 1967

CHAPTER VII

SUMMARY AND CONCLUSIONS

Laboratory and field studies were conducted to identify the physical, organic or chemical effects involved in the natural sealing of canals or reservoirs under prolonged submergence.

Laboratory experiments on sediment migration into sands were conducted and gamma ray scanning procedures utilized to evaluate migration and retention on the soil surface and to compare sediment retention with measured changes in saturated hydraulic conductivity in soil columns.

A simplified equation relating the deposit ratio, σ, or volume of sediment retained at any level in a soil column to the hydraulic conductivity was developed and verified with laboratory results. These studies showed that with 50-150μ sands and introduction of various sized sediments, reduction in hydraulic conductivity to 3 to 5 percent of the original values can occur. Ninety-four to ninety-eight percent of the reduction takes place in the top 20mm of the columns as 25 to 68 percent of the sediment did not penetrate the soil matrix. Small size (<2μ) sediment penetrates the sand more readily than larger sediments and provides a more effective sealing layer as it accumulates on the surface. Gamma ray scanning proved to be a fast effective means of determining the deposit ratio within soil columns. Comparison of estimated deposit ratios by Stein's equation, a simplified hydraulic equation, and gamma ray analysis showed that the simplified equation yielded as good or better results than Stein's equation.

Procedures for estimating changes in hydraulic conductivity of

Portneuf silt-loam soils of southern Idaho due to soil-water-chemical effects were studied. Techniques developed by McNeil (1968) using measured conductivities during percolation of mixed salt solutions were used to estimate probable changes in conductivity of silt-loam due to clay swelling. Results showed that measured changes in saturated hydraulic conductivity of disturbed columns could not be accounted for by clay swelling. Since steps were taken to minimize microbiological activity in this series of tests, the measured reduction in conductivity were attributed to plugging of soil pores by physically dislodged and redeposited (dispersed) particles.

Measurements of saturated hydraulic conductivity on undisturbed soil cores taken from the bottom of an operating canal showed reductions with time similar to that of disturbed samples during percolation of non-sterile irrigation water. The top layers exhibited decreases to 20 percent of initial values with lower layers sometimes exhibiting no decrease. Comparison of the initial conductivity of a core with the top layer of fine sediments intact with the conductivity of a core with the layer removed showed a K value 25 times lower than for the core with the top layer intact. These measurements indicate the reasons for large observed changes in overall loss rates for unlined canals after the first season.

Field tests were made on an operating canal in which comparisons were made of ponded seepage rates, inflow-outflow rates and estimates of seepage rates from permeability tests.

These comparisons showed that estimates of losses for proposed canals in silt loam soils can be as much as five times greater than actual operational losses. Measurements by inflow-outflow methods show

seasonal declines in total losses which can be attributed to changes in hydraulic conductivity of the soil.

Soil moisture tension measurements below the operating canal showed seasonal declines in elevation potential with major fluctuation over the season. The hydraulic gradient in the top .08m (.25 ft) of the canal bottom showed an increase to five times the initial gradient whereas the gradient in the lower layers remained relatively constant. This indicates that the major decrease in seepage rates is due to changes in conductivity of the top sealing layer. The responses of tensiometers below a section of the canal from which the top layer had been removed were nearly identical to those with the layer intact. The mechanisms causing reduction in hydraulic conductivity are in effect with or without the sealing layer.

Measurements of soil moisture below the canal invert were made at two stations to examine the effect of removing the top 2.5cm of soil on the canal bottom. No significant differences in the seasonal change in the soil moisture was measured at the two stations indicating that the presence of an initial sealing layer does not affect the seasonal change in seepage.

Results of the laboratory and field tests indicate that sedimentation, microbiological activity, soil-water-chemical effects, and physical dispersion of the silt fraction can effect hydraulic conductivity of the soils beneath canals and reservoirs. For the Portneuf silt-loam soils, the effect of clay swelling due to changes in the chemical content of percolating water causes minimal reduction in hydraulic conductivity. The major reduction in conductivity is caused by physical dispersion of the silt fraction in the top layer of the soil. This

reduction in conductivity due to dispersion appears to be reversible with drying. Accumulation of sediment on the canal bottom causes long term decrease in seepage rates, however, the relative magnitude of the reduction is less than that caused by dispersion. The role of microbiological activity in seepage reduction is apparently significant under some situations but not in others. Difficulty was encountered in laboratory sedimentation tests with growth under non-sterile conditions in sand columns. However, in the conductivity measurements of Portneuf silt-loam soil, no apparent difference in conductivity was measured under sterile or non-sterile conditions. Data from these experiments is not sufficient to evaluate the relative effort of microbiological activity on seepage rate changes in operating canals and reservoirs.

Determination of the deposit ratio, σ, using equation (19) will allow the evaluation of the location or migration of sediment into a soil matrix by monitoring the change in hydraulic conductivity during a sedimentation run on laboratory columns. Using this procedure on soil columns taken along proposed new canal routes estimates of sediment migration into the soil matrix can be used to estimate the decrease or permanence in seepage reduction from sedimentation. Also, if mechanical mixing of sediments is contemplated as a means of decreasing the hydraulic conductivity of soil in canal bottoms, the resulting hydraulic conductivity expected for any specific deposit ratio can be estimated from a single measurement of initial porosity and hydraulic conductivity.

The procedures developed by McNeal and Coleman (1966) and applied in this study can be used to predict the relative effect on seepage of clay swelling for percolation of waters of various qualities. For example, where waters from different sources are interchanged in a

system, relative differences in seepage due to clay swelling can be predicted for planning purposes. Likewise the expected decrease in seepage due to physical dispersion of fine particles within the soil matrix as opposed to clay swelling can be evaluated using procedures developed in this study.

Recognition of and quantification of the effects of seepage reduction on sedimentation and soil-water-chemical effects can prevent costly design errors not only for canal systems but for smaller developments such as holding ponds for irrigation water supply or even landscaping developments.

CHAPTER VIII

RECOMMENDATIONS

The broad scope of this investigation prevented a thorough evaluation of many factors affecting operational seepage losses in canal systems. Several additional research endeavors should be pursued:

1) An evaluation of the type of biotic environment of the benthic area of canals and reservoirs conducive to the development of sealing on the surface or beneath the soil surface. Microbiological sealing is not always the predominant effect in a natural sealing process under prolonged submergence. Possible alteration of the benthic environment, either through soil amendments or slight changes in water quality may serve as very economical means to achieve significant seepage reduction.

2) Procedures developed to determine relative effects on seepage due to soil-water-chemical interactions for Portneuf silt-loam soil need to be applied to other major soil groups in Idaho and other areas where open channel conveyance of irrigation water is common.

3) Additional studies on the sediment migration into sand-soil matrices should be performed with the objective to develop quantitative relationships between sediment size, media size, penetration, distance and seepage velocities. Results of these studies would be helpful in evaluating long term operating seepage rates of proposed new canals due to natural sedimentation or to estimate effects to artificial introduction of sediments.

LITERATURE CITED

Allison, L. E. 1947. The effect of microorganisms on permeability of soil under prolonged submergence. Soil Science 63:439-540.

Beavers, A. H. and L. Jones. 1966. Elutriator for fractionating silt. Soil Science Society of American Proceedings 30:126-128.

Behnke, Jerold J. 1969. Clogging in surface spreading operations from artificial groundwater recharge. Water Resources Research 5(4):870-876.

Bodman, G. B. and M. Fireman. 1950. Changes in soil permeability and exchangeable cation status during flow of different irrigation waters. International Congress Soil Science, Transcript 4th (Amsterdam, Netherlands) 1:397-400.

Bondurant, J. A., R. V. Worstell, and C. E. Brockway. 1969. Plastic casings for soil cores. Soil Science 107:70-71.

Bouwer, Herman. 1965. Theoretical aspects of seepage from open channels, Journal of the Hydraulics Division, American Society of Civil Engineers 91 (HY3) Proceedings Paper 4321:37-59. May.

Brockway, C. E., and R. V. Worstell. 1969. Groundwater investigations and canal seepage studies. Progress Report No. 2. Engineering Experiment Station. University of Idaho, 70 p, 1967. June.

Camp, Thomas R. 1964. Theory of water filtration. Journal of the Sanitary Engineering Division, American Society of Civil Engineers 90(SA4):1-30. August.

Carman, P. C. 1938. Journal of Society Chemical Industry 57(225) as cited in Scheidegger (1957).

Childs, E. C. and Collis-George, N. 1950. The permeability of porous materials. Proceedings Royal Society of London A201:395-405.

Christiansen, J. E. 1944. Effect of entrapped air upon the permeability of soils. Soil Science 58:355-365.

Chung, Yung Chi. 1970. The sedimentation of natural channels. Unpublished M. S. Thesis, University of Idaho. 50 p

Eliassen, Rolf. 1941. Clogging of rapid sand filters, Journal of the American Water Works Association 33(926).

Filmer, R. W. and A. T. Corey. 1966. Transport and retention of virus sized particles in porous media. Sanitary Engineering Paper No. 1, Colorado State University.

Foster, L. J. 1941. Placing the All-American canal in operation. Civil Engineering, pp 580-583, October.

Freeze, R. Allen. 1971. Three dimensional, transient, saturated-unsaturated flow in a groundwater basin. Water Resources Research 7(2):347-365.

Gardner, R. 1945. Some soil properties related to the sodium salt problem in irrigated soils. U. S. Department of Agriculture Technical Bulletin 902, 28 p.

Glenn, J. Harlan. 1968. Relationship of water quality and soil properties to seepage problems. Proceedings 2nd Seepage Symposium, Phoenix, Arizona. pp 1-7.

Glover, R. E. 1963. An evaluation of quantitative importance and the factors governing canal seepage losses. Technical Memorandum to Chief, Technical Engineering Analyses Branch, U. S. Bureau of Reclamation, 6 p.

Gupta, Rajinder P. and Dale Swartzendruber. 1964. Entrapped air content and hydraulic conductivity of quartz sand under prolonged liquid flow. Soil Science Society of America Proceedings 28:9-12.

Gupta, Rajinder P. and Dale Swartzendruber. 1962. Flow associated reduction in the hydraulic conductivity of quartz sand. Soil Science Society Proceedings 24:6-10.

Harr, M. E. 1962. Groundwater and seepage. McGraw Hill Book Company, New York, 315 p.

Hart, P. F. C. 1963. Experience with seepage control in the Pacific Northwest. Proceedings Seepage Symposium. Phoenix, Arizona, pp 167-175.

Hayden, C. W. and W. H. Heineman, Jr. 1967. A hand-operated undisturbed core sampler. Soil Science 106:153-156.

Hendricks, D. and C. C. Warnick. 1959, 1960, 1961. A study of the control of canal seepage, Progress Report Numbers 1, 2 and 3. University of Idaho Engineering Experiment Station.

Hubbert, M. K. 1956. Darcy's law and the field equations of the flow of underground fluids. American Institute of Mining, Metallurgical and Petroleum Engineers, Transactions 207:222-239.

Iwasaki, Tomihisa. 1951. Some notes on sand filtration. Journal of the American Water Works Association 29:1591-1602.

Jackson, R. D., R. J. Reginato and W. E. Reeves. 1962. A mechanical device for packing soil solumns. Agricultural Research Service. U. S. Department of Agriculture. ARS 41-52, 10 p.

Jeppson, R. W. 1969. Free-surface flow through heterogeneous porous media. Journal of the Hydraulics Division, American Society of Civil Engineers 95:363-381.

Jeppson, R. W. and William R. Nelson. 1970. Inverse formulation and finite difference solution to partially saturated seepage from canals. Soil Science Society of America Proceedings. 34:9-14.

Johnson, Curtis E. 1958. Effect of chlorination on some physical and biological properties of a submerged soil. Soil Science Society of America Proceedings 22:244-246.

Kozeny, J. 1927. S. Ber. Weiner Akad. Abt. 11a 136, 271, as cited in Scheidegger 1957.

Laliberte, G. E., A. T. Corey, and R. H. Brooks. 1966. Properties of unsaturated porous media. Hydrology Paper Number 17, Colorado State University, 40 p.

Martin, J. P. and S. J. Richards. 1969. Influence of the copper, zinc, iron, and aluminum salts of some microbial and plant polysaccharides on aggregation and hydraulic conductivity of Ramona silt loam. Soil Science Society of America Proceedings 33:421-423.

Muckel, Dean C. 1959. Replenishment of groundwater supplies by artificial means. Technical Bulletin Number 1195, U. S. Department of Agriculture, Agriculture Research Service. 51 p.

Muscat, M. 1946. The flow of homogeneous fluids through porous media. J. W. Edwards, Inc., New York. 736 p.

McNeal, B. L. 1968. Prediction of the effect of mixed salt solutions on soil hydraulic conductivity. Soil Science Society of America Proceedings 32:190-193.

McNeal, B. L., D. A. Layfield, W. A. Norvell, and J. D. Rhoades. 1968. Factors influencing hydraulic conductivity of soils in the presence of mixed salt solutions. Soil Science Society of America Proceedings 32:187-190.

McNeal, B. L., W. A. Norvell, and N. T. Coleman. 1966. Effect of solution composition on the swelling of extracted soil clays. Soil Science Society of America Proceedings 30:313-317.

McNeal, B. L., and N. T. Coleman. 1966. Effect of solution composition on soil hydraulic conductivity. Soil Science Society of America Proceedings 30:308-312.

Pillsbury, A. F. 1950. Effects of particle size and temperature on the permeability of sand to water. Soil Science 70:299-300.

Polubarinova-Kochina P. Ya. 1962. Theory of groundwater movement, (translated from the Russian by J. M. Roger deWeist), Princeton University Press, Princeton, New Jersey. 613 p.

Quirk, J. P. and R. K. Schofield. 1955. The effect of electrolyte concentration on soil permeability. Journal of Soil Science 68:163-178.

Rasmussen, W. W. and B. L. McNeal. 1973. Predicting optimum depth of profile modification by deep plowing for improving saline sodic soils. Soil Science Society of America Proceedings 37:432-437.

Reeves, A. B. 1954. Linings for irrigation canals. Presented at Annual Meeting, National Reclamation Association, Portland, Oregon, November.

Reeve, R. C., C. A. Bower, R. H. Brooks, and F. G. Gschwend. 1954. A comparison of the effects of exchangeable sodium and potassium upon the physical condition of soils. Soil Science Society of America Proceedings 18:134-132.

Richards, L. A. Capillary conduction of liquids through porous mediums. Physics, Vol. 1:1931.

Risenaur, A. E., R. W. Nelson and C. N. Knudsen. 1963. Steady Darcian transport of fluids in heterogeneous partially saturated porous media. Part 2. The computer program. Atomic Energy Commission Research and Development Report HW-72335 PT2. 80 p.

Risenaur, A. E. and R. W. Nelson. 1965. Some influences of soils and water table depths on seepage from lined and unlined canals. Atomic Energy Commission Research and Development Report HW-SA-2890. 72 p.

Risenkampf, B. K. Hydraulics of groundwater. State University of Saratovsky. Part 1, Vol. 1, No. 1, 1938.

Robinson, A. R. and C. Rohwer. 1959. Measuring seepage from irrigation channels. Agricultural Research Service, U. S. Department of Agriculture Technical Bulletin Number 1203, Washington, D. C. Government Printing Office. 82 p.

Scheidegger, A. E. 1957. The physics of flow through porous media. MacMillan Company, New York. 256 p.

Shen, R. T. 1958. Sediment sealing with bentonite in a dune sand. CER Number 58RTS 25, Colorado State University Research Foundation. 135 p.

Stein, P. C. 1961. A study of the theory of rapid filtration of water through sand. Ph.D. Thesis, Massachusetts Institute of Technology, Cambridge, Mass. as reported by Camp.

Tiedeman, D. A. and C. T. Coffey. 1966. Soil moisture changes beneath a canal, U. S. Department of the Interior, Bureau of Reclamation Report Number EM-725. 17 p, 41 illustrations.

U. S. Bureau of Reclamation. 1963. Final report. Silting and seepage investigation North Platte Project, Wyoming-Nebraska, March. 61 p.

U. S. Bureau of Reclamation. 1971. Use of water on federal irrigation projects. Minidoka Project, Northside Pumping Division, Idaho. Vol. 1. Crop and Irrigation Data. pp 103-106.

U. S. Bureau of Reclamation. 1914. Project History - Minidoka Project Idaho.

U. S. Department of Agriculture. 1954. U. S. salinity laboratory diagnosis and improvement of saline and alkali soils. Handbook No. 60. 160 p.

Warnick, C. C. 1949. Methods of evaluating seepage losses from irrigation canals. Progress report on special research project No. 20, Engineering Experiment Station, University of Idaho, Moscow, Idaho. 48 p.

Wyllie, M. R. and Gardner, G. H. F. 1958. The generalized Kozeny Carman equation. World Oil, March and April.

APPENDIXES

Appendix A

Evaluation of Mass Absorption Coefficients for Container Materials

Mass absorption coefficients, α, of possible container materials were evaluated using the gamma ray scanner with various thicknesses of material. Table 16 contains the data for α determinations of plexiglas, steel and aluminum.

Table 16. Mass absorption coefficients of solid materials

Material	Density ρ g/cm^3	Thickness x cm	Average Coefficient I_o [L1]	Absorption Coefficient-α cm^2/g [L2]
Plexiglas	1.16	9.59	50,499	.15963
		6.56	88,583	.15952
Steel	7.407	.328	20,784	1.09618
		.565	1,451	1.27238
		.984	306	.94413
Aluminum	2.64	1.250	135,597	.23861
		1.875	94,309	.23243
		2.500	63,308	.23471

[L1] Average of 10, 10 second counting periods with gamma ray facilities settings of:

Window	0.00
Threshold	035
Discriminator	5.00

[L2] Equation (20) $\ln \frac{I_o}{I} = \alpha x \rho$

I_o = 298,000 counts

Appendix B

Evaluation of Mass Absorption Coefficients for Soil and Distilled Water

Soil was packed in a 7.70cm long, 5.08cm diamater plexiglas column. Gamma ray intensity was measured at 11 intervals throughout the length of the column. The same column was used for determination of the mass absorption coefficient of distilled water. Results are shown in Table 17.

Table 17. Mass absorption coefficients of soil and distilled water

Material	Density ρ g/cm^3	Thickness x cm	Average Count I_o	Average Coefficient-α cm^2/g
Soil [L1]	1.7008	5.08	34,504	.23745
Distilled Water [L2]	.9976	5.08	113,164	.16821

[L1] Soil is 50μ-150μ sand packed with a density of 1.7008 g/cm^3 and porosity of 0.3752

[L2] Room temperature was 22.7°C, therefore ρ = .9976 g/cm^3

VITA

Charles Edward Brockway

Candidate for the Degree of

Doctor of Philosophy

Dissertation: Investigation of Natural Sealing Processes in Irrigation Canals and Reservoirs

Major Field: Engineering

Biographical Information:

Personal Data: Born at Ketchum, Idaho, December 4, 1936. Married to Carol Marie Smith, Hailey, Idaho, August 16, 1958; three children - Ann, Karen and Charles.

Education: Attended elementary school in Ketchum, Idaho; graduated from Hailey High School, Hailey, Idaho, in 1955; received the Bachelor of Science degree from University of Idaho in Civil Engineering in 1959; completed requirements for the Master of Science degree in Civil Engineering at the California Institute of Technology in 1960.

Professional Experience: 1960-61, foundation engineer for Converse Foundation Engineering Company, Pasadena, California; 1961-63, Instructor in Engineering at Boise College, Boise, Idaho; 1963-65, hydraulic engineer with the U. S. Bureau of Reclamation, Denver, Colorado; 1965 to present, Assistant and Associate Professor, Civil Engineering, University of Idaho.